ADVANCED PROPULSION POWER DISTRIBUTION SYSTEM FOR NEXT GENERATION ELECTRIC/ HYBRID VEHICLE

PHASE I : PRELIMINARY SYSTEM STUDIES

FINAL REPORT

by

Bimal K. Bose
Min-Huei Kim

The University of Tennessee
Department of Electrical Engineering
419 Ferris Hall
Knoxville, Tenn. 37996-2100

for
NASA Lewis Research Center
Cleveland, Ohio 44135

June 5, 1995

NASA Contact: Dr. M. David Kankam
Power Technology Division
Electrical Components and Systems Branch

ADVANCED PROPULSION POWER DISTRIBUTION SYSTEM FOR NEXT GENERATION ELECTRIC/HYBRID VEHICLE

1. Project Objective

The primary objective of this project is to establish the viability of high frequency ac (HFAC) for propulsion power distribution system in the next generation advanced electric/hybrid vehicle that tends to satisfy the PNGV (Partnership for Next Generation Vehicles) goals [1]. In justifying this validity, the HFAC system is to be compared with the traditional dc distribution system in terms of cost, weight, performance and other capabilities, and its overall superiority is to be established. Any possible drawbacks are also to be highlighted. Before attempting the above design trade-off study, a comprehensive study will be made for the possible power and energy sources in the next generation, and based on this study, the most viable distribution system will be established for the near term (year 2002 for PNGV Goal 3) technology basis.

2. Summary

The report essentially summarizes the work performed in order to satisfy the above project objective. In the beginning, different energy storage devices, such as battery, flywheel and ultra capacitor are reviewed and compared, establishing the

superiority of the battery. Then, the possible power sources, such as IC engine, diesel engine*, gas turbine and fuel cell are reviewed and compared, and the superirity of IC engine has been established. Different types of machines for drive motor/engine generator, such as induction machine, PM synchronous machine and switched reluctance machine are compared, and the induction machine is established as the superior candidate. Similar discussion was made for power converters and devices. The IGBT appears to be the most superior device although MCT shows future promise. Different types of candidate distribution systems with the possible combinations of power and energy sources have been discussed and the most viable system consisting of battery, IC engine and induction machine has been identified. Then, HFAC system has been compared with the DC system establishing the superiority of the former. The detailed component sizing calculations of HFAC and DC systems reinforce the superiority of the former. A preliminary control strategy has been developed for the candidate HFAC system. Finally, modeling and simulation study have been made to validate the system performance. The study in the report demonstrates the superiority of HFAC distribution system for next generation electric/hybrid vehicle.

3. Introduction

Electric vehicles (EV) were introduced practically from the beginning of this

----

* Diesel engine is strictly an IC engine

century. However, their importance for transportation was greatly diminished as gasoline-powered internal combustion engine (ICE) continued to improve and its electric self-starter was commercially introduced. During the 1930's, the number of electric vehicles on road practically vanished to zero because of heavy competetion with the ICE-powered cars. During the Arab oil embargo of 1970's, the electric vehicle research and development activity was pushed to the forefront by various Government-sponsored and privately funded research programs around the world. The prime focus at this stage was fuel saving so that the dependence on imported oil could be reduced. This burst of enthusiasm gradually died as the price of gasoline fell. In the 1980's, the environmental pollution (particularly the urban pollution) problem and the corresponding global warming effect became a major concern in our society. The pollution problem along with the urge for fuel saving, once again became a major motivation for EV research. It is interesting to note here that in USA oil constitutes 42% of total energy consumtion, and the major part of this oil is consumed in automobile transportation. Again, more than 50% of our oil is imported from outside.

It appears that this time we are very serious about EV's because environmental pollution is a problem that will not go away easily. In October 1990, the California Air Resources Board (CARB) established rules that mandate 2% of all vehicles sold in California in 1998 must be zero emission vehicles (ZEV). This quota increases to 5% by 2001 and to 10% by 2003. These regulations have been adopted by the states of New York and Massachussetts, and are being actively considered by about twelve other states

3

in the US. The California rules not only had serious impact in USA, but had wide reverberations in Europe and Japan. It appears that governments, prominent auto industries and universities around the world are persuing serious development effort for advancement of EV's , and published literature in this area is abounding. In September 1993, the US Government along with the big three automakers (GM, Ford and Chrysler) declared a historic partneship program for next generation vehicles (PNGV) [1] . The salient PNGV goals that are to be fully implemented in prototype vehicle before the year 2003 can be summarized as follows:

- A state-of-the-art vehicle that has three times the present fuel efficiency (80 miles/gallon)

- Emission level: 0.125 HC (gms/mile)

   1.7 CO   "

   0.2 NO_x "

- Acceleration: 0 - 100 kmh (0 - 60 mph) in 12 secs.

- Range: 610 km (280 miles)

- Capacity : 6 passengers

- Curb weight : 900 kg

- Luggage : 90 kg

- Drive train : 190 kg

- Useful life: 160,000 km (100,000 miles)

Although it is not mentioned as an EV, it has to be an hybrid electric vehicle

(HEV) obviously with regenerative braking energy capture capability in order to meet the desired fuel efficiency and range goals. To achieve the PNGV goals at an acceptable consumer price, challenging R & D in a number of related technology areas will be needed.

4. Electric and Hybrid Electric Vehicles

Table 1 gives the summary of key EV programs around the world [78] with the salient vehicle data. The traditional EV uses battery as an energy source, dc distribution bus and a converter-fed propulsion motor which can be either dc or ac. However, the disadvantages of dc machine coupled with the recent advancement of power electronics technology has favoured ac motor drives. Replacing a conventional gasoline-powered ICE vehicle with an EV eliminates the air pollution problem in urban area. However, the battery is to be charged with utility power that is usually generated by a fossil fuel or nuclear power station. Of course, regular night charging can be done by off-peak utility power which is economical. Recent studies have indicated that switching from ICE vehicle to electric vehicle not only causes overall energy saving but also reduces the environmental pollution effect. Fig. 1 shows the fuel chains for gasoline-powered ICE vehicle and EV charged with coal-based power [60]. In a federal urban driving cycle (FUD) , the ICE vehicle gives a poor efficiency of 12.24% with the overall fuel chain efficiency of 10%. On the other hand, an EV gives efficiency of 51.6% with the total fuel chain efficiency of 18%. It may be mentioned here that coal generates 56% of US

Table 1: Electric Vehicle Programs and Vehicle Data

Program	Vehicle	Range (km) @(km/h)	Top Speed (km/h)	Gross Weigh (kg)	Pay-load (kg)	Accelerat. (0-x km/h)	Energy Consum. (kWh/kmh)	Battery Data Type	Energy (kWh)	Volt. (V)	Weight (kg)	Transmission	Drive	Grade Ability %	Motor Type	Drag Coef.	Notes
ETV-1 GE	4-seater	87/C-cyc 120/D-cy	96	1793	270	8.8 (0-50) 23.7 (0-80)	0.29/city	Pb-acid	32.6	108	500	single 5.48:1	front-wheel		DC separ.	0.3	regeneration onboard charg
EXT-I Ford	Escort 2 seater		96	1725	180	6.7 (0-50) 18 (0-80)	0.18/FUDS	Pb-acid	17	204	560	2-speed auto 15.52, 10.15	front-wheel	30	AC (IM)	0.39	Ef=70%@dri Ef=57%@reg
EXT-II Ford	Aerostar Van	160+ 227/80	96	2310	260	<20 (0-80)	0.16/48 0.25/FUDS	Na-S	50	204	500	2-speed auto 21.2, 13.8	rear-wheel planetary g	30	AC (PMSM)	0.44	elec. P/S drive-by-wire
DSEP Eaton	Minivan T115	212/48 85/FUDS	105	2720	550	<20 (0-80)	0.16/48 0.30/Funds	Ni-Fe	30	168	500	2-speed auto 24.8,14.1	front-wheel	25	AC (IM)	0.38	4h offboard cha regen 10%
G-Van Magna	GMC Rally	96	90	4360	680 c 450 p	13 (0-50)	0.52	Pb-acid	44.3	216	1280.	single 8.7:1	rear-wheel	18	DC	0.46	P/B, P/S, regeneration
TEVan Chrysler	Minivan	195/50	105	2815	550 c 410 p	8.2 (0-50) 25 (0-96)	0.27	Ni-Fe	39	180	820	2-speed auto 15.3, 8.4	front-wheel		DC		elec. P/B, P/S regeneration
IMPACT GM	2-seater	193/89	160	1160	160	8.5 (0-96)	0.07/90	sealed Pb-acid	13.6	320	400	single planet. 10.5:1	front-wheel		AC2 (IM)	0.19	onboard charge regeneration
LA-301 CAT	4-seater 25kW IC	96(bat.) 240(ICE)	120	2110	340	7 (0-50) 17 (0-80)	0.16/C-cyc	sealed Pb-acid	10.9	216	500	2-speed auto	front-wheel		DC		onboard charger regeneration
BMW E1	2+2 Coupe	260/50 144/FTP	120	1180	300	6 (0-50) 18 (0-80)	0.13	Na-S (ABB)	19	120	200	single speed planetary g.	rear-wheel	>25	AC (BDCM)	0.32	regeneration 6-8h recharge
BMW E2		430(ICE)	120	1215	300	6.5 (0-50) 15.5 (0-80)		Na-S (ABB)	28.8	180	265		rear-wheel		AC (BDCM)	0.32	9h recharge
Ecostar Ford	4 seater hybrid	320/40 160/FUD	120	1850	390	12 (0-80)		Na-S	30		360	single speed planetary g.	front-wheel	30	AC (IM)		100 mi@FUDS 6 h charging
MEVP GE	compact van	260/FUD 276/88		1590 (curb)		4.4 (0-50) 14.4(0-96)		Na-S	50	336	450	single speed 12.2:1	front-wheel	34	AC (IM)	0.34	
FEV Nissan	2+2 Coupe	240/40 160/70	130	900 (curb)	4 pasgr	3.6 (0-40) 20(-400m)	0.075	Ni-Cd	11.6	280	200	planetary g. single 12:1	front-wheel	35	AC (IM)	0.19	superquick 15min recharge
Chico VW	2+2 seate hybrid	60 (bat.)	130	1135	350	19 (0-80) 30 (0-100)	0.13	Ni-Cd (ABB)	3.5	72	140	5 speed manual	rear-wheel		AC (IM)		2cyl, 25kW ICE
VW City Stromer	4 seat Jetta	80/50 65/70	100	1690	280	13 (0-50) 27 (0-70)	0.20/50 0.25/70	Na-S (ABB)		180	276	5 speed	front-wheel	30	DC separ.		regeneration
VERD PSA	4-seater hybrid	72/40 750/100	130	1910	320	7 (0-50) 23 (-400m)		Ni-Cd	5.3	230	210	single speed 5.8:1	rear-wheel	30	DC2 in series		52kW ICE 41kW generator
IZA TEPCO	4-seater	548/40 270/100	176	1573 (curb)		3.5 (0-40) 18 (-400m)	0.06/40	sealed Ni-Cd	28.8	288	531	in-wheel motor x 4	4-wheel	32	AC (BDCM)	0.19	P/B, P/S, air in-wheel motor

c-cargo
p-passenger
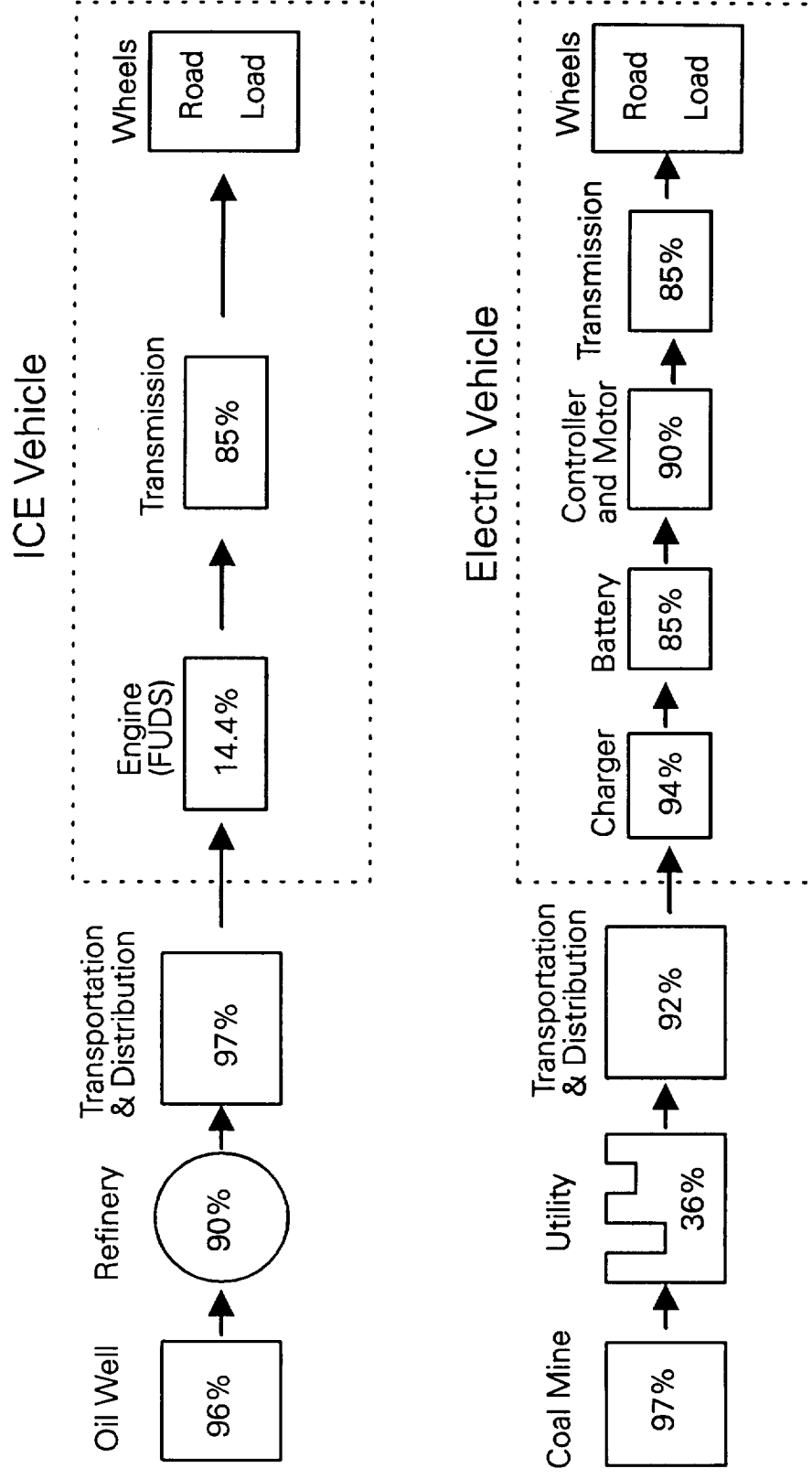
FIG. 1: FUEL CHAINS FOR GASOLINE-FUELED ICEV AND EV CHARGED WITH COAL-BASED POWER

ICE Vehicle

Oil Well 96% → Refinery 90% → Transportation & Distribution 97% → Engine (FUDS) 14.4% → Transmission 85% → Wheels (Road Load)

Electric Vehicle

Coal Mine 97% → Utility 36% → Transportation & Distribution 92% → Charger 94% → Battery 85% → Controller and Motor 90% → Transmission 85% → Wheels (Road Load)

electrical energy, and the corresponding share for oil and nuclear power are respectively 3% and 22%. In addition to energy saving, EV needs less maintenance and the "fuel" is more economical, but the bulky battery is expensive and has a limited cycle life. The EV has also a limited range and limited acceleration capability at high speed, i.e., can not definitely meet the performance of a gasoline car. However, statistics have shown that more than 70% of cars in USA are used for limited range commuting application where EV is satisfactory.

In HEV, a power source (usually an IC engine) assists the energy storage source to get a good compromise of EV and IC-powered vehicle in terms of fuel economy, pollution, range extension and versatility, and of course, with additional cost. The EV mode is mainly active in urban driving with zero emission whereas the engine mode essentially serves as the vehicle's range extender. The two modes can be strategically combined for optimal performance and energy management. The HEV drive configuration can be either in parallel or in series mode. In parallel mode, the electric motor power and engine power are directly combined on the drive shaft, whereas in the latter configuration, the power from the engine-generator is parallelled with that of the battery and feed a single converter-fed propulsion motor. It can be shown that the series system is more efficient, practical and gives a better drivability. It appears that both EV and HEV will share the market equitably in future. Eventually, in the long run the EV's will dominate the market when the energy source becomes economical.

5. Propulsion Power Distribution System

Fig. 2 shows the general block diagram for advanced propulsion power distribution system for next generation HEV that can possibly meet the PNGV goals. Basically, it is a series hybrid drive system where the energy storage source and the power source contribute electrical power to a common bus that drives an ac motor through a variable voltage variable frequency (VVVF) converter. Traditionally, dc power distribution system has been considered for electric vehicle. Recently, NASA has demonstrated the viability of high frequency (20 kHz) single-phase power distribution system for aerospace applications [2][3]. The first application considered was an "all electric" secondary power system for a commercial plane . In this study, all existing secondary power system functions were performed by electrically powered systems operating from a dual redundant 20 kHz power distribution system. In this application, the high frequency power system resulted in both a significant weight reduction and an increased efficiency. The second system design was evaluated for the power distribution system of the NASA orbiting Space Station. The Space Station, as presently planned, will have an initial power capability of 75 kW and will eventually grow to 300 kW. Evaluation of this design showed that the intrinsic low weight and high efficiency of the 20 kHz system would result in an initial cost savings of about 100 million dollars. Several other applications under consideration are: Naval Air ship program, electrically operated flight controllers for Shuttle II, and the newly proposed

- BATTERY
- FLYWHEEL
- ULTRA CAPACITOR
- [SUPER CONDUCTING MAGNET (SMES)]

POWER FLOW

TRANS-MISSION

AC MOTOR

M

CONVERTER (VVVF)

ENERGY STORAGE

CONVERTER/GENERATOR

DC or HIGH FREQUENCY AC

OPTIMAL ENERGY MANAGEMENT & CONTROL

- INDUCTION MOTOR
- PM SYNCHRONOUS MOTOR
- SWITCHED RELUCTANCE MOTOR

USER INTERFACE

AUXILIARY SYSTEM

GENERATOR/CONVERTER

POWER SOURCE

POWER FLOW

- IC ENGINE
- GAS TURBINE
- FUEL CELL
- [DIESEL ENGINE]
- [STIRLING ENGINE]

POWER FLOW

FIG. 2: GENERAL BLOCK DIAGRAM OF ADVANCED PROPULSION POWER DISTRIBUTION SYSTEM FOR NEXT GENERATION HEV

10

transatmospheric vehicle. It appears that high frequency ac distribution system for EV/HEV has some special advantages which will be discussed later. The battery has been the traditional energy storage source, but flywheel or ultra capacitor can also be the alternate storage device. The superconducting magnet energy storage (SMES) can possibly be a viable source in the long run. The battery or ultra capacitor can be directly connected to dc distribution bus but needs an inverter for HFAC distribution system. On the other hand, a flywheel needs a dc machine (or converter-fed ac machine) drive for dc bus or an ac machine with a frequency changer for HFAC bus. Normally, an IC engine is the power source for HEV, but other possible candidates may be gas turbine, fuel cell, diesel engine or Stirling engine . An engine/turbine can be connected to the dc bus through a dc machine (or converter-fed ac machine) or an ac machine with frequency changer for HFAC bus. On the other hand, a fuel cell needs an inverter for HFAC bus but can be connected directly on a dc bus. The ac machine can be induction, permanent magnet (PM) synchronous or switched reluctance type, as indicated in the figure. The various components of the system will be described later.

The main directions of power flow are indicated in the figure.

The various modes of operation of the drive system can be described as follows:

Mode 1: Acceleration from energy storage source

The vehicle drive motor accelerates from the energy storage source. Since the storage source has limited power capability, acceleration at high speed or speeding on

11

a high grade is not possible. This mode is principally valid in urban driving where the vehicle has truly zero emission.

Mode 2: Decelerate by regenerative braking

The storage source always gets back the recovered energy extracted from the kinetic energy of the vehicle. This mode also has zero emission. Evidently, Modes 1 and 2 (pure EV mode) are truly valid for zero emission urban driving. Note that a conventional IC engine car has no regeneration capability, and therefore, the efficiency is so poor. The efficiency of such a car will dramatically improve if braking energy could be recovered.

Mode 3: Engine/turbine start-up mode

An engine/turbine power source requires electric starting which is normally done by an auxiliary battery through a starter. Instead of separate starting, it is more economical to use the propulsion energy storage source and start the engine through the main generator/converter where the generator acts as a motor. Apparently, the storage source should have the minimum energy available to do this function even it is not being used for driving the vehicle.

Mode 4: Acceleration from power source

Once the engine has started, the power can be used to accelerate the vehicle as in an IC engine powered car. This mode is for highway driving where zero emission

is not strictly demanded, or in city driving, if the battery is nearly discharged.

Mode 5: Combined power and energy source driving the vehicle

This made is valid normally for highway driving where acceleration is required at high speed and the power demand can not be satisfied by either energy storage or power source. It is also valid for speeding on a high grade.

Mode 6: Power source charging the energy storage.

As indicated before, the energy storage source should be always at a minimum charge (say, a battery). This charge is needed not only for engine starting, but also for bypassing a vehicle on a highway, or climbing a high grade where the power source needs the assistance of the battery. If SOC (state of charge) falls below a limit, say 0.2, the spare capacity of the power source will charge the battery to bring to the level of SOC = 0.3. Such a charging is very inefficient compared to that of utility charging, but is unavoidable during driving.

All the above modes of operation indicate that control and energy management of a HEV are very complex. A well-designed control methodology is to be formulated, based on analytical and simulation study, and implemented digitally with powerful DSP's (digital signal processor).

6. Energy Storage Devices

6.1. Battery

Electric storage battery has been the "heart and soul" of EV even from the beginning of this century when EV was first introduced. It will possibly remain so for the years to come. Among all the components of the EV propulsion system, the power electronics technology is well-developed, the machine and control technologies are well-developed, but the battery possibly remains the weakest link in the system. It has been the main barrier for consumer acceptance of EV in the market. Today's propulsion battery is considered too heavy, too expensive, has low cycle life and gives low vehicle range which makes it essentially suitable for daily urban commuting. For this reason, battery has been the prime focus of R & D for a long time. In 1990, the US Advanced Battery Consortium (USABC) consisting of Department of Energy (DOE), the big three automakers (Chrysler, Ford and General Motors) and Electric Power Research Institute (EPRI) was established to systematically sponsor R & D activities for EV battery technology. The USABC established near-term, mid-term and long-term research goals which will be discussed later.

Unlike other applications, the EV battery has to be specially designed and should meet some special cost and performance goals. These are essentially specific energy (Wh/kg), energy density (Wh/L), specific power (W/kg), power density (W/L) , cycle life (years), and of course, finally the most impoertant parameter is cost ($/kWh). There are various trade-off considerations in designing the battery in an EV. The energy storage

capability is the key performance parameter of a battery that determines the range of EV. In a gasoline-powered car, it has been estimated that 1 kg of gasoline can store 55 times more energy than that of 1 kg of lead-acid battery . Increasing the battery weight can increase the energy storage, and that can give longer range of EV, but soon the cost becomes prohitive . Typically, battery weight should be limited below 1/3 of the vehicle curb weight. Besides energy, the power capability of battery is equally important. This parameter determines the acceleration/deceleration capability and gradeability of the vehicle. In urban driving, the maximum vehicle speed is usually limited, and therefore, the power requirement can be easily met. For longer vehicle range and higher acceleration/deceleration capability at higher speed, the assistance of an engine power source (hybrid vehicle) is more desirable. The life cycle of a battery is limited mainly due to frequent charge/discharge cycles. Replacing an expensive battery every few years adds highly to the life-cycle cost of EV, and this is another deterrant factor for non-popularity of EV.

Besides the prime performance factors of battery as discussed above, the other factors of consideration are maintainability, safety, reliability, material recyclability, charging delay, "fuel gauging" and charge equalization. The charging of battery from utility system is preferrable at off-peak hours when utility system has surplus power capacity. External charging circuits can be used that operates at unity power factor on the line. The converters of the drive system can also be specially designed to perform this charging function. The time delay in charging is another problem in EV application

15

from way-side charging station. While gasoline tank takes a minute to fill, battery charging may need a few hours. Fast charging is possible but it tends to decrease the battery life. superconducting magnent Again, fast charging from a residential power source is difficult because of limited power capacity. It has been estimated that the limited power capacity of an utility distribution system does not permit fast charging of a large number of EVs simultaneously. The "fuel gauging" (or state-of-charge determination) accuracy problem has not yet been solved satisfactorily. The techniques developed so far give only very approximate gauging information. An EV battery requires a large number of cells in series to get the desired terminal voltage that is optimum for storage energy and converter-motor system. The equalization of charge on individual cells is important, otherwise the battery life tends to get short.

Description of Battery Types

There are several types of battery under consideration for EV application. These are: Lead-Acid, Nickel-Cadmium, Sodium-Sulfur, Zinc-Air, Lithium-Polymer, Nickel Metal Hydride, Nickel Iron, Zinc Bromide, Sodium Nickel Chloride , Nickel-Zinc, Nickel Hydrogen and Lithium Iron Disulfide. Table 2 gives the battery technology status [79] summarizing the performance parameters of a few important batteries. It also includes the USABC goals in mid-term and long-term. Table 1 gives the application of battery types in key EV projects.

Table 2: Battery Technology Status

Technology	Cell Voltage Volts	Operating Temp. °C	Specific Energy Wh/Kg 3H rating	Energy Density Wh/L	Specific Power W/Kg	Power Density W/L	Life Cycle [Years]	Cost $/Kwh	Enegy Eff. %
NEAR TERM BATT.									
Lead Acid	2.1	3.5 to 70	35	80-90	125-230	230-600	500[3]- 600[4]	70-130	-
Nickel Cadmium	1.25	-30 to 50	55	120	190	330	2000[10]	600	-
MID TERM BATT.									
USABC goals		-30 to 65	80-100	135	150-200	250	600[5]	<150	-
Nickel Metal Hydride	1.4	-20 to 60	65	175	150	400	600[2]	-	80
Sodium Sulfur	2.08	300 - 400	85	115	120	180	350[2]	600	91
Sodium Nickel Chloride	2.59	250 - 350	130	170	168	225	1000[5]	-	-
LONG TERM BATT.									
USABC goals		-40 to 85	200	300	400	600	1000[10]	<100	-
Zinc Air	1.62	25 - 65	130	120	50	65	70	110	-
Lithium Iron Disulfide	1.62	400 - 450	165	240	375	550	500(2)	110	-
Lithum Polyer	2.8 - 4.5	0 -100	160	260	200	210	300(1)	200	-
Nickel Iron	-	-	50	118	100	-	900	200	58
Nickel Zinc	-	-	67	142	105	-	114	-	77
Zinc Bromine	-	-	79	56	40	-	334	-	75
Lithium monosulfide	-	-	66	133	64	-	163	-	81

The lead-acid battery is possibly the best compromise in energy density, power density, life-cycle, cost and other criteria. It has been widely used in the past and present projects, and will possibly remain so in the near future. Lead-acid batteries are easily available in mass scale, but are not yet in high volume production. It can be shown that 40-50 miles range in urban driving is easily possible with lead-acid battery that will ot exceed 30% of vehicle curb weight. Recently, Horizon Battery Technologies, Inc. (HBTI) with joint venture between Electrosource and BDM Technologies and strategic alliance with EPRI promised to manufacture lead-acid battery that even exceeds the USABC mid-term goals. The Horizon battery specs. can be summarized as follows [21]:

Specific energy (Wh/kg)   -- >45

Specific power (W/kg)   -- 450-500

Energy density (Wh/L)   -- 90

Charge-dischage cycles   -- 900

Normal charge (h)   -- <3

Rapid recharge (min.)   -- 8 (to 50%) - 30 (to 99%)

Cost ($/kWh)   -- 400

Nickel-Cadmium battery is more expensive because of raw material costs. But, it has relatively high energy density, power density and long life compared to lead-acid battery. Many Japanese EV projects prefer Ni-Cd battery. The battery is safe and sealable. It has higher internal resistance (than lead-acid). Cadmium is not

environmentally safe and recycling may be a problem.

Sodium-Sulfur battery has high energy capability. Hence it is good for obtaining high range. But its power is low , thus acceleration capability of the vehicle may be limited. Its cost is reasonable compared to Ni-Cd battery. One drawback is that the battery operates at high temperature (about 300 deg.C) to keep the sodium and sulfer molten within insulated capsules. The battery must be pre-heated to operating temperature and maintained at that temperature during operation. However, once operating, the battery produces enough heat to maintain temperature if adequate thermal insulation is provided. The energy density tends to get limited by the necessity of the packaging and thermal insulation restraints. The battery has the advantages of very low self-discharge, maintenance-free operation and abuse tolerance. The technology is still relatively expensive, but work is in progress to develop lower cost technology and make it competetive for EV market. It seems that not much work has been done on its recycling aspect.

Zinc-Air has good energy capability, but it has low power and short life. Its process is also complicated. Its air supply must be carefully scrubbed of carbon dioxide. Lithium-Polymer battery may be the compromise of all the good properties required for EV. At present, it is still in research stage. It has good power and energy capability and the cost is lower than that of Ni-Cd battery. Its cost will further come down when it is put into regular production.

Nickel-Metal Hydride battery seems to be more promising for the high energy capability, and it has been under development for several years. It is more expensive than other types of batteries, and is not easily available. The cells are abuse tolerant and can be overcharged and over-discharged at moderate levels without damage to the battery. Cells of very low internal resistance can be constructed. The hydride alloy is endothermic on discharge which improves the thermal performance of the cell. As the cell discharges , the hydride alloy is de-hydrided which requires the input of heat to the electrode. Thus, the heat being generated by the cell is partially offset by the heat being absorbed by the hydride electrode. The cycle life is good and could be substantially improved as the system matures. It is also non-toxic.

Nickel iron batteries have been under development for a number of years and have demonstrated potential for long life. The low cell voltage needs large number of cells in series and makes reduction of non-active components/weight important for higher system voltage. The low cell resistance and smaller change in resistance as a function of DOD (depth of discharge) are distinct advantages. However, the life cycle cost would be higher.

Zinc Bromide battery systems are being developed world wide. This technology has a potential for low cost, as the system's components lend themselves to mass production and are made of readily available and inexpensive materials. The system has an advantage for application to larger vehicles.

Nickel hydrogen battery is perhaps the most intensively studied and extensively tested battery system, particularly for aerospace applicatioins. It offers excellent energy density, high abuse tolerance and highest level of reliability of any battery system in existance. The cells can be extensively overcharged and over-discharged without any damage. Although the battery is somewhat expensive, it has a long life cycle and can be guaranteed for the operating life of a vehicle.

6.2. Flywheel

A flywheel (FW) as an energy storage element has been investigated for a long time for different applications. It has been considered for commercial transit bus, and several experimental vehicles have been built using flywheels for automobile applications. A flywheel stores mechanical or kinetic energy (compared to chemical energy in a battery) which is proportional to the moment of inertia (J) and the squared angular velocity (w_r). The mechanical energy is converted to electrical form through a coupled machine-converter system. The machine acts as a generator when the kinetic energy is extracted for vehicle acceleration, whereas it acts as a motor in braking when the vehicle kinetic energy charges the flywheel. Since the stored energy varies as square of the speed, 75% of the stored energy can be utilized by varying the speed in 2:1 range. However, a flywheel requires initial charging from the utility source through a converter. It is usually constructed in a ring form (instead of plate form) to increase the

21

moment of inertia for the same amount of material. Instead of metal, it normally uses light-weight and high strength composite material to economize the cost, but the storage energy is increased by increasing the speed that sometimes exceeds 100,000 rpm. Because of the square relation, it is more economical to increase speed rather than moment of inertia. The friction and aero-dynamic loss of the FW-machine system is very critical. For a prolonged stoppage of the vehicle, the flywheel may loose the energy and may require recharging. It is normally placed in a vacuum chamber and active bearing is more desirable to minimize the friction loss. Maintaining a good vacuum in an automobile environment can be a challenge. The gyroscopic effect of the flywheel can be a safety concern which should be adequately addressed. The machine-converter system has to handle the high frequency because of the high machine speed. A speed reduction gear can be installed at the expense of additional cost and poorer system efficiency.

A flywheel energy storage has the following advantages over the battery:

- Higher power capability

- Quick charging capability

- Longer service life and recyclability

- Higher round trip efficiency (total energy in vs. energy out)

Flywheel systems have been considered both for HEV and EV. It has also been considered for load levelling in a battery-fed EV where it supplies/absorbs the peak power during acceleration/deceleration and helps to prolong the battery life. Prototype

flywheel systems have been demonstrated with a specific energy of 5 Wh/kg and specific power of 375 W/kg for transit bus applications. Additional research and development efforts in flywheel storage system should focus on increasing the specific energy and reducing the cost of flywheel systems. Further R & D offers the potential to reduce material costs, provide lightweight containment, and simplify overall system integration. Potential technical solutions include improved processing and production of high-performance fibers, wet filament winding, in-situ or rapid curing, and multi-layer containment shielding based on low-cost metal matrix and polymer composites.

6.3. Ultra Capacitor

Recent advances in super/ultra capacitor (UC) technology has renewed interest for its application in EV/HEV. The energy storage density of UC is two order of magnitudes higher than the traditional electrolytic capacitors. However, compared to battery, the energy density is very low.

A UC is basically a chemical double layer capacitor (CDLC) that utilizes large surface area electrodes and a liquid electrolyte to form a charge storage layer as shown in Fig. 3. The thickness of this layer is on the order of a few angstroms. Materials such as carbon blacks and Raney metals with surface areas of several hundred square meters per gram had been used in the early CDLCs. The carbon black has a higher energy density but a lower power density because of the material's higher resistivity. On the

(a) Parallel Plate Capacitor

(b) Principle of Liquid
Double Layer Capacitor

(c) Practical Liquid
Double Layer Capacitor
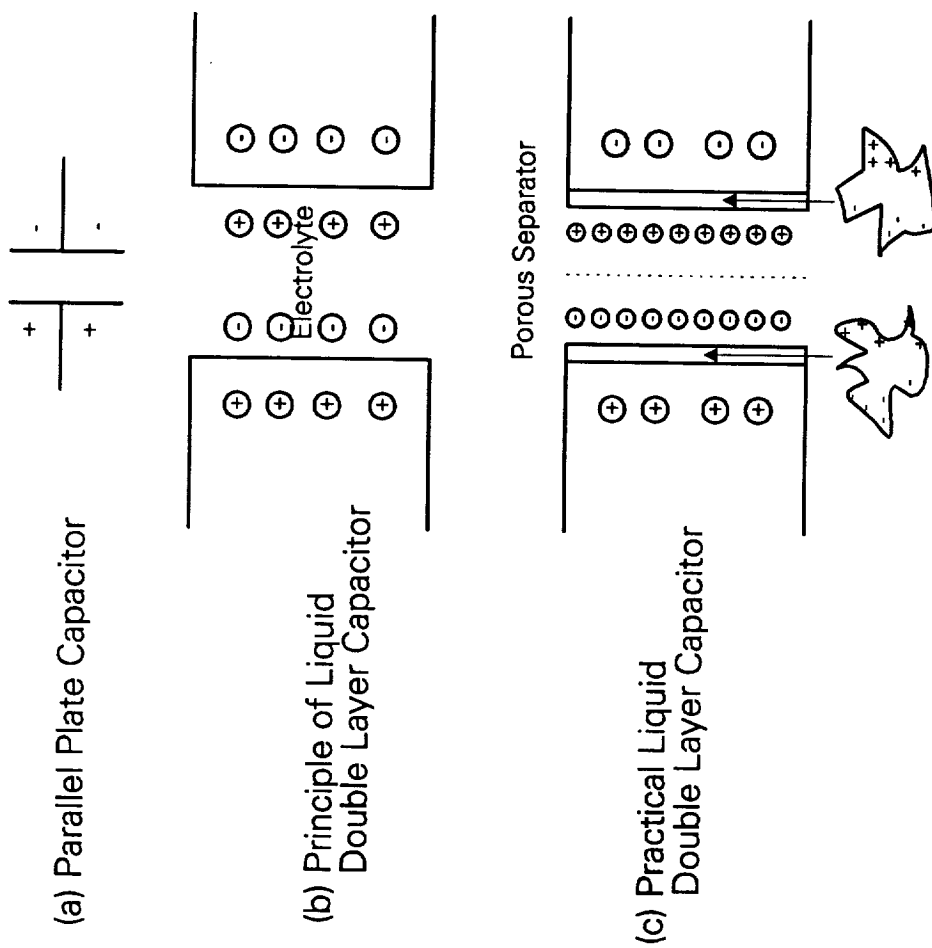
FIG. 3: STRUCTURE OF ULTRACAPACITOR

24

other hand, Raney metals have low resistivity but also low surface area and low energy density. By mixing carbon black and metals, a compromise can be achieved that will increase both the energy and power densities simultaneously. The energy density of new materials has increased two orders of magnitude over Raney metals, and for new CDLCs it has practically reached one-tenth that of lead-acid battery. In CDLC, the interface between the conductor and a liquid electrolyte forms a layer capable of storing charge, as shown in Fig. 3(b). In order to achieve high energy storage density, the thickness of this barrier must be on the order of a few angstroms, and the electrode materials must have high surface areas. By effectively utilizing high surface area materials, the A/d (area/distance) ratio can approach 10, or the capacitance approaches a farad for 1-cm^2 planar area. Table 3 [35] lists some large surface area materials for double layer capacitor applications. Fig. 3(c) shows the practical implementation of UC where a capacitor cell consists of two segments of large surface area material, is immersed in a high conductivity electrolyte, and separated by a porous membrane.

Although characterized by low energy density, UC's have high specific power and high charge/discharge energy efficiency. The former permits very high charge/discharge rate. Therefore, combining high energy density battery with UC capable of handling high transient power requirement (load levelling) may provide an attractive solution to prolong the battery life. Ultra capacitors that are commercially available today have a specific energy of about 1-2 Wh/kg. Laboratory prototype ultra capacitors have recently been demonstrated with a specific energy of about 2 to 5 Wh/kg and power density of

25

Table 3 : Large Surface Area Materials

Materials	Approximate Surface Areas	Comments
Raney Metals	50 - 200 m²/g	Compatibility problems with high conductivity acidic electrolytes
Rare Earth Oxides	300 - 500 m²/g	Compatible with electrolytes
Carbon Blacks	1500 m²/g	Compatible with electrolytes; Modest resistivity
Pillared Clays	250 m²/g	High resistance

2 to 4 kW/kg. Aero-capacitors which are based on the use of aerogels with aqueous or organic electrolytes, have projected specific energies of 4 to 8 Wh/kg. The key technical challenges are to improve the UC's low specific energy and reduce costs. Research and develoment offers the potential to improve UC materials, such as carbon/metal fiber composites, monolith foamed carbon, foamed carbon with a binder, doped polymer layers on carbon paper, and mixed metal oxides (ceramic) on metal foil. Table 4 gives a summary of ultra capacitor technology and Table 5 gives the Rigone plot for UC's and some key batteries.

Ultra capacitors are definitely very expensive for EV application, and another problem is that they are available in very low voltage rating. A large number of them can be connected in series and placed directly across the battery for load levelling. Or else, low voltage capacitor bank can be interfaced through a dc-dc converter at additional cost , loss of reliability and poorer efficiency.

6.4. Superconducting Magnetic Energy Storage (SMES)

In principle, the energy for EV propulsion can also be stored in inductive coil in the form of magnetic energy. The current in the coil can be initially established from utility system through a converter. The magnetic energy can be used to accelerate the vehicle, and then be recovered during deceleration. The power loss in ordinary wire at room temperature will make the system very bulky and inefficient. If the coil is placed

Table 4 : Ultracapacitor Technology Status

Name	Electrode Material	Wh/Kg	Wh/L	W/Kg (pk)	Cost	Voltage	Basis for Projection
Panasonc	Carbon	2.2	2.9	400	Low	3 V	Lab tests
Pinnacle Research	Maxed Oxides (Ru, Ta)	0.8	3	2,000	High	1 V	Lab Testing
Insitiute	Mixed Oxides Advance Design	2-3	10	>500	Med	—	projections
Maxwell/ Auburn	Carbon/Metal Aqueous	1.2	2	800	Med	1 V	Lab Tests
	Carbon/Metal Organic	7	9	2,000	Med	3 V	Lab Tests
Livermore Nat'l Lab	Aerogel Carbon Particulate	1	1.5	—	Med	1 V	Lab Tests
Sandia Nat'l Lab	Synthetic, activated carbon	1.4	1.7	1,000	Med	1 V	Lab Tests
Los Alamos Nat'l Lab	Conducting polymer on carbon	10	—	>500	Low	—	Projections
Federal Fabrics	Carbon	20	—	>500	Low	—	Projections

28

Table 5 : Rigone Plot for Ultracapacitors and Batteries
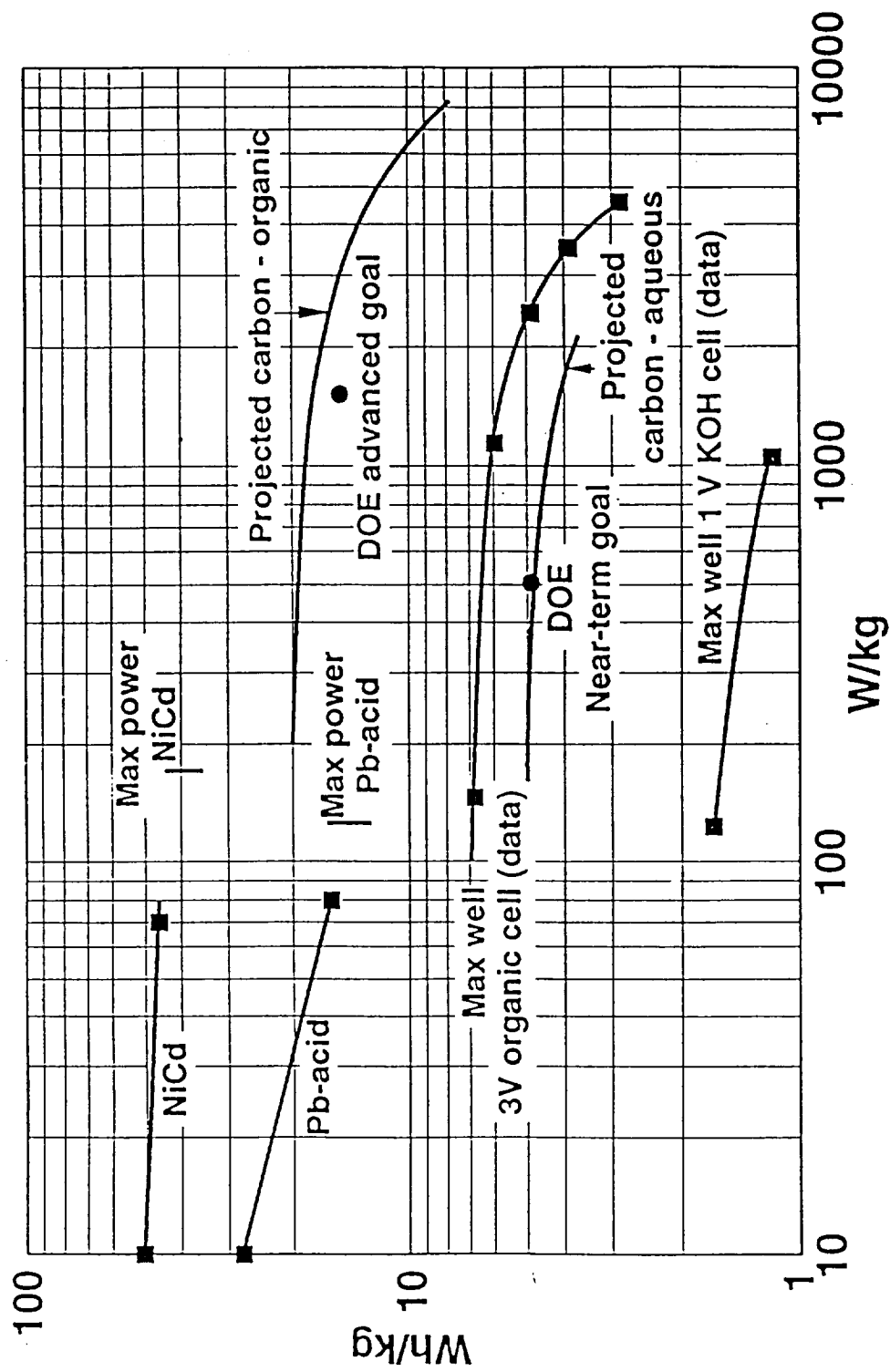
in superconducting environment (cryogenic cooling) , the metal resistivity tends to be zero , and such a system tends to be very efficient although at a high cost. The SMES system has been considered for utility system energy storage, cooling of synchronous machine field winding and other applications, but such a storage system will be prohitively expensive for EV application. Of course, high tenperature superconductivity offers some promise in the future.

6.5. Comparison of Energy Storage Devices

Table 6 gives the approximate comparison among the energy storage devices. Since SMES system is yet very expensive, it is excluded from the table. Again, lead acid battery has been considered as the basis for comparison. As discussed before, a hybrid system, such as battery/flywheel or battery/ultra capacitor can be used combining the advantages of both although at a higher cost. From the table, it can be concluded that battery remains as the viable energy storage device in the foreseeable future.

Table 6: Comparison of Energy Storage Devices *

	Battery	FW	UC
Specific Energy (pu)	1	0.125	0.1
Specific Power(pu)	1	3	20
Cost(pu)	1	1.2	2
Availability	Good	Medium	not good
Safety	Good	not good	Good
Maintenance	Good	Medium	Very Good
Cycle Life	Limited	Large	Very Large
Charge/Discharge	Good	Moderate	Very Good
Comments	Available technology	Available technology	Needs R&D

* Numerical comparison should not be taken seriously

7. Power Sources

As mentioned before, the installation of a power source along with the energy storage source not only increases the range of HEV but also improves the gradeability and acceleration capability at high speed. The important criteria of power source selection are fuel economy, emission characteristics, specific power, and cost. Two

possible power sources, i.e., engine or fuel cell can be used although the former has been traditionally preferred. Fig. 4 gives the tree of heat engines. Both continuous-combustion and intermittent-combustion engines can be used, and in both categories, combustion may occur either internal or external to the engine. The Stirling-cycle engine, which has existed since the early 1800s, is a continuous-external-combustion engine that uses a gaseous working fluid. The leading continuous-internal-combustion candidate is based on the Brayton cycle. The most important option in this engine class is the non-reciprocating version, the gas turbine. The intermittent internal combustion engine requires periodic ignition which may be accomplished either spontaneously, as a result of compression of the charge or by electrical spark. The ignition in this type engine may be effected in either a homogeneous or a stratified charge of fuel and air. The compression-ignited stratified-charge engine is recognized as diesel engine. On the other hand, spark-ignited homogeneous and stratified charges constitute viable possibilities for the automobile. A brief description of the viable engine types are given below.

7.1. IC Engine

The spark-ignition internal combustion engine (commonly known as IC engine) has long been known as the traditional power source for the general gasoline-powered vehicle. Since its invention in late nineteenth century and the subsequent invention of electric self-starter in the early part of this century, the engine has gone through
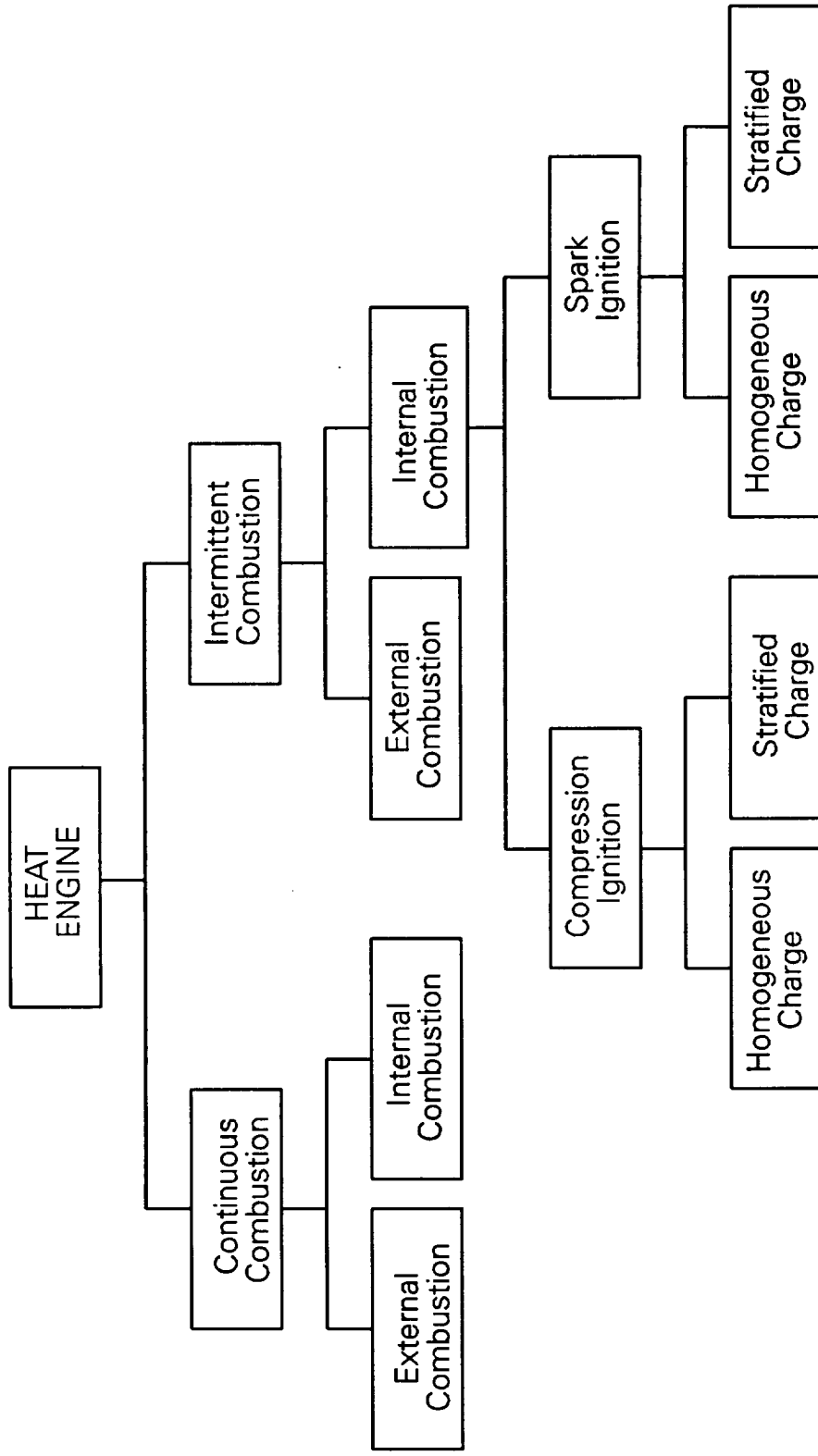
FIG. 4: HEAT ENGINE TREE

33

evolutionary improvement over a long period of time. Modern turbo-charged engine has smaller size and higher efficiency which is improved further by microprocessor-controlled fuel injection. It is possibly the best candidate for HEV power source, and will remain so in the early part of the next century.

Fig. 5 shows the typical characteristics [59] of a four-stroke IC engine where the constant efficiency contours are given in the plane of normalized mean effective pressure (related to engine output torque) vs. engine shaft speed. These contours are specified in terms of brake specific fuel consumption (BSFC) with units of grams of fuel per kWh of delivered energy. Using the heat content of gasoline as 33.2 kWh/g, the percentage efficiency values are calculated and noted on these contours. The heavy line contours indicate the effect of five-speed transmission (not usually valid in HEV). Also shown are the hyperbolae of constant engine power with normalized power levels of 1 to 36. An optimal efficiency locus spanning the range of engine power is shown by the dashed contour FGCDE. The highest efficiency (30%) is obtained at the point D where BSFC = 274 g/kWh. In a normal vehicle operation, the engine speed varies widely and because of the wastage of braking power the total efficiency hardly exceeds 15% (see Fig. 1). In a parallel hybrid system, the engine also runs at variable speed but the braking energy is recovered in the battery. However, in a series hybrid system, the engine speed can be independently controlled for any power demand, and therefore, optimum efficiency locus can be achieved.

34
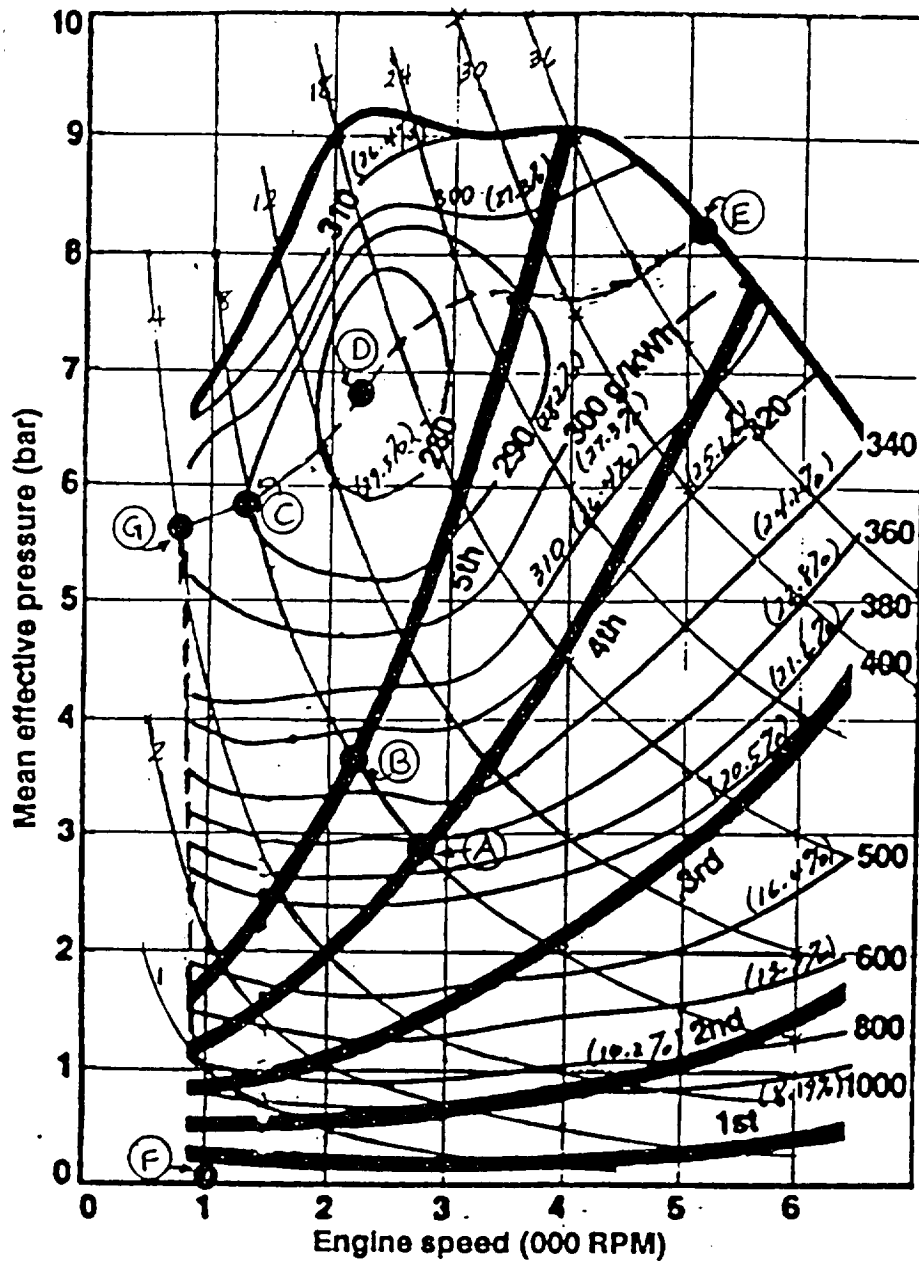
**FIG. 5: TYPICAL CHARACTERISTICS OF
FOUR-STROKE IC ENGINE**

The use of un-leaded gasoline and catalytic converter in the tail pipe have significantly reduced emission characteristics of IC vehicles. The typical emission (gms/mile) of a mid-size automobile can be given as 0.20/0.63/3.43/0.35 (SO_2/NO_x/CO/HC) whereas the PNGV goals are respectively 0/0.20/1.70/0.125. Instead of gasoline, some alternative fuels, such as methanol, ethanol and CNG can give different fuel economy and emission characteristics . Some typical parameters of commercial IC engines can be summarized in Table 7 (supplied by Ford). These parameters can be scaled appropriately for HEV.

Table 7: Typical IC Engine Parameters

Engine Rating (L, P @ N)	Shipped Weight (kg)	Wt. Specific Power (kW/kg)	Vol. Specific Power (kW/L)
5.0, 112, 3200 (V8)	260	0.43	22
2.5, 112, 5800 (V6)	175	0.64	45
1.8, 93, 6200 (V4)	130	0.73	52

L = Displacement in L, P = Power in kW, N = RPM @ rated power

It has been shown that advanced engines which show good fuel economy are lean burn in nature, as indicated in Fig. 6 [36]. This means that excess oxygen in the fuel-air mixture promotes more complete combustion. As a result, it reduces emission of HC and CO but increases NO_x. Various evolutionary and proposed revolutionary adaptions of lean burn engines hold great future promise relative to meeting fuel economy targets, while achieving success in areas, such as cost effectiveness, manufacturability, customer acceptance, overall performance and emissions. Lean burn engines which offer potential for significant fuel gains are: (1) spark-ignited, direct fuel injected, stratified-charge engines and (2) direct fuel injected diesel engines. A number of research versions of both of these engine types have been demonstrated by various government and commercial agencies but no production prototypes have yet demonstrated the efficiency and emission targets of PNGV. Projected advances in emission after-treatment for lean burn engines will further improve the PNGV emission goals.

7.2. Diesel Engine

Diesel engine is also a candidate for HEV drive. It has a superior fuel economy (about 13% advantage) over the gasoline ICE because of the greater energy content of a gallon of diesel fuel compared to gasoline. The diffusion combustion of its fuel spray avoids the knock problem accompanying the premixed combustion of the traditional spark-ignition ICE, so the diesel is free to use a higher compression ratio. Again, diffusion combustion allows load to be controlled by varying the overall fuel-air ratio in

37
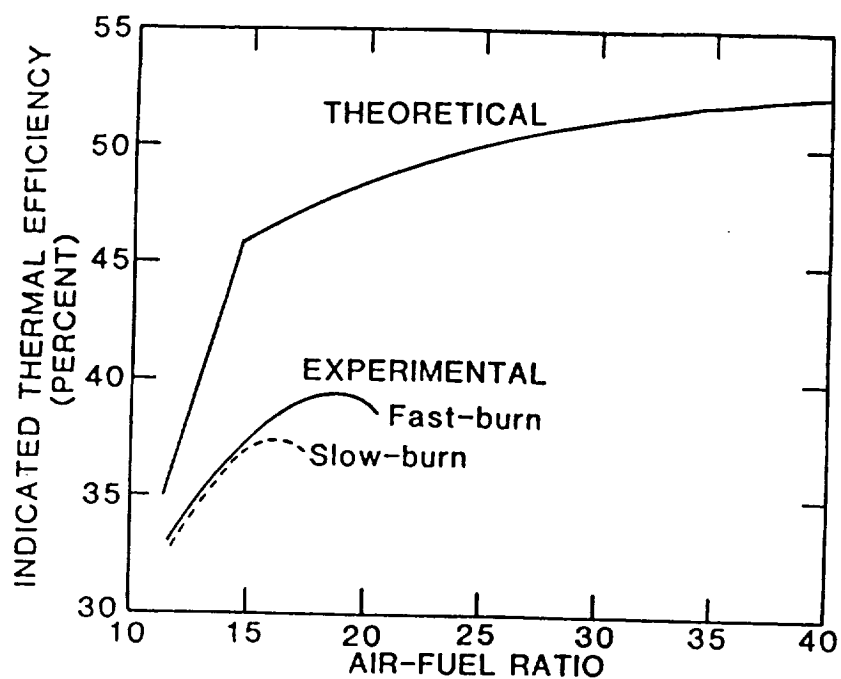
FIG. 6: EFFECT OF AIR-FUEL RATIO ON THERMAL EFFICIENCY
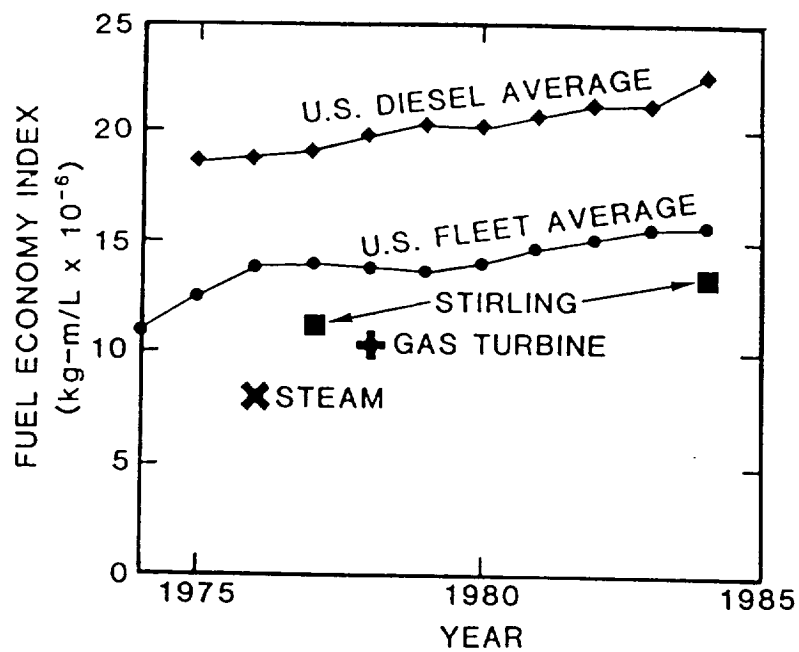
FIG. 7: FUEL ECONOMY INDEX FOR VARIOUS ENGINE TYPES

the cyclinder, thus avoiding the part-load pumping loss of the traditional spark-ignition ICE during the intake stroke.

The diesel automobile first appeared in the market about 50 years ago. More popular in Europe than in the USA, its market penetration in USA peaked at 6% in 1981, and now less than 1%. Half of the dozen companies that once built diesel cars for the U.S. market has dropped out. There are a variety of reasons behind the disaffection of the U.S. consumer for the diesel car. Among them are the decline in fuel prices, which had once been projected to be two to three times their current level, imposition of extra tax on diesel fuel by the U.S.government, higher first cost of diesel car, higher noise level and exhaust odor and fumes associated with today's diesel engine. Despite such shortcomings, the diesel remains the most fuel-efficient engine known that is suitable for passenger-car propulsion. Faced with the long range grim prospects for petrolium, it is difficult to ignore this engine until a more efficient alternative is identified.

The diesel continues strong in the heavy-duty truck market. It has also found a niche market in light- and medium-duty trucks and vans some of which are used in personal transportation. The most challenging emission regulations for diesel have been those for NO_x and particulate matter.

7.3. Stirling Engine

A Stirling engine receives heat at elevated temperature from an external source and converts a fraction to work rejecting the remainder at a low temperature. Stirling engine has many advantageous characteristics. These include silent operation, low exhaust emission levels, superior fuel economy at steady state, the ability to operate on any liquid fuel (gasoline, diesel oil, kerosine, propane or methane), low cyclic torque variation, and a flat part-load characteristics similar to that of a diesel engine. It is conceivable they could be used in automobile. In fact, during the past decade or more, several cars, trucks and buses with Stirling engine propulsion have effectively demonstrated their capability. Nevertheless, despite such favourable factors, it is difficult to believe that Stirling engine will ever be preferred in automobiles in competition with IC engines. They are expensive, have large warm-up time and have poor performance in urban driving cycle. Excessive manufacturing cost also remains a barrier for consumer acceptance.

7.4. Gas Turbine

Gas turbines of large capacity have been traditionally used in central power stations, and continued research over the period of last two decades has greatly improved their performance. The regenerative gas turbine in a smaller scale model is a desirable candidate for HEV because it is free of noise and vibration associated with intermittent combustion and reciprocating pistons, it can be made small and light, and it normally has an excellent torque-curve shape for road-vehicle use. In a laboratory

setting, it has demonstrated low emission level (0.41/3.4/0.4 g/mile HC/CO/NO$_x$ at low mileage. A particular advantage of gas turbine is that variety of fuels, such as diesel oil, natural gas, gasoline or methanol can be used. The single point in fuel economy index of Fig. 7 [36] from a turbine-powered car built by Chrysler for DOE compares very unfavourably with other types of engines. The thermal efficiency of gas turbine increases with inlet temperature, regenerator effectiveness, and other component efficiencies. It has now been established that automotive gas turbine has to incorporate structural ceramics in its hot parts, including the highly stressed turbine rotor. This is expected to permit raising inlet temperature from today's level of around 1050 deg.C with high temperature metal alloys to as much as 1350 deg.C. Government programs have made progress in making ceramic gas turbine components technically viable, especially in the difficult area of improving the strength and reliability made of high temperature structural ceramic materials. Several of these critical high temperature ceramic components have been fabricated and successfully rig-tested in a research setting.

The gas turbine regenerator reduces the fuel required to reach a specified turbine inlet temperature. At the same time, it cools the engine exhaust gas and helps to contain the noise emanating from the turbine exhaust. Again, unfortunately, the efficiency of compressor and turbine are sensitive to size. As ceramics permit higher turbine inlet temperature, the engine airflow requirement for a specified power rating decreases. This causes additional problem of improving upon established efficiency levels when engine rated power is decreased to match the HEV drive requirement.

Nearly all automotive gas turbines demonstrated to date have been of the free-shaft type in which a compressor and a turbine mounted on a common shaft serve as a gasifier to feed a supply of compressed hot gas to a downstream power turbine.

A HEV with a free-shaft gas turbine can operate at single speed on-off mode contributing to the best performance of the engine. It is interesting to note that recently AB Volvo of Sweden has announced its Environmental Concept Car (ECC) [54] which is a hybrid using gas turbine power source. The 20 kW, 100,000 rpm turbine uses nickel alloy in the combustion chamber and is fuelled by diesel oil.

7.5. Fuel Cell

Fuel cell is a potential viable power source for HEV application and has been considered for use over a number of years. They are attractive because they convert fuel energy directly into electricity without the need for combustion (as in an engine), can achieve high efficiency (2 to 3 times better than gasoline engine), virtually gives no emission (100 to 1000 times less), inherently modular, no wear-and-tear due to rotating parts, and is noise-free.

The operating principle of fuel cell is shown in Fig. 8. Basically, it is a reverse process of electrolysis of water where water breaks down to hydrogen and oxygen gases with the help of electricity. The construction of a fuel cell is similar to a battery, except that it does not undergo a material change, and consequently, it operates as long as the

Hydrogen Fuel (H₂)

$H_2 \rightarrow 2H^+ + 2e$

Electrode

Electrolyte

$2H^+$

Electrode

$\frac{1}{2} O_2 + 2H^+ + 2e \rightarrow H_2O$

Anode (-)

Cathode (+)

$2e \rightarrow$

$\leftarrow 2e$

V_L

V_{Cell}

V_{FC}

Electrical Load

Fuel Cell Auxiliary Loads

Reaction for a Phosphoric Acid Electrolyte

Air (O₂ and N₂)
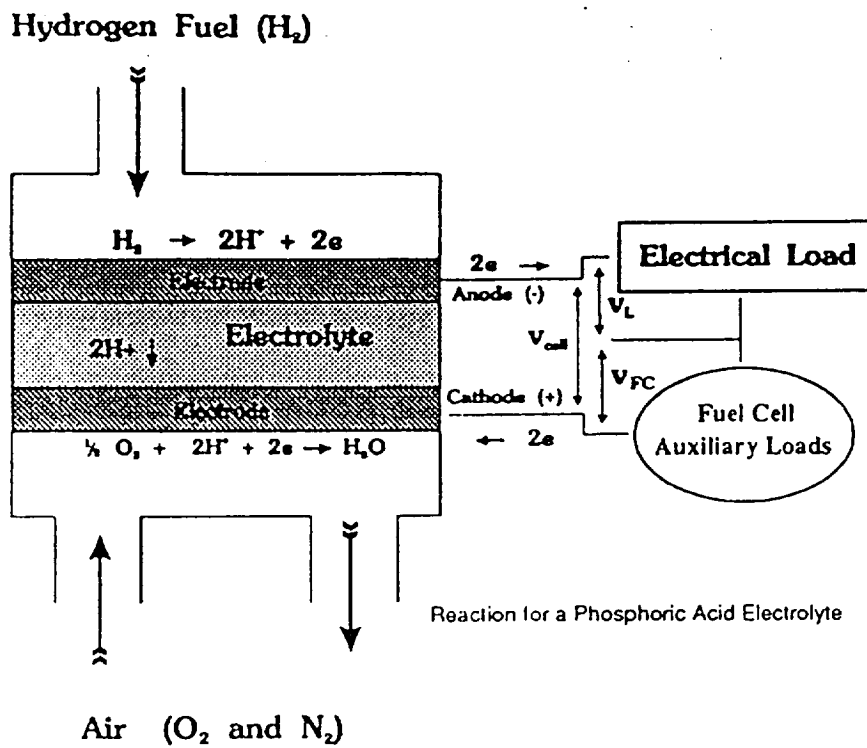
FIG.8: OPERATING PRINCIPLE OF FUEL CELL
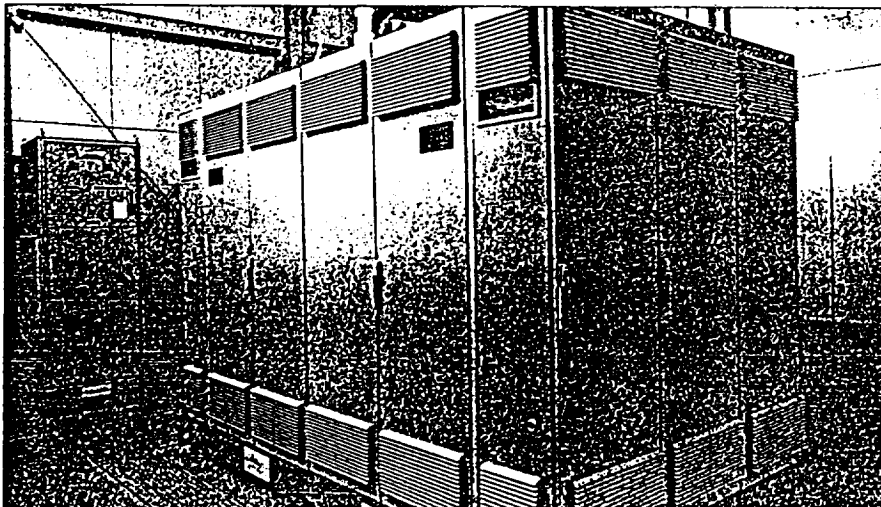
FIG. 9: 20 KW SOFC UNITS IN KANSAI ELECTRIC
POWER CO.

fuel is available. The hydrogen and oxygen gases in fuel cell are supplied externally and they react through electrolyte. First, the electrons are separated from the hydrogen molecules by a catalist (reduction) creating hydrogen ions (no electrons). The ions then pass through the electrolyte to the oxygen side. The electrons can not pass through the electrolyte and are forced to take an external electrical circuit which then leads to the oxygen side. When electrons reach the oxygen side, they combine with the hydrogen ion and oxygen creating water. Large amount of heat is generated as a result of the reaction that raises the cell temperature. The terminal dc voltage (like a battery) can be directly tied to the distribution bus or converted to ac through an inverter. The hydrogen can be stored as hydrogen-containing fuel, such as methane, methanol or ethanol which may be reformed to liberate hydrogen for fuel cell consumption. The oxygen can be supplied directly from air.

The theoritical efficiency in a hydrogen-oxygen fuel cell is 83%. Efficiencies of practical fuel cells using pure hydrogen and oxygen range from 50% to 65% based on lower heating value. The theoritical voltage of the hydrogen-oxygen cell operating at one atmosphere and 25 deg. C is 1.23 volts. Under electrical load, the cell voltage falls to 0.6 - 0.8 due to polarization effect. Therefore, multiple cells are connected in series in a fuel cell stack.

Fuel cells are classified on the basis of the electrolyte used in the cell. The technologies that are appropriate for application in HEV include phosphoric acid fuel

cell (PAFC), molten carbonate fuel cell (MCFC), solid oxide fuel cell (SOFC), proton excange fuel cell (PEMFC), direct methanol fuel cell (DMFC) and polymer electrolyte fuel cell (PEFC). Table 8 [47] summarizes the characteristics of some of the above fuel cells. The PAFC is possibly the more mature technology and is nearest to commercialization. They have been used in manned spacecraft program and tested in electric utility service, such as peak load-shaving and spinning reserve. Their auxiliaries are too complex to make them practical for transportation power.

Fuel cells are recently being used widely in low to medium size utility power plants in metropoliton areas where efficient energy conversion and low emission are essential. They have also been considered for urban transit buses, but today, they are too expensive (around $1000/kW) and bulky for automobile applications. Besides, their start-up time and transient response are very sluggish. Fig. 9 shows installation of two 20 kW SOFC units in Kansai Electric Power Co [50]. As mentioned before, a fuel cell power plant is definitely more efficient than that of an IC engine, but the estimate has shown that the payback period for fuel saving in an automobile would be 34 years. For cross-country tracks this figure is eight years whereas for locomotives and commercial buses it is four years.

Among the fuel cells, the PEMFCs have the potential to achieve the power density required for cars but R & D are required to reduce cost and optimize performance. Development of PEMFC systems for the next generation vehicle would

45

Table 8 : Projected Characteristics of Various Fuel Cell Types

Cell Type	Major Application Potential	Estimated Commercial	HHV[a] Effic. (%)	Cell Temp. (C)	Main Cell Materials	Emissions g/GJ NO_x	SO_x[b]	Ka/MWh CO_2
Phosphoric Acid (PAFC)	Dispersed Electric	1996	41(80)	200	Carbons	1.1	0	450
	On-Site Cogen.	1992-5	36-40(70)			1.1[c]	0[c]	510-460
Molton Carbonate (MCFC)	Dispersed Electric	1996-8	48-55	650	Steels	4.1	0	385-335
	On-Site Cogen.	1996-8	45(70)			4.1	0	410
	Central Power	2000+	>50			5.7	11.4	<645
Solid Oxide (SOFC)	On-Site Cogen.	2002	42(70)	1,000	Ceramics	2.6	0	440
	Central Power	2002+	45			14.2	34.0	715
Polymer (PEFC)	Vehicle	2000+	-	80	Polymers	-	-	-

(a) Fuel higher heating value to net ac electricity; cogeneration in parenthesis
(b) So_x based on 4 percent sulfer coal
(c) Measured

focus on the technical areas needed to minimize size and weight, reduce costs, improve overall system efficiency, increase response rate, and reduce start-up time.

The R & D activities in this area may include improved membrane development, advanced fuel cell stack designs, more efficient air compression systems, improved onboard hydrogen storage technology, compact-lightweight rapid-response fuel processors, and versatile water and thermal management. For SOFCs, development efforts will be focussed on reducing system operating temperature to more manageable levels. For DMFCs, which are based on modifications to conventional PEMFC or SOFC technologies, key aspects of the development program will be to increase power density and raise system efficiency to levels comparable with those of other fuel cells.

7.6. Comparison of Power Sources

Approximate comparison chart for different power sources is given in Table 9 where Stirling engine was excluded.

Table 9: Comparison of Power Sources *

	ICE	DE	GT	FC
Cost (pu)	1	1.2	1.3	2
Weight (pu)	1	1.2	1.1	2
Emission	medium	high	small	smaller
Availability	good	good	good	not good
Practicality	good	good	good	not good
Efficiency (pu)	1	1.2	1.3	1.8
Safety	good	good	medium	very good
Noise	medium	higher	medium	none
Control Complexity	medium	medium	high	small
Comments	Available technology	Available technology	Needs R &D	Needs R&D

* Numerical comparison should not be taken seriously

8. Drive Motor/Engine Generator

A hybrid vehicle drive system (see Fig. 1) requires a propulsion motor and a generator coupled to the engine power source (if engine is used). Practically, the same type of machine can be used as a motor and as a generator. The main requirements of

the motor are ruggedness, high torque-to-inertia, high peak torque capability, high speed operation, low noise, minimum maintenance, small size, ease of control, and above all, low cost with the control converter. The peak power rating of the motor is about 70 to 100 kW. While the motor runs at variable speed, the generator usually runs at constant speed for optimum efficiency of the engine. The main machine candidates are cage type induction motor, PM synchronous motor and switched reluctance motor. The separately excited dc motor has the advantages of low-cost converter, easy control, inherent stability and inherently fast transient response. However, the disadvantages are heavy and expensive machine, brush wear, lower speed range, commutator noise and continuous maintenance requirement. The dc machine has been traditionally the strong candidate from the beginning, but low power electronics cost and high performance control development in the recent years are favouring ac machines.

8.1. Induction Motor

Induction motor has been traditionally the workhorse for industrial drives, and is possibly the best candidate for EV/HEV application. The machine is very rugged, has very high speed capability (may be up to 15,000 rpm), and the size is considerably small compared to dc motor. There are no brushes and commutators, and therefore, no maintenance is required. The machine has high efficiency, reliability and is cheaper than other types of motor. It has nonlinear torque-speed characteristics, but with modern vector control, the characteristics are linear like a dc machine and gives dc

49

machine-like fast transient response. The machine has high peak torque capability (because of large thermal time constant), and operation can easily be extended to high speed field-weakening region. At low speed high torque operation , the machine requires forced cooling like other machines.

8.2. PM Synchronous Motor

The PM synchronous motor does not need any brushes and slip rings like wound-field machine, and thus reliability is high. Using modern high energy density neodymium-iron-boron magnet, the machine has higher power density and thus lower weight compared to other types of motors. The PM machine has no rotor loss (unlike induction motor) , and therefore, the efficiency is higher and cooling is somewhat simplified. Since the flux is constant, the motor efficiency tends to be poor at light load. With high stator current in fault mode, there is the possibility of rotor magnet demagnetization. The PM machines can be classified as surface magnet type and interior magnet type. The former is again categorized as trapezoidal and sinusoidal machines. The surface magnet machines operate at constant flux and field-weakening operation is not possible whereas the interior magnet machine permits field-weakening operation but efficiency is sacrificed because of large leading power factor current. The trapezoidal machine has somewhat higher power density (15%). All PM machines can be operated in dc machine (decoupled) mode giving high transient response. The PM

machines have been used in a number of EV projects.

The synchronous reluctance motor is similar to PM machine but does not have magnet in the rotor. Recently, there has been a lot of improvement in this class of machine, but it can not be considered viable for EV application.

8.3. Switched Reluctance Motor

The interest in switched reluctance motors (SRM) has revived recently and the published papers in the literature is abounding in this area. It has been considered for EV applications. The motor is very simple in construction, rugged, and can operate in high speed (in excess of 15,000 rpm). The machine is claimed to have comparable efficiency and power-to-weight ratio with induction motor. However, the machine has pulsating torque and acoustic noise problems.

8.4. Comparison of Machines

Table 10 [66] gives the typical of comparison characteristics of induction, PM synchronous and switched reluctance motors. The dc machine is not a viable candidate but it is included in the table because people are generally familiar with dc machine for speed control applications. Synchronous reluctance and interior PM machines are not

Table 10: Comparison of Motor Characteristics

	DC Brush Type	Induction	Brushless (PM)	Switched Reluctance
Peak Efficiency (%)	85 - 89	94 - 95	95 - 97	<90
Eff.@ 10% load (%)	80 - 87	90 - 92	79 - 85	78 - 86
Max. RPM	4,000 - 6,000	9,000 - 15,000	4,000 - 10,000	>15,000
Cost/Peak Shaft Kw ($/Kw)	10	8 - 12	10 - 15	6 - 10
Relative cost of control electronics	1.0	3.5	2.5	4.5
Ruggedness	Good	Excellent	Good	Good
Reliability	Fair	Excellent	Good	Good

included in the table. Considering all the characteristics, induction motor seems to be the best choice.

9. Converter

A converter usually interfaces the propulsion motor and the engine generator as indicated in Fig. 1. The propulsion motor converter takes the input supply (ac or dc) and converts it to variable frequency variable voltage (or current) supply for the ac machine. Variable frequency supply permits variable speed operation of the machine whereas variable voltage proportional to frequency permits rated flux operation that permits fast transient response of the machine. Of course, at light-load steady state operation (steady state cruising) , the machine flux can be programmed for improvement of efficiency. The converter should be capable for four-quadrant operation of the machine, i.e., motoring and braking regeneration in both forward and reverse directions. The converter generates symmetrical three-phase machine voltage by PWM (pulsewidth modulation). The converter efficiency is determined by its conduction and switching losses. At high switching frequency , converter loss increases but the machine loss decreases because the leakage inductance (acting as lowpass filter) decreases the harmonic copper loss, and thus improving the machine efficiency. The converter-machine system is to be designed optimally for efficiency, reliability and cost.

What is the best power semiconductor device for the converter? In the HEV

53

power range, IGBT appears to be the best device although MCT (MOS-controlled thyristor) is a potential candidate. The scenario for IGBT and MCT are summarized in Tables 11 and 12, respectively. Both the devices are MOS-gated, but IGBT is a mature device with high voltage and current capability, high switching frequency and square safe operating area (SOA). The square SOA permits the converter to operate without snubber. However, IGBT has a higher conduction drop (2.5 V) which is possibly its only disadvantage. In contrast, commercially available MCT has lower rating , but its conduction drop is low. The non-square SOA of the device requires snubber except the soft-switched device which will be discussed later. Future MCT, based on N-type material is expected to be introduced with improved SOA and higher voltage and current capability. All the present power semiconductors are based on silicon material. Future power devices based on new type of material, such as silicon carbide and diamond show the prospect of low conduction drop, high switching frequency and high temperature operation will have large impact on the converter technology.

10. Candidate Distribution Systems

In this section, several candidate distribution systems based on the possible energy storage and power sources will be identified and their merits and demerits will be discussed qualitatively. The features become obvious because they are dictated by the characteristics of the power and energy sources. The SMES, diesel and Stirling engines will be excluded although the possibility of diesel should not be ruled out. The induction

54

IGBT SCENARIO

. FAST EVOLUTION SINCE INTRODUCTION
   IN 1983

. SIMPLE STRUCTURE - SIMPLE PROCESSING

. "SMART POWER" CAPABILITY

. SQUARE SOA - ADVANTAGE OF SNUBBERLESS
   OPERATION

. APPROACHING LOWER ON-VOLTAGE, FASTER
   RISE AND FALL TIMES

. STATE-OF-THE-ART HIGH POWER DEVICE
   - 2000 V, 325 A

. STATE-OF-THE-ART HIGH POWER INTELLIGENT
   CONVERTER MODULE - 1200 V, 600 A

. APPROACHING 1 MW POWER LEVEL USING
   3-LEVEL CONVERTER

MCT SCENARIO

. VERY SLOW EVOLUTION SINCE INTRODUCTION
   IN 1988

. COMMERCIALLY INTRODUCED BY HARRIS
   IN 1992

. VERY COMPLEX STRUCTURE - COMPLEX
   PROCESSING (POOR YIELD)

. HARRIS DEVICE SPECS. (MCTV75P60E-1)
   P - TYPE

   -600 V, 75 A
   CONDUCTION DROP = -1.3 V
   JN. TEMPERATURE   = -55 °C TO 150 °C
   SURGE CURRENT   = 2000 A
        DI/DT   = 2000 A/ μS

. NON-SQUARE SOA - NEEDS SNUBBER

. "SMART POWER" CAPABILITY - NOT AVAILABLE

. IMPROVED FEATURES OF N-MCT

machine will be assumed in all cases for both the drive motor and engine-generator. All the candidate distribution systems are derived from Fig. 2.

10.1. IC Engine - Battery DC/HFAC Distribution

This system is described later in detail in Figs. 10 and 13. In near term (next 10 years), this appears to be the most viable system.

10.2. IC Engine - Ultra Capacitor DC/HFAC Distribution

The topology of the system is same as above except the battery is replaced by the ultra capacitor. The UC has the advantage of large power capability but the energy capability is poor compared to battery. At present state of technology, it is very expensive. The UC can also be placed in parallel with the battery to enhance the battery power capability.

10.3. Gas Turbine - Battery DC/HFAC Distribution

The distribution system remains same as before except the IC engine is replaced by the gas turbine. The gas turbine should operate at high speed, and therefore, a speed reduction gear is necessary for the generator-converter system. Although turbine is

lighter and generates less noise, the gear adds weight, noise and additional power loss. The efficiency is less than IC engine. High efficiency turbine development based on structural ceramics will take long time. The system is expensive and efficiency is poor.

10.4. Gas Turbine - Ultra Capacitor DC/HFAC Distribution

The topology is the same as above but obviously it is a very expensive system.

10.5. IC Engine - Flywheel DC/HFAC Distribution

The flywheel is coupled to a generator/motor to convert mechanical energy into electrical energy which is further coupled to the distribution system through a converter. For a high speed flywheel, a reduction gear is needed. For a dc distribution system, a synchronous machine - load commutated inverter or induction machine - PWM voltage-fed inverter can be used. For HFAC system, ac -ac frequency changer (described later) should be used. The system cost is high but the life cycle cost may be low because of long service life of flywheel.

10.6. Gas Turbine - Flywheel DC/HFAC Distribution

Both gas turbine and flywheel require generator - converter system and the

58

system is definitely expensive.

10.7. Fuel Cell - Battery DC/HFAC Distribution

The fuel cell can be directly connected to the bus like battery in a dc system but requires inverter for HFAC system. The system has high efficiency, low emission and is noise free, but it is bulky and expensive.

10.8. Fuel Cell - Ultra Capacitor DC/HFAC Distribution

The system is more bulky and expensive than above.

10.9. Fuel Cell - Flywheel DC/HFAC Distribution

The system is bulky and expensive.

10.10. General Comparison and Selection of Candidate System

Table 13 gives the general comparison of the candidate systems

Table 13: General Comparison of Candidate systems *

	ICE-Battery	ICE-UC	GT-Battery	GT-UC
Cost (pu)	1	1.5	1.3	1.8
Weight (pu)	1	1.5	1.1	1.6
Emission	medium	medium	small	small
Availability	good	not good	good	not good
Practicality	good	not good	good	not good
Efficiency (pu)	1	1.05	0.8	0.85
Safety	good	good	medium	medium
Noise	medium	medium	medium	good
Control Complexity	medium	medium	high	high
EV Range (pu)	1	0.7	1	0.7
Total Range (pu)	1	1	1.1	1.1
Comments	Available technology	Needs R&D	Needs R&D	Needs R&D

ICE-FW	GT-FW	FC-Battery	FC-UC	FC-FW
1.2	1.5	2	2.5	2.2
0.8	0.9	2	2.5	2.2
medium	small	small	small	small
good	good	not good	not good	not good
good	good	not good	not good	not good

0.8	0.7	1.2	1.25	0.9
not good	not good	good	good	not good
medium	medium	none	none	medium
high	high	small	small	medium
0.7	0.7	1	0.7	0.7
1	1.1	1.1	1.1	1.1
Available technology	Needs R &D	Needs R&D	Needs R &D	Needs R&D

* Numerical figures in the table should not be taken seriously where right technology is not available.

From overall comparison in the table, it appers that ICE - Battery system is the best for near-term HEV application.

11. DC vs. HFAC Distribution

The power supply distribution system in HEV interconnecting the energy storage source, power source and the propulsion motor can be based on dc, biased HFAC, or HFAC. The HFAC again can be based on single-phase or polyphase (two or three phase). Whatever the case may be, the system should be optimally designed for cost and performance considering the characteristics of the system components. Fortunately, in HEV system (unlike that of space power distribution system), the components are in close proximity. Therefore, modular design with minimum lead length is

most desirable.

11.1. DC Distribution

DC distribution is traditionally preferred for EV/HEV application, and a typical system for HEV is shown in Fig. 10. Here, the dc link is directly connected to the battery terminal. The engine power source is connected to the dc bus through a starter/generator and a converter. The dc supply is converted to variable frequency variable voltage ac through an IGBT inverter for the ac machine terminal. While the propulsion motor runs at variable speed in four-quadrant mode, the engine-generator can be operated at one speed (in fact, programmable speed is desirable as shown in Fig. 5) for optimal efficiency. The converter-machine operates only in two-quadrants (starter and generator) with one direction of rotation. The machine starts in motoring mode at zero speed for starter function, and as the speed reaches a threshold value, the engine starts and converts the machine to generating mode. In both of these modes, the machine gets excitation current from the converter. The voltage and frequency at the generator terminal are constant because of constant speed operation, but the torque will vary depending on the power demand. At light load steady state condition, the flux on both the machines can be programmed to optimize the efficiency.

The inverter output voltages are controlled by sinusoidal PWM technique. The most common method is to compare a high frequency triangular wave with three-
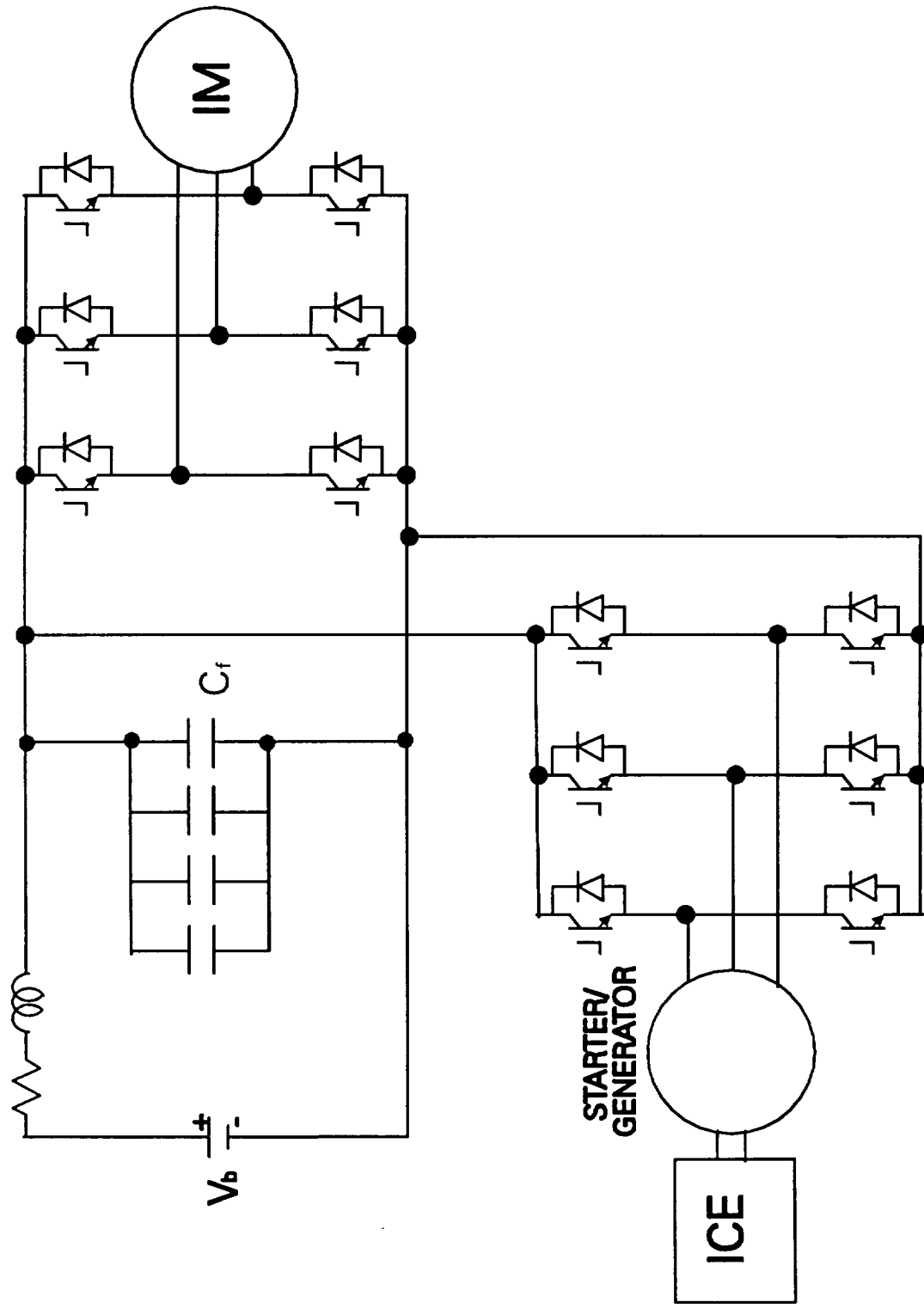
FIG. 10: DC PROPULSION POWER DISTRIBUTION SYSTEM

63

phase sinusoidal reference waveforms. At the intersection of sine and triangular waveforms, the devices in each phase of the inverter are switched to obtain the sinusoidal PWM (SPWM) pattern at the inverter output. The output voltage is varied by varying the amplitude of the reference signals, whereas the output frequency is varied by varying the frequency of the reference waveforms. The PWM voltage range can be extended by injecting triplen harmonic components in the reference wave. Recently, space vector PWM technique has been introduced which is very convenient to implement by digital and microprocessor based systems. The space vector approach gives not only better quality PWM wave than that of SPWM but the voltage magnitute is also increased by about 15%. Modern high speed IGBT can operate at switching frequency upto 20 kHz. The dc link voltage appears directly across the inverters, and the power devices are "hard-switched" in comparison to "soft-switching" which will be described later. In hard or stressed switching, the device handles the full voltage and current, and therefore, switching loss is high. A snubber can soften the rise and fall of these parameters, but overall loss may be higher. High switching loss decreases efficiency of the converter and increases loading on the cooling system. In fact, the switching frequency of a hard-switched converter is limited on the basis of converter loss.

A large electrolytic filter capacitor is connected at the battery terminal to bypass the harmonic currents generated by the converters. It has been shown that excessive harmonic current reduces the battery life by sulphation effect. Electrolytic capacitor is more economical than ac capacitor, but it is more lossy , operating temperature range

is low, and has less reliability and life. The size of the capacitor is large because it
is determined by harmonic current capability rather than filtering capability.

11.2. HFAC Distribution

Biased HFAC Distribution

A conventional dc distribution system, shown in Fig. 10, has a number
of disadvantages. The converters, as discussed before, use hard-switching technique,
i.e., the devices turn-on and turn-off with full voltage and current at the time of
switching. This causes high switching loss, and therefore, the efficiency of the
inverter is decreased to some extent. It also causes additional cooling burden on the
inverter. It should be noted here that the switching loss is highly influenced by the
reverse recovery current of the bypass diode on the opposite side of the phase-leg.
A low recovery current diode can considerably improve this loss. As discussed
before, this switching loss criteria essentially dictates the PWM switching frequency,
and an inverter of this power range (using modern high speed IGBT) can hardly use
more than 10 kHz switching frequency. With hard-switching, the switching stress on
the device is high that impairs its MTBF. Modern IGBT's are available with square
SOA (safe operating area) so that snubberless clamped voltage design is possible.
However, a snubber is desirable to relieve the switching stress (and loss) of a device
although   overall   switching   loss   may   increase

because of snubber dissipation. Energy recovery snubbers have been proposed (and used commercially) for high power converters at the expense of additional power circuit components.

A biased HFAC system can be defined as a soft-switched system where the converter devices experience unidirectional voltage. This can also be defined as resonant link dc (RLDC) system . Power flow directions in Fig. 2 for different modes of operation should be possible in RLDC system. The unidirectional or biased HFAC voltage has the advantage that a high frequency power device (IGBT, BJT, etc.) can easily withstand this voltage.

The concept of soft-switched high frequency link cycloconverter was originally demonstrated by Bose [12] . Divan [84] proposed the concept of RLDC converter in place of a conventional hard-switched inverer which caught wide interest of the technical community. In RLDC inverter, the dc voltage is converted to high frequency (50 - 60 kHz) unidirectional resonant pulses through a L-C resonant circuit. These voltage pulses cross zero periodically and permit zero voltage switching (ZVS) of the inverter switches. A power device turning on or off at zero voltage or zero current causes soft-switching. The advantages of such soft-switching inverter can be summarized as follows:

- Switching at zero voltage (or current) practically eliminates the switching loss.

This improves efficiency of the inverter.

- The devices no longer need any snubber, resulting less device count and improving reliability.

- Higher efficiency permits less need of cooling.

- Less heat dissipation permits integration of the inverter in less volume.

- The device switching stress is low improving its MTBF.

- The EMI problem is less because of soft rise and fall of PWM voltage pulses.

- Lower dv/dt and di/dt are beneficial for the device and machine load.

Since the invention of RLDC soft-switching principle, a large number of papers have been published suggesting many soft-switching techniques. One major problem in RLDC converter is that it has severe voltage penalty (3 to 4 times) on the devices. A passive clamping method that clamps the device voltage typically by a factor of 2.5 was proposed . Subsequently, active clamping technique was proposed to limit the voltage by a factor of 1.6. The author (Bose) [85] proposed a novel current initialization contro to improve on the clamped method. Later, a quasi-resonant RLDC scheme was also proposed by the author .

Fig. 11 shows a typical resonant link dc distribution system, and Fig. 12 shows the resonant link voltage and current waves in different modes. The active clamping with current initialization technique has been used in the circuit. The capacitor C_r charges to the battery dc voltage which is then converted to resonant voltage pulses
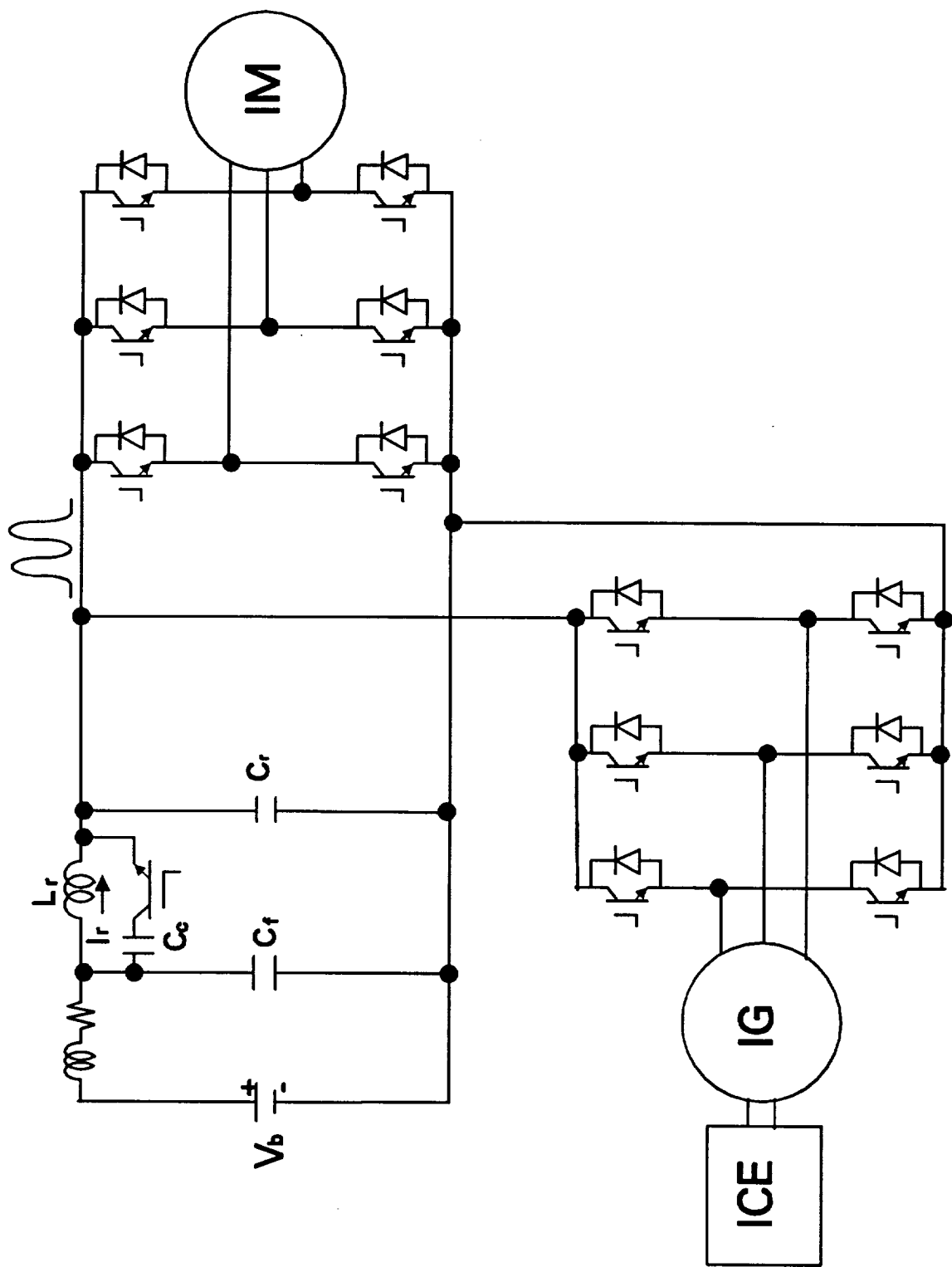
**FIG. 11: RESONANT LINK DC (BIASED AC)
DISTRIBUTION SYSTEM**

68
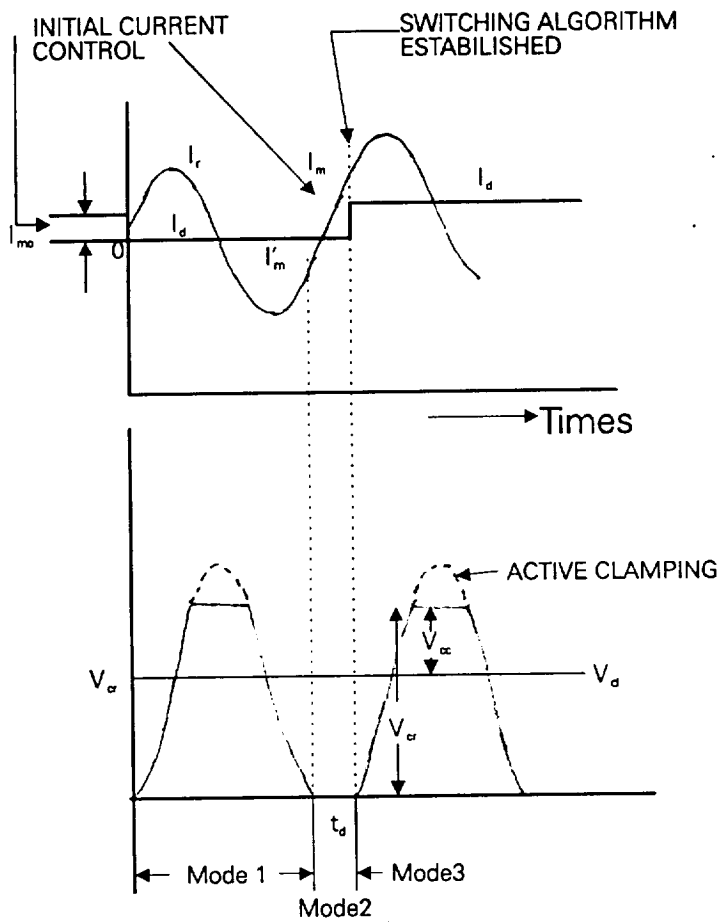
FIG. 12: RESONANT LINK VOLTAGE AND CURRENT WAVES IN DIFFERENT MODES

69

through the L_r - C_r resonant circuit, as shown . The programmable initial current I_m in the inductor is established by switching on the inverter devices. This will tend to raise the dc link voltage by a factor of 2. The capacitor C_c and the bypassed IGBT will actively clamp the link voltage typically by a factor of 1.6.

Although large number of resonant link, resonant pole and quasi-resonant converter schemes have been published in literature, the industry so far has not paid much attention to them. Inspite of the advantages of soft switching, the converters are to be overdesigned because of voltage penalty and additional components are required. The discrete nature of PWM method causes the machine harmonic current penalty higher. The clamping lengthens the resonant pulsewidth and causes the harmonic problem worse. Of course, higher resonance frequency can alleviate this problem. It is difficult to design the resonant circuit to handle high power at high frequency. The usual disadvantage of dc system , i.e., low machine voltage, also remains.

Single Phase / Polyphase Distribution

Single Phase Distribution

A single-phase HFAC distribution system which is most viable for HEV in near term is shown in Fig. 13. It uses a battery (possibly lead acid battery) as the energy
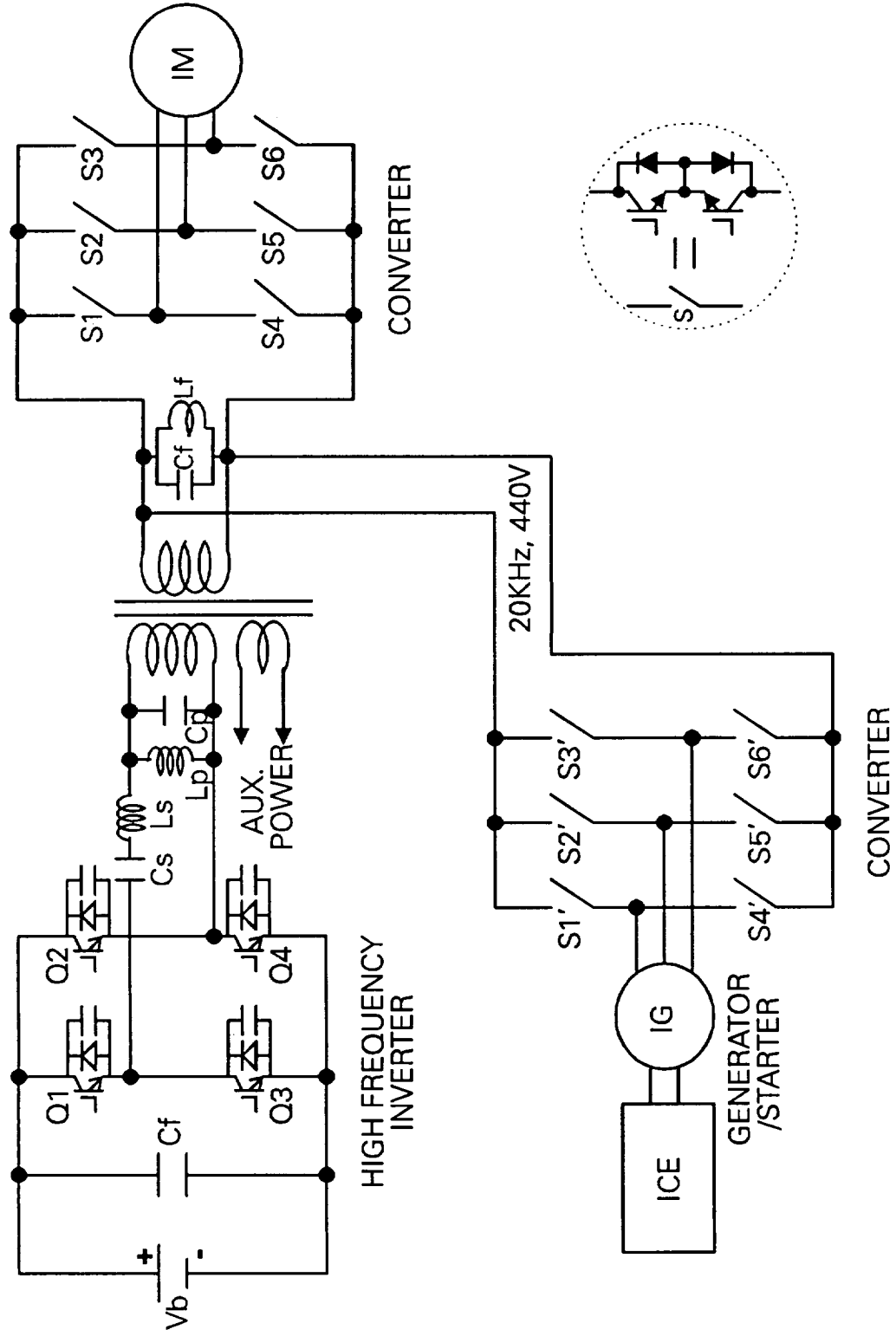
FIG. 13: SINGLE PHASE AC DISTRIBUTION SYSTEM

71

source and IC engine as the power source. Both the motor and the generator use the cage type induction machine due to its inherent advantages, and the power converters use IGBT switches. Tentatively, 20 kHz, 440 V HFAC distribution system (as considered for space application) will be assumed. This will be discussed later. The dc voltage of the battery is inverted to HFAC through a H-bridge resonant inverter. This type of inverter has the advantages that the output voltage is easily sinusoidal and the devices switch at zero voltage eliminating the switching loss. The inverter output voltage is boosted (and isolated) by a HF transformer, and then supplied to the converters which feed the drive motor and the generator, respectively. The resonant inverter selected in this application is called hybrid resonant type[16] because it contains both series and parallel resonant circuits. The inverter output should have good voltage regulation irrespective of battery voltage and loading, and its harmonic content should be minimal. A traditional series resonant converter (SRC) can provide output with low high frequency harmonics content when adequately loaded. It does not have circulating currents between the tank and the input source because the only current path goes through the output load. However, when the output current is reduced, the filtering of the high frequency harmonics decreases dramatically, i.e., at no load there is no attenuation. This characteristic makes the converter inadequate for application where the load varies from no load to full load. A parallel resonant converter (PRC) can be designed to provide good attenuation of high frequency harmonics from no load to full load. Since   the   output   is   in   parallel   with   the

resonant capacitor, the converter behaves like voltage source which can be designed with very low load sensitivity. However, the high attenuation of the harmonics and the load insensitivity require a design with significant circulating current through the resonant capacitor. The switches have to conduct the load current plus the current through the resonant capacitor. The hybrid converter combines good properties of both SRC and PRC inverters.

The inverter voltage is controlled by generating a quasi-square wave voltage at the input of the resonant circuit, as shown within the Fig. 14. This means that at the lowest battery voltage and maximum load the voltage wave is square wave whereas for the highest battery voltage and no load the wave has minimum pulsewidth (delta angle). Fig. 14 shows the fundamental and harmonic voltage components (odd) with different pulsewidth angle. Evidently, harmonic magnitudes worsen at reduced pulsewidth.

The converter for drive motor converts the HFAC voltage into variable voltage variable frequency supply for the drive motor. Since each switch has to withstand ac voltage and conduct in both directions, the equivalent ac switch configuration using inverse-series IGBTs are indicated in Fig. 13. This configuration is preferrable to inverse-parallel or diode-bridge with a single device. Integral ac switch is not yet available commercially, but will possibly find a market place when sufficient demand is established. The converter operates with zero voltage switching, and the resulting advantages were discussed in the previous section. The circuit can be defined as integral
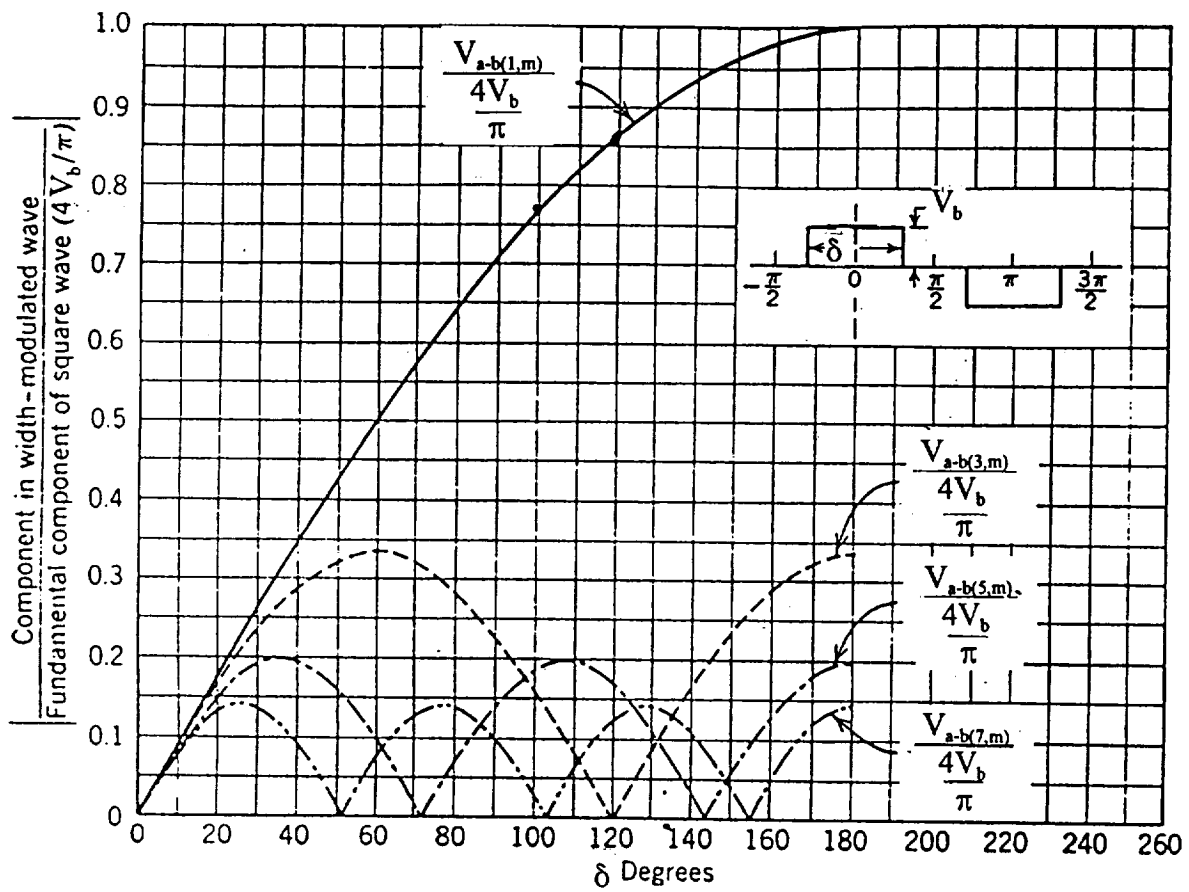
FIG. 14: RESONANT INVERTER OUTPUT
CHARACTERISTICS WITH DELTA ANGLE

half-cycle (IHC) converter [8] because the output PWM waves are synthesized by discrete half cycles basis. This type of PWM has the disadvantage that the output harmonic content is higher than that of dc fed system. Obviously, machine is to be designed with higher leakage inductance or the link frequency is to be higher for reasonably low harmonic current. IHC converter operation will be discussed further later.

The converter for the generator operates in similar mode except the fundamental voltage and frequency are constant on the generator. This is because the ICE/generator operates at constant speed but variable torque to generate variable power. A programmable speed control is also possible for further improvement of efficiency.

The HF transformer not only couples the converters for motor and generator but also supplies the auxiliary power need of the vehicle. This is a distinct advantage in HFAC system. The secondary voltage can be selected by appropriate turns ratio to directly supply the ac load or rectified to dc for dc type load. In either case, there are the advantages of higher efficiency and reduced size with HFAC supply. The transformer core is usually made of ferrite material but amorphous metal also shows future promise. Fig.15 shows the hysteresis loops for different materials indicating that amorphous metal will give significant size reduction compared to that of ferrite.
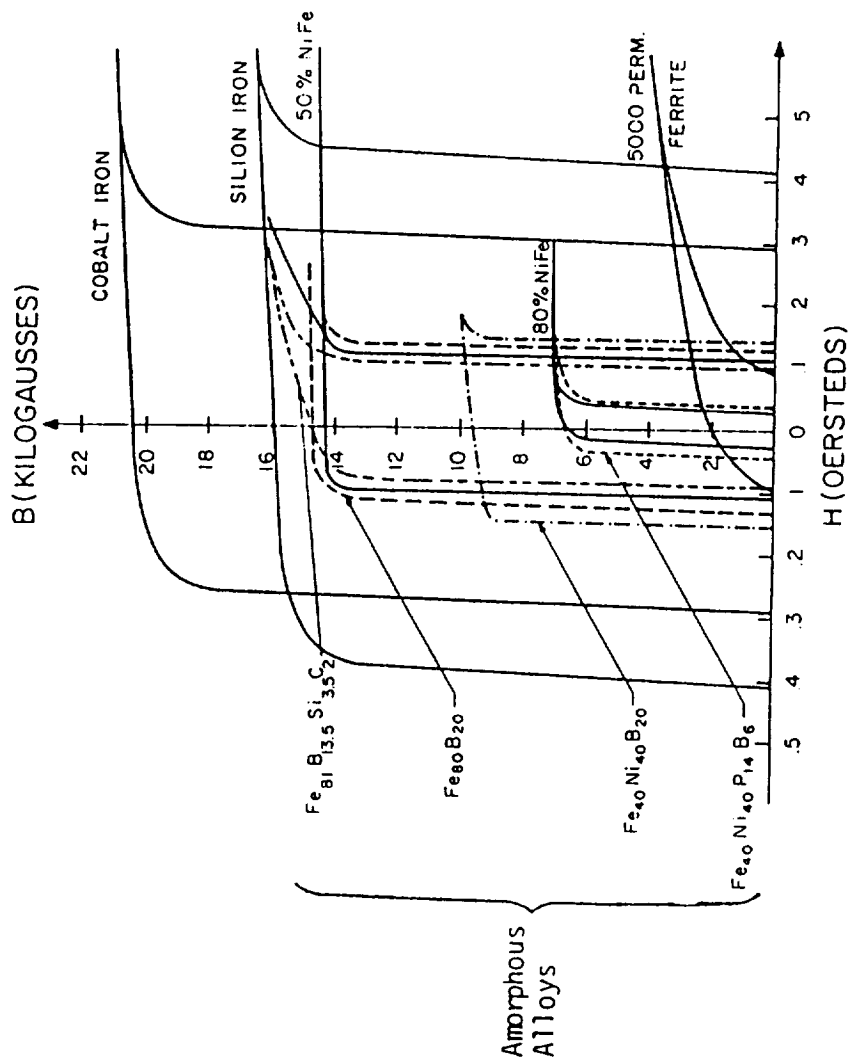
FIG. 15: HYSTERESIS LOOPS OF VARIOUS MAGNETIC MATERIALS

76

Polyphase Distribution

As an alternative to single phase system shown in Fig. 13, a possible two phase HFAC system is shown in Fig. 16. The dc voltage is inverted to two-phase ac with the help of two H-bridge inverters (resonance circuits are not shown for simplicity) operating independently. The independent 90 deg. phase-shifted sinusoidal voltages are controlled by pulsewidth modulation, as described before. The two-phase HFAC voltage is boosted by a transformer with the center point grounded, as shown. Both the machines (motor and generator) are wye-connected with grounding of the neutral point. The converters are same as in single phase system. Because of neutral grounding of the machines and the transformer, only phase voltage is impressed across each ac switch. However, neutral connection will cause significant triplen harmonic current loading of the machines and the converters. The system is definitely uneconomical compared to single-phase system.

A possible topology for three-phase HFAC system is shown in Fig. 17 . The three H-bridge resonant inverters generate three-phase HFAC, as shown. Three-phase HFAC is then converted to variable voltage variable frequency ac for the motor/generator terminal with the help of nine-switch (ac) matrix converter. The soft-switched matrix converter operating in this mode is not yet known in the literature. Anyway, the system is not worth of investigation because it appears so uneconomical compared to single-phase system. One advantage in a three-phase system is that active power flow tends
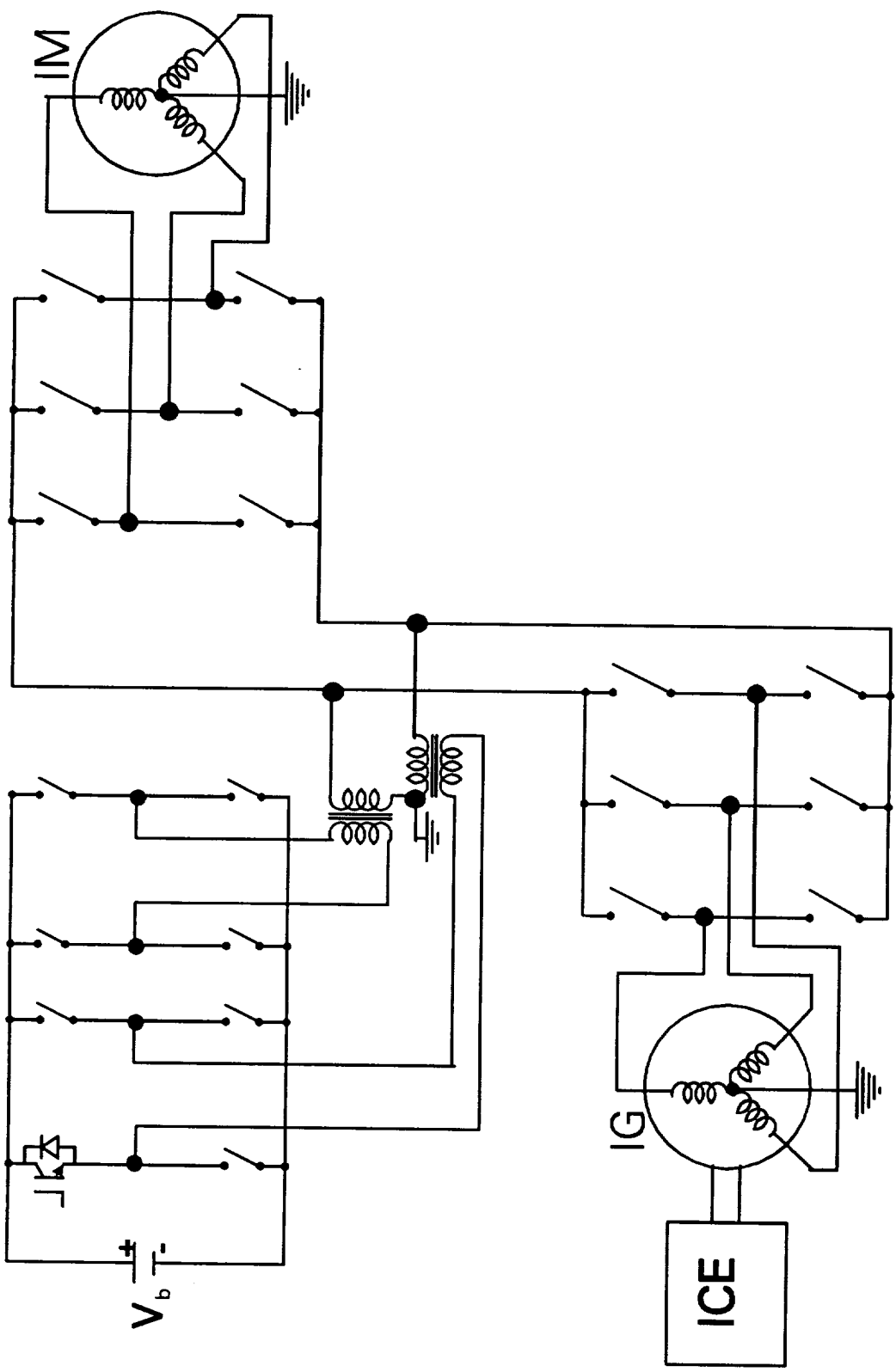
FIG. 16: TWO-PHASE AC DISTRIBUTION SYSTEM

78
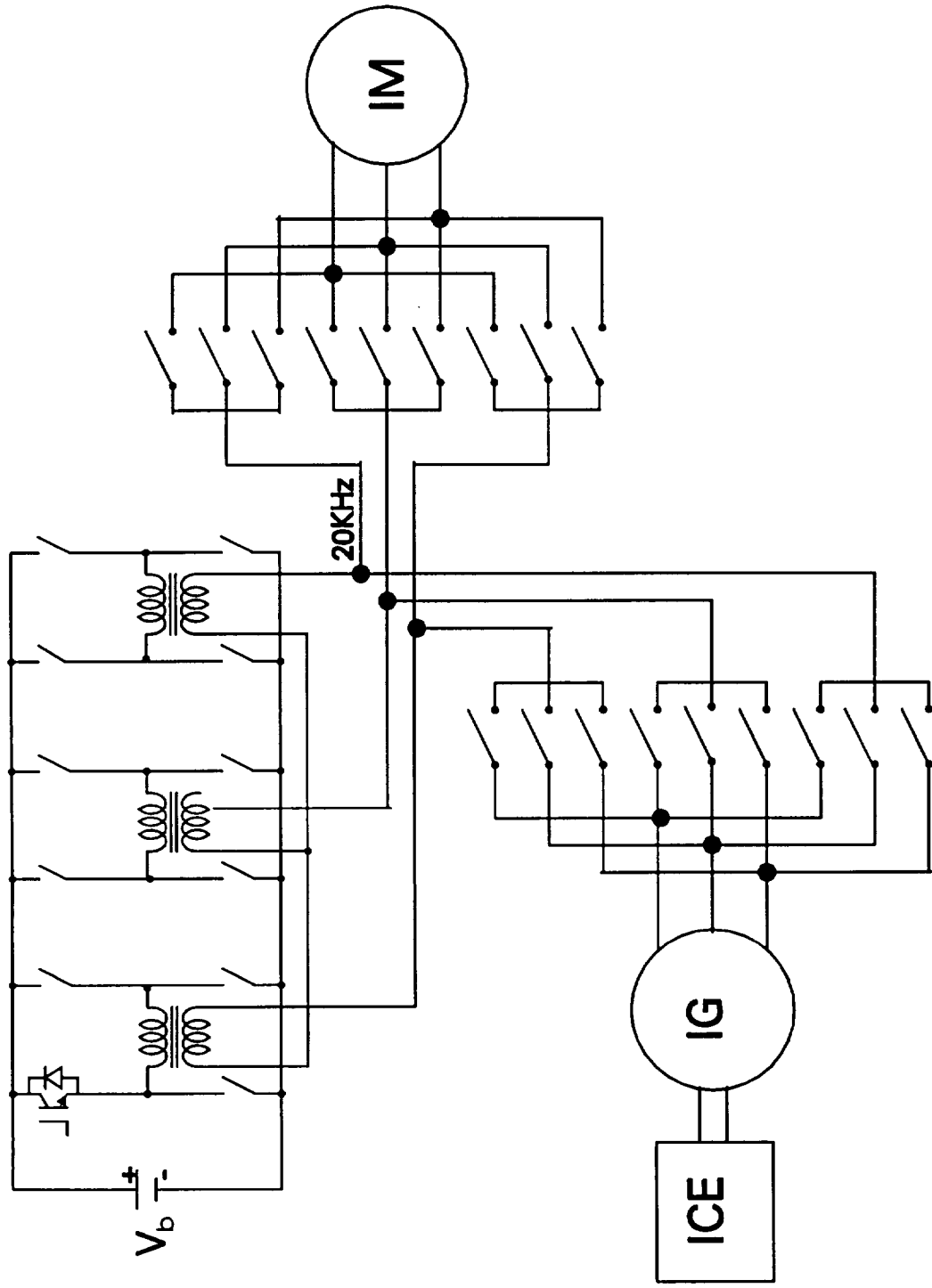
FIG. 17: THREE-PHASE AC DISTRIBUTION SYSTEM

79

to remain constant alleviating the modulation problem of the link voltage.

Distribution Frequency and Voltage

The selection of distribution voltage and frequency is very crucial for the system. One advantage in HFAC system, as mentioed before, is that the battery voltage can be independent because of the HFAC transformer used. Traditionally, 20 kHz, 440 V system has been considered for space application. Therefore, it is tempting to use the same values for HEV application.

Higher frequency has the following advantages:

- The HF transformer and the passive circuit components become smaller

- The harmonic ripple on the machine side is smaller causing less loss, i.e., improved efficiency.

- The filter capacitor becomes smaller.

- Auxiliary power circuits become smaller.

However, the disadvantages are:

- The power device switching speed should be higher for ZVS operation, otherwise device switching will occupy larger angular interval.

- The dv/dt and di/dt withstand capability of the devices and the machines should be higher.

- EMI effect will be worse.

In near term, it appears that 20 kHz frequency is optimum.

The selection of higher voltage has the following advantages:

- The distribution circuit current loading will decrease making it more economical.

- Machines and converter current ratings will decrease making them more economical.

However, the devices will have to handle higher voltage and the machine harmonics will increase causing loss of efficiency. Selection of 440 V appears to be a good choice, but with the presently available IGBT voltage rating, the link voltage can be boosted to higher value. This is discussed in the section of numerical design. In next generation, as IGBT switching speed is further improved, or other high frequency devices (such SiC) become available, both voltage and frequency can be boosted . These will make the system more economical and give better performance.

12. Component Sizing for Candidate HFAC System

In this section, an approximate sizing calculation will be done for the main components of the selected HFAC candidate system shown in Fig. 13. In this calculation, a number of assumptions will be made based on the current or near-term technology.

81

In fact, component sizing calculation for dc system described in the next section will be based on similar assumtions so that comparative figures-of-merit can be obtained for the HFAC system.

Drive Machine - Converter Sizing

The drive motor will be assumed to have peak output power of 100 kW (specified) or 134 hp. This figure appears practical for a mid-sized car because the HEV is desired to have the same driving capability of a ICE vehicle. The machine peak power is utilized for high speed acceleration when both the ICE and the battery work simultaneously. Since the machine has large thermal time constant and the acceleration power is required for a short time, the steady state power rating may be low (depends on the duty cycle). Assuming 2:1 ratio,

The steady state power rating = 100/2 = 50 kW, i.e. 67 hp

Assume motor efficiency = 0.95 (somewhat optimistic) at both 50 kW and 100 kW,

The corresponding input power = 52.63 kW and 105.3 kW, respectively. Consider a half-bridge version of the IHSC (integral half-cycle converter) which is shown in Fig. 18 (a). The corresponding load voltage wave at maximum output (square wave) is shown in (c). At any instant in the circuit there will be conduction drop due one IGBT and one diode. Therefore,

the machine phase rms voltage V_p = 4/pi (440 2 2/2 pi - 5.5) / 2 = 173.4 V

82

FIG. 18: (a) HALF-BRIDGE EQUIVALENT CIRCUIT OF
INVERTER
(b) HFAC LINK VOLTAGE WAVE
(c) LOAD VOLTAGE AT SQUARE WAVE

FIG. 19: INDUCTION MOTOR CURRENT COMPONENTS

V at square-wave where

> HFAC voltage V_s = 440 V (rms)

> IGBT drop = 3 V (pessimistic)

> Diode drop = 2.5 V (pessimistic) and π =3.142

(The drops are taken from POWEREX power semiconductor data book) [86]

At linear PWM range, the rms sine wave voltage = 173.4 * $\pi/4$ =136 V

and the corresponding line voltage (V_L) = 235 V.

The square-wave line rms voltage = 173.4 $\sqrt{3}$ = 300.3 V

Since the inverter can operate successfully in quasi-PWM range, a 250 V machine can

be used. Using space vector PWM, the linear PWM range can be extended further

permitting higher line voltage machine.

Assume power factor (cos ϕ) at 50 kW = 0.85

Therefore, steady state rms line current = 50,000/ (Ef. * $\sqrt{3}$ * 250* 0.85) = 143 A

where Ef (efficiency) = 0.95

The flux component of current i_{ds} = $\sqrt{2}$*143*sin 31.8 = 106.6 A

The torque component of current (i_{qs}) at 50 kW = $\sqrt{(\sqrt{2}*143)^2 - 106.6^2}$ = 171.9 A

> and at 100 kW = 343.8 A

The maximum rms line current = $\sqrt{(343.8^2 + 106.6^2)/2}$ = 254.5 A

Fig, 19 shows the current phasor diagram.

With IHS converter, the motor stator current ripple will be somewhat high unless the

machine is designed with high leakage inductance.

Assuming 5% peak ripple current, the peak machine current = 254.5 $\sqrt{2}$* 1.05 = 377.9

A. The IGBT should be selected to carry this current.

Select a 4-pole machine with maximum speed of 15,000 rpm

The maximum inverter frequency = 4. 15,000/120 = 500 Hz

The vehicle is assumed to have one transmission gear ratio such that 15,000 rpm corresponds to 100 mph speed.

The corresponding angular velocities are

$$2 \pi \ 15,000/60 \ = 1570 \ r/s \ at \ 15,000 \ rpm \ (100 \ mph)$$

$$= 942 \ r/s \ at \ 9,000 \ rpm \ (60 \ mph)$$

$$= 471 \ r/s \ at \ 4,500 \ rpm \ (30 \ mph)$$

The machine torque at 100 kW output is

$$100,000/1570 = 63.7 \ Nm \ at \ 15,000 \ rpm$$

$$= 106.2 \ Nm \ at \ 9,000 \ rpm$$

The vehicle will be assumed to operate in pure EV or zero emission mode in city driving.

In this mode, assume that 0 to 30 mph acceleration is required in 5 s.

Given: Curb weight = 900 kg

Luggage = 90 kg

Wt. of 6 passengers (72.3kg or 160 Lbs each) = 434 kg

Drive train wt. with battery (assumed) = 526 kg
(conservative)

Total wt. = 1950 kg   (Compares favourably with GE ETX 1, ETX 2

BMW E2)

85

Vehicle kinetic energy $1/2\ mV^2 = 1/2\ J\ W_m^2$

$$\text{or } J = m\ V^2\ /W_m^2 = 1950 * V^2\ /471^2 = 1.576 \text{ MKS unit}$$

where V = 13.4 m/s (corresponds to 30 mph), or W_m = 471 r/s

Assume that the vehicle accelerates 0 - 30 mph in 5 s at pure inertia load (neglect load torque).

$$\text{Acceleration torque } T_e = J\ W_m/t = 1.576 * 471/5 = 148.4 \text{ Nm}$$

Therefore, battery power needed = $T_e W_m$ = 148.4 * 471 = 69,896 W

Select nominal battery power rating = 70 kW

Since vehicle peak power = 100 kW, the base or corner speed = 30. 100/70 = 42.9 mph, i.e. 6,435 rpm, or 673.6 r/s, and the corresponding torque is 100,000/673.6 = 148.5 Nm

The corresponding inverter frequency = 500 * 6,435/15,000 = 214.5 Hz

Fig. 20 shows the motor characteristics at different speed. The motor field weakening speed ratio = 15,000 : 6,435 = 2.33 : 1

The average torque between 42.9 mph and 60 mph (field weakening) is (148.5 + 106.2)/2 = 127.4 Nm.

Acceleration time 0 to 60 mph:

0 - 42.9 mph : 1.576 * 673.6/148.5 = 7.15 s

42.9 - 60 mph : 1.576 * (942 - 673.6)/127.4 = 3.32 s

i.e. total time = 7.15 + 3.32 = 10.47 s (PNGV goal = 12 s)

This time is somewhat optimistic because friction and aerodynamic loads were
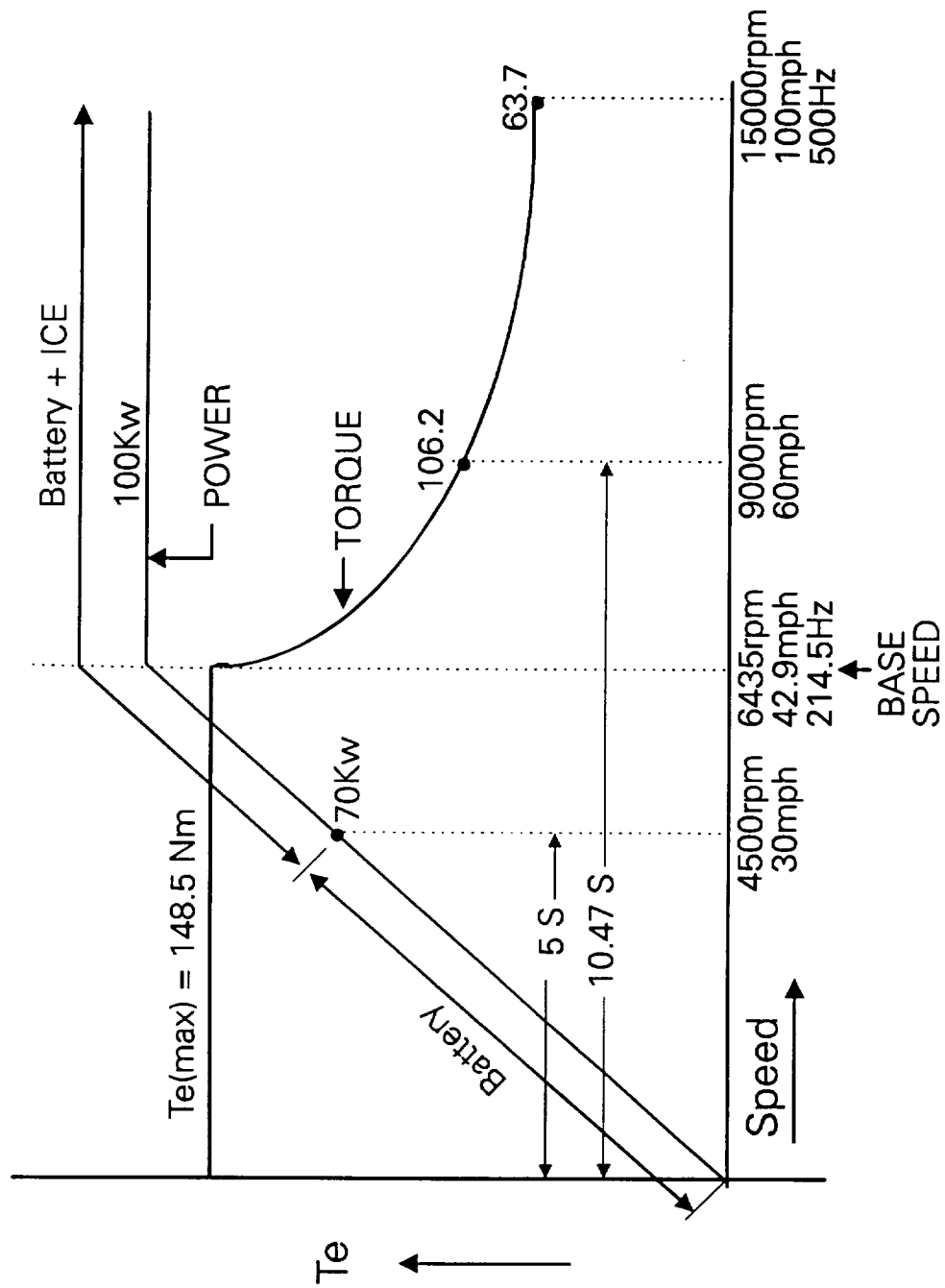
FIG. 20: MOTOR DRIVE CHARACTERISTICS AT DIFFERENT SPEED

87

neglected.

Fig. 21 shows the typical road-load [59] as a function of vehicle velocity and percentage grade [60]. It indicates that at steady state, the vehicle demands 48 kW power at 100 mph with 0% grade, and at 60 mph with 8% grade.

The motor cost = 100 * 2.75 = $275 (assumed $2.75/ peak kW)

and motor weight = 52.63 /(0.85 * 2) =31 kg (assumed 0.5 kg/KVA)

The converter rating = $\sqrt{3}$ * 250 * 254.5 = 110.2 KVA

Converter wt. = 110.2/5 = 22 kg (assumed 0.2 kg/KVA)

Converter cost = 110.2 * 20 = $2,204 (assumed $20/KVA)

Peak IGBT voltage = 440$\sqrt{2}$ = 622 V

The IGBT will see somewhat higher voltage because of modulation of HFAC voltage. Peak device current = 377.9 A

Select POWEREX IGBT type 1S621K40 which has rating of 1000 V, 400 A. Table 14 gives the POWEREX IGBT selector guide [86].

It is a single device with built-in fast-recovery bypass diode. New third generation IGBT has somewhat improved characteristics.

Note that the device has excess voltage margin. To utilize this voltage margin, HFAC voltage can be increased. For the same power level, higher voltage will cause less current loading, tending the converter and machine to be more economical.

The ideal HFAC rms voltage (V_s) = 1,000/$\sqrt{2}$ = 707.2 V

Consider practical V_s = 600 V (i.e., 15.5% margin for V_s fluctuation)

The motor terminal rms voltage at square wave = (4/π)[600$\sqrt{2}$/π - 5.5]($\sqrt{3}$/ $\sqrt{2}$) = 412.4

88
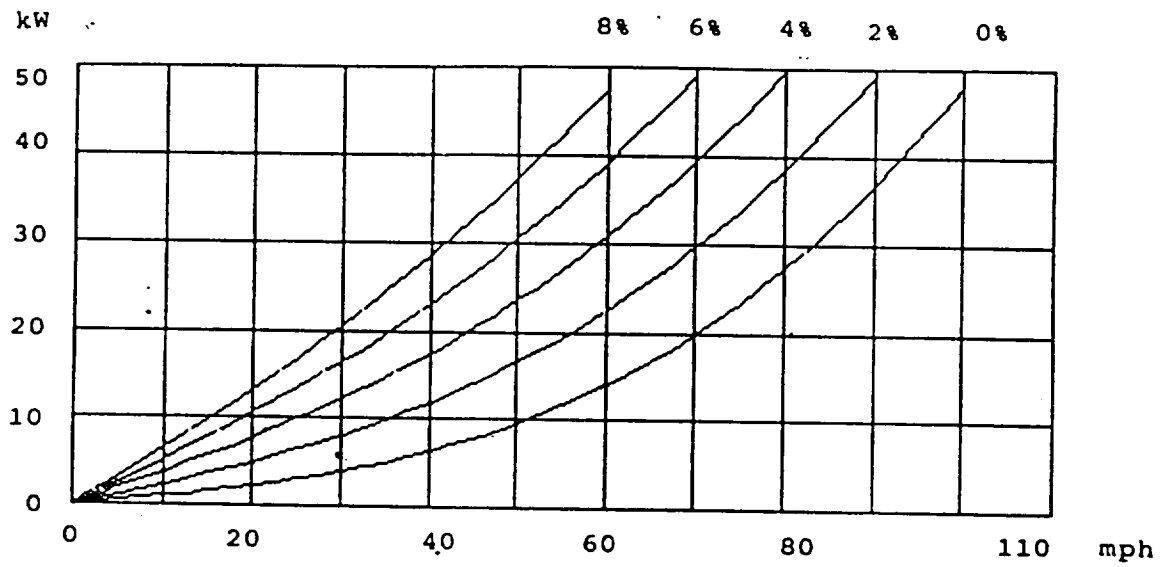
**FIG. 21: ROAD-LOAD AS A FUNCTION OF VEHICLE
VELOCITY AND PERCENTAGE GRADE**
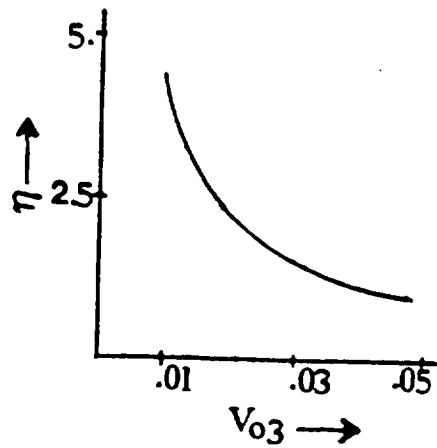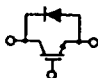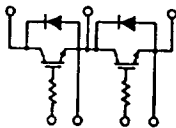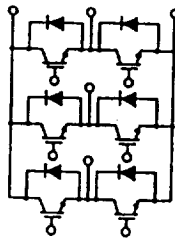
**FIG. 22: RATIO (η) AS FUNCTION OF THIRD HARMONIC
VOLTAGE**

89

Table 14 : POWEREX IGBT SELECTOR GUIDE

Circuit Diagram		V_CES (V)	I_c (A)									
			15	25	50	75	100	150	200	300	400	600
Single		600								IS626030	IS626040	IS621K60
		1000							IS621K20	IS621K30	IS621K40	IS621260
		1200							IS621220	IS621230	IS621240	
Dual		600		ID2260A2	ID226005	ID226075	ID226010	ID226015	ID226020	ID126030	ID126040	
		1000		ID221KA2	ID221K05	ID221K75	ID221K10	ID121K15	ID121K20			
		1200		ID2212A2	ID221205	ID221275	ID221210	ID121215	ID121220			
Six-IGBT		600	IEF260A1	IEF260A2	IEF26005	IET26075	IET26010					
		1000	IEF21KA1	IET21KA2	IET21K05							
		1200	IEF212A1	IEF212A2	IET21205							

☐ Under Development

90

V.

The motor terminal peak voltage in linear PWM = $600\sqrt{2}/\pi$ - 5.5 = 264.5 V

The corresponding rms line voltage = $264.5\sqrt{3}/\sqrt{2}$ = 324 V

Therefore, machine line rms voltage at quasi-PWM can easily be raised from 250 V to 340 V (i.e., 36%)

The corresponding motor currents are:

Line rms current (steady state) = 143 * 250/340 = 105.1 A

i_{ds} = 106.6 * 105.1/143 = 78.7 A

i_{qs} = 171.9 * 105.1/143 = 126.3 A

The peak machine current = $\sqrt{78.7^2 + 126.3^2}$ * 1.08 = 285.7 A

where 8% ripple current was assumed because for the same frequency (20 kHz) higher HFAC voltage will cause more machine ripple current (slightly increasing the harmonic loss). But, fundamental copper loss will decrease.

We can safely select 1S621K3D type IGBT with rating of 1,000 V, 300 A (lower current rating). In summary, higher HFAC voltage has the following features:

- One size lower IGBT

- Lower conduction loss improves converter efficiency

- Machine will be slightly economical

- Machine iron loss will slightly increase but copper loss will decrease slightly improving the efficiency

Ideally, the IGBTs in the inverter will not need snubber because of ZVS (zero voltage switching), but a small capacitor should be connected across each for protection.

Sizing of Battery

The battery side supplies roughly 70% of the motor peak power need and the rest is supplied by the ICE generator. Assume:

Converter efficiency = 96%

HF transformer efficiency = 99%

and resonant inverter efficiency = 98%

The battery power rating = 100 * 0.7/(0.95 * 0.96 * 0.99 * 0.98) = 79.1 kW where the motor efficiency is 95%

Select battery nominal voltage = 300 V (125 no. 2.4 V cells in series)

Assume minimum battery voltage = 210 V (70%)

and maximum battery voltage = 390 V (130%)

As discussed before, selection of battery voltage depends on a number of trade-off considerations.

Select the Horizon lead-acid battery with the parameters given before.

The battery weight = 79,100/450 = 176 kg (optimistic)

The battery storage energy = 176 * 45 = 7.92 kWh

From Fig. 21, the car needs 3.5 kW power at steady speed of 30 mph

Therefore, the vehicle range at 80% DOD (depth of discharge) = 7.92*0.8*30/3.5 = 54.3 miles. This range should be satisfactory for daily commuting in EV mode. Of course, heavier battery is needed to increase the range.

The battery cost = 7.92*400 = $3,168 which is somewhat high.

[If the lead-acid battery is selected from Table 2, the corresponding parameters are:

Battery weight = 79,100/125 = 632.8 kg (very heavy)

Energy storage = 632.8 * 35 = 22.1 kWh (very high)

Urban range = 22.1 * 0.8 * 30/3.5 = 151.5 miles (very high)

Cost = 22.1 * 70 = $1,547 (very low)]

The battery maximum currents:

79,100/300 = 263.7 A at 300 V

79,100/210 = 376.7 A at 210 V

79,100/390 = 202.8 A at 390 V

Assume the battery lead equivalent resistance = 0.1 Ohm and inductance = 100 uH.

The capacitor will bypass the harmonic currents injected by the inverter.

Sizing of Resonant Inverter

The resonant inverter operates in quasi-square wave (or single-pulse PWM) to regulate the HFAC voltage for variation of load and battery voltage. It will operate in square wave mode at minimum battery voltage.

$a_1 = (4V_b/\pi) * \sin \delta/2 = 4 * (210 - 5)/\pi = 261$ V for $\delta = 180$ deg, where IGBT drop of 2.5 V has been assumed. For same inverter output voltage,

$\delta = 88$ deg at $V_b = 300$ V, and $\delta = 64$ deg at $V_b = 390$ V

The inverter carries the maximum current at the lowest battery voltage. At this

condition, the input current wave is nearly single-phase full-wave rectified.

Therefore, inverter peak current = 376.7*π/2 = 591.8 A which is carried by each device.

The device peak voltage = 390 V.

Select POWEREX IGBT type 1S621K60 which has ratings of 600 V, 600 A. The single device has a bypass diode built-in.

Inverter output power = 79.1 * 0.98 =77.5 kW (Ef. = 0.98)

Assume displacement factor = 1.0, and distortion factor = 0.8

Therefore, inverter rating = 77.5/0.8 = 96.9 KVA

The inverter cost = 96.9 * 10 = $969 (assumed $10/KVA)

The inverter weight = 96.9 * 0.15 = 14.5 kg (assumed 0.15Kg/KVA)

The resonant circuit of the inverter can be designed based on Jain and Tanju's paper [6]. The design criteria are as follows:

- The output voltage wave should have reasonably low third harmonic distortion. This is the dominant harmonic at the output.

- The total reactive rating of the resonating network and circulating current losses should be reasonably low.

These criteria are plotted respectively in Figs. 22 and 23, where V_{03} = 3rd harmonic content of the output voltage, $\eta = X_s/X = wL_s/wL_p$, P_{cl} = circulating power loss, $\digamma$ = resistance of circulating path, S_T = reactive rating of the resonant network and K = a constant factor.

Assuming equivalent resistive load at the inverter terminal, R_B = 440*440/96,900 = 2.02

94
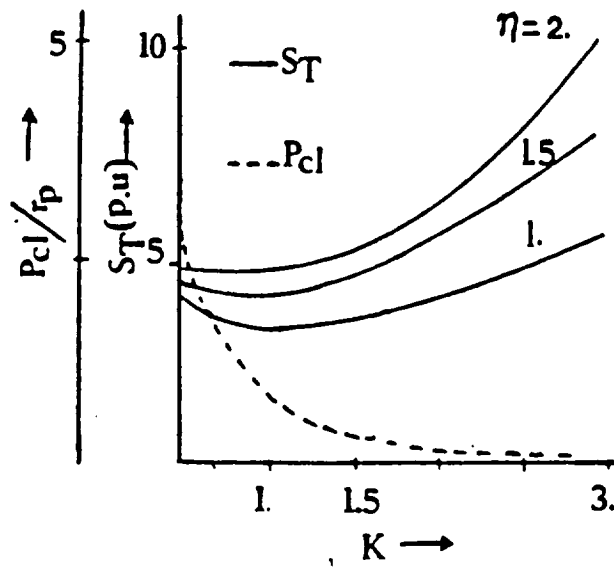
FIG. 23: LOSSES IN PARALLEL RESONANT NETWORK
(P_{cl}) AND REACTIVE RATING (S_T) AS FUNCTION
CONSTANT K
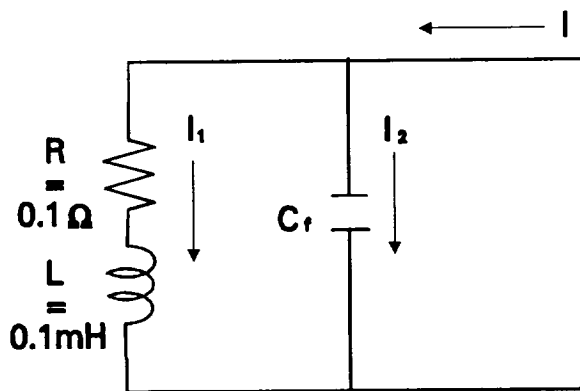
FIG. 24: EQUIVALENT CIRCUIT OF BATTERY FILTER

Ohms. In Figs. 22 and 23, select $\eta = 1.5$ and K = 1.2.

Therefore, $L_S = K \eta R_B/w_0 = 28.95$ uH

$$C_S = 1/K\eta R_B w_0 = 2.19 \text{ uF}$$

$$L_P = KR_B/w_0 = 19.3 \text{ uH}$$

$$C_P = 1/KR_B w_0 = 3.28 \text{ uF}$$

where K = 1.2, $\eta = 1.5$, $R_B = 2.02$ and $w_0 = 2 \pi \ 20{,}000$,

Sizing of Filter Capacitor

In worst case, the resonant inverter input current is single-phase full wave rectified dc with a peak value of 591.8 A at $V_b = 210$ V. The current wave will contain even harmonics where the 2nd harmonic component will have maximum magnitude. The filter can be designed so that only 10% of second harmonic current can flow through the battery. The equivalent circuit of the filter is shown in Fig. 24. The 2nd harmonic current $i_2 = 4 * 591.8/3\pi = 251.1$ A. The battery circuit impedance $Z_1 = 0.1 +$ j $(2\pi \ 40*10^3*0.1*10^{-3}) = 0.1 + J \ 25.1$ Ohm, where the frequency is 40 kHz.

The capacitor impedance $Z_2 = 1/(JwC) = - J \ 10^6 /(2\pi \ 40*10^3*C) = - J \ 3.98/C$ Ohm

Therefore, $Z_1 + Z_2 = 0.1 + J \ (25.1 - 3.98/C)$

i.e., $| Z_1 + Z_2 | = \sqrt{0.01 + (25.1 - 3.98/C)^2}$

since $| I_1/(I_1 + I_2) | = 0.1$, $| Z_1/(Z_1 + Z_2) | = 0.1$

Therefore, $3.98/C = 0.1 \sqrt{0.01 + (25.1 - 3.98/C)^2}$

solving this equation C = 1.74 uF

Since the capacitor size is small, a non-electrolytic (ac) capacitor of 2 uF, 600 V can be selected.

Sizing of Transformer

The high frequency transformer (see Fig. 13) will handle roughly 70% of the motor peak power and the rest will be handled by the ICE generator. This of course ignores the auxiliary power need by the transformer. At the time of battery charging by the ICE generator, the power will be relatively low. Either amorphous metal or ferrite core, as discussed before, can be used.

The transformer secondary rms voltage = 440 V

Load displacement factor = 0.9 (assumed)

Load distortion factor = 0.8 (assumed)

Primary rms voltage = $261/\sqrt{2}$ = 184.6 V

Therefore, transformer rating = 105.3*0.7/(0.96*0.9*0.8) = 106.6 KVA

Turns ratio = 184.6 : 440 = 1 : 2.38 (primary : secondary)

Primary current = 106,600/184.6 = 577.5 A

Transformer weight = 106.6 * 0.2 = 21.3 kg (assumed 0.2 kg/KVA for ferrite)

[Using amorphous metal, the weight = 21.3 * 5/16 = 7 kg since flux density = 16 k. gauss compared to 5 k. gauss for ferrite]

Transfor cost = 106.6 * 5 = $533 (assumed $5/KVA)

Sizing of ICE - Generator - Converter

The IC engine will be directly coupled with the induction machine as generator. Assume that the ICE operates at constant speed of 5,000 rpm and the IG is directly coupled to it. A speed-up gear could make the machine more economical but the gear weight and losses are added.

The power ratings are:

Engine rating = 105.3 * 0.3/ (0.96 * 0.95) = 34.6 kW

(assuming generator efficiency = 0.95 and converter efficiency = 0.96)

Generator rating = 34.6 * 0.95 = 32.9 kW or 38.7 KVA (assuming power factor = 0.85)

Converter rating = 32.9 * 0.96 = 31.6 kW or 39.5 KVA (assuming disp. factor = 1.0 and dist. factor = 0.8)

Engine weight = 34.6 * 1.0 = 34.6 kg (assumed 1.0 kg/kW)

Engine cost = 34.6 * 15 = $519 (assumed $15/kW)

Generator weight = 38.7 * 0.6 = 23.2 kg (assumed 0.6 kg/KVA)

Generator cost = 32.9 * 3.75 = $123.4 (assuming $3.75/kW)

Converter weight = 39.5 * 0.25 = 9.9 kg (assumed 0.25 kg/KVA)

Converter cost = 39.5 * 20 = $790 (assumed $20/KVA)

Generator frequency = 4*5,000/120 = 166.7 Hz (assumed 4 pole machine)

Select generator line rms voltage = 250 V (same as the motor) .

Generator rms line current = 38,700/($\sqrt{3}$* 250) = 89.4 A

Generator full load torque = 32,900* 60/(2π 5,000) =62.8 Nm

Fig. 25 shows the engine generator characteristics.

The peak device current = 89.2 √2 * 1.05 = 132.4 A

Select POWEREX IGBT type 1S621K20 which has the ratings of 1,000 V, 200 A

[If 600 V HFAC link voltage is selected, the generator line current = 89.4*250/340

= 65.7 A

Then, the device peak current = √2 * 65.7*1.06 = 98.5 A, i.e., an 100 A IGBT could be

selected]

13. Component Sizing for DC System

Drive Machine - Converter Sizing

The dc system is shown in Fig. 10. As in HFAC system, we will assume 300 V

battery and 100 kW (peak power) drive motor. Since the machine must always operate

in PWM mode, its voltage rating should be based on the minimum battery voltage.

Machine phase rms voltage at minimum battery voltage = (4/π) (105 -5)/√2 = 90 V

for sq. wave (assumed device drop = 2.5 V), line voltage = 90 √3 = 155.9 V. Linear PWM

range = 155.9 * 0.785 = 122.4 V. Take 83.3% of sq. wave for quasi-PWM range, i.e.

155.9 * 0.833 = 130 V. Evidently, machine voltage rating is very low demanding large

current for same power rating.
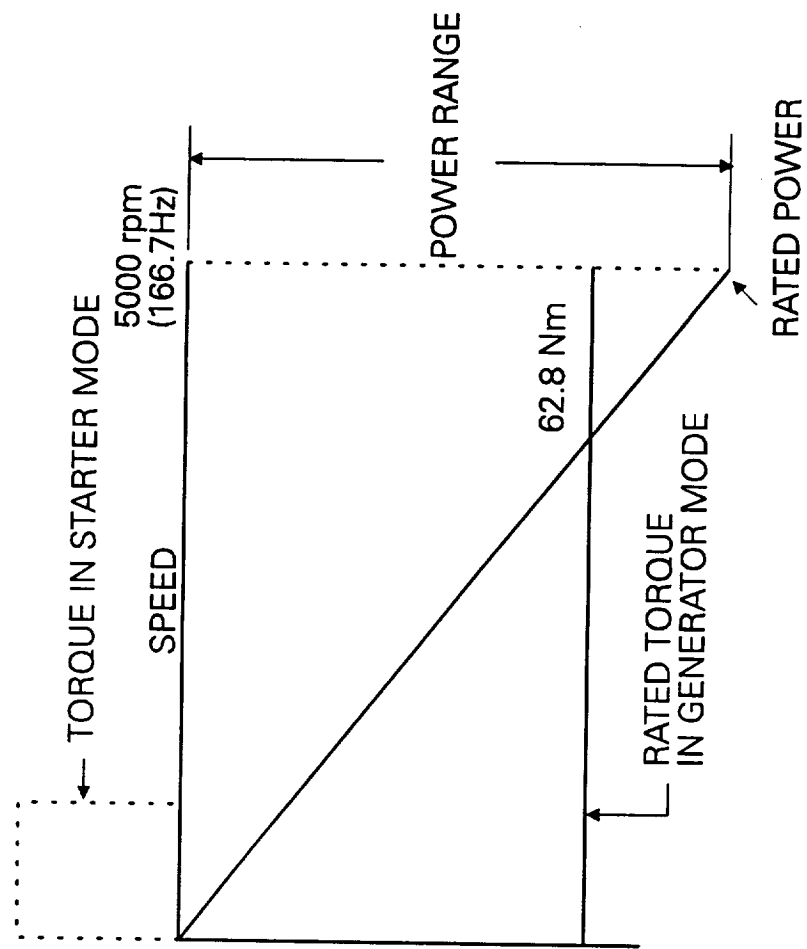
FIG. 25: ENGINE GENERATOR CHARACTERISTICS

100

Motor line rms current at steady state = 50,000/($\sqrt{3}$ * 130 * 0.85 * 0.95) = 275 A

(assumed motor Eff. = 0.95 and PF = 0.85)

i_{ds}= $\sqrt{2}$ * 275 * sin 31.8 = 202.2 A

i_{qs} = $\sqrt{2}$ * 275 * 0.85 = 330.5 A and at 100 kW = 661 A

The maximum rms line current = 489 A

Peak IGBT voltage = 390 * 1.2 = 468 V (assumed 20% overshoot)

Peak IGBT current = 489$\sqrt{2}$ * 1.03 = 712 A (assumed 3% peak ripple current)

The harmonic voltage at machine terminal will be somewhat less causing less ripple current.

Select POWEREX IGBT type 1S626040 with the ratings of 600 V, 400 A

(Note that two devices are needed in parallel with the corresponding matching problem)

Sizing of Battery

The battery ratings will practically remain the same

Sizing of ICE - Generator - Converter

Peak power input to motor-converter = 100/(0.95 * 0.94) = 112 kW

(assumed converter Eff. = 0.94)

Peak power from ICE-generator side = 112 * 0.3 = 33.6 kW (30% share)

The ICE-generator will be designed to carry this as the steady state power

ICE power rating = 33.6/(0.94 * 0.95) = 37.63 kW (assumed gen. Eff. = 0.95
and conv. Eff. = 0.94)

Generator power rating = 33.6/0.94 = 35.74 kW, i.e. 42 KVA

Generator rated rms current = 35,740/($\sqrt{3}$*130*0.85) = 186.7 A

Generator terminal voltage will be the same as motor voltage

Peak IGBT current = 186.7$\sqrt{2}$ * 1.03 = 271.9 A

Select POWEREX IGBT type 1S621K30 which has ratings of 600 V, 300 A

Sizing of Filter Capacitor

The criteria for filter design will be the same as in HFAC system.

The filter capacitor is to be designed to sink harmonic currents generated by both the
generator-converter and motor-converter. The detailed calculation is very complex. Only
approximate calculation will be done on the basis of Ziogas [17] paper.

The general harmonic current expression is given as

$$
I_{i,l} = \frac{9V_b}{2} [\sum_{m=1,5,\ldots}^{\infty} \frac{(C_{m+1})(C_m)}{|Z_m|} \cos(l\Theta + \gamma_1)
$$
$$
(for \ k = m + l)
$$
$$
+ \sum_{k=1,3,\ldots}^{\infty} \frac{(C_k)(C_{k+1})}{|Z_k + l|} \cos(-l\Theta + \gamma_2)
$$
$$
(for \ m = k + l)
$$
$$
+ \sum_{m=1,5,\ldots}^{l-1} \frac{(C_m)(C_{l-m})}{|Z_m|} \cos(l\Theta - \delta_1)]
$$
$$
(for \ k = l - m)
$$

where $\quad$ l = 6, 12, 18

$$\Upsilon_1 = \theta_m - \theta_{m+1} + \phi_m$$

$$\Upsilon_2 = \theta_{k+1} - \theta_k + \phi_{k+1}$$

$$\delta_1 = \theta_m + \theta_{1-m} + \phi_m$$

Motor-inverter output power = 100/0.85 = 117.6 KVA

Motor line voltage = 130 V

Therefore, 1 pu power = 117,600/3 = 39,200 VA

$\quad$ 1 pu voltage = 130 V

$\quad$ 1 pu current = 39,200/130 = 301.5 A

The carrier frequency currents will be ignored, and design will be based on the 6th

harmonic current, i.e., $I_{i,6}$= 301.5 A

Generator- rectifier input power = 42 KVA

Therefore, 1 pu power = 42/3 = 14 KVA

$\quad$ 1 pu voltage = 130 V

$\quad$ 1 pu current = 14,000/130 = 107.7 A

Therefore, $I_{i,6}$ = 107.7 A

Higher harmonic currents are of smaller amplitude and will be neglected.

Although $I_{i,6}$ components of the converters are at different frequencies, it will be

assumed to correspond to the generator frequency, i.e., 166.7 Hz.

Therefore f_6 = 166.7 * 6 =1000.2 Hz and total $I_{i,6}$ = 301.5 + 107.7 = 409.2 A

For the parallel filter equivalent circuit with the battery R = 0.1 Ohm and L = 100 uH

103

$Z_1 = 0.1 + J\ 2\ \pi\ 1000.2 * 0.0001 = 0.1 + J\ 0.63$ Ohm

$Z_2 = 10^6 /(2\pi\ 1000.2C) = 159/C$

$Z_1 + Z_2 = 0.1 + J\ (0.63 - 159/C)$

i.e., $|\ Z_1 + Z_2\ | = \sqrt{0.01 + (0.63 - 159/C)^2}$

Assuming the same ripple current(25.1A) as in HFAC system

i.e., $|\ I_1/I\ | = 25.1/409.2 = 0.061$

$159/C = 0.061\ \sqrt{0.01 + (0.63 - 159/C)^2}$

Solving the equation C = 4,314 uF

An ac capacitor of 5,000 uf, 500 V can be selected

14. Comparison of DC and HFAC Systems

The following table gives the comparison of ratings and parameters of power circuit components for the same vehicle performance

Table 15: Comparison of Power Circuit Components

HFAC	DC
Drive Motor:	
Type = Induction	"
Peak power = 100 kW or 134 hp	"

104

Rated power = 50 kW or 67 hp   "

Line voltage = 250 V   130 V

Power factor = 0.85 at 50 kW   "

Poles = 4   "

Maximum speed = 15,000 rpm   "

Maximum frequency = 500 Hz   "

Corner speed = 6,435 rpm   "

Corner frequency = 214.5 Hz   "

Field-weakening range = 2.33:1   "

Maximum line current = 254.5 A   489 A

Rated line current = 143 A   275 A

Efficiency at rated load = 0.95   "

Maxumum torque = 148.5 Nm   -

Weight = 31 kg   20% higher

Cost = $275   20% higher

Converter for Motor:

No. of devices = 12 IGBTs   "

            = 12 diodes   "

Device ratings = 1000 V, 400 A   600 V, 400 A (2 in parallel)

Power rating = 105.3 kW or 110.2 KVA   "

Efficiency = 0.96   0.94

Weight = 22 kg   20% higher

Cost = $2,204   20% higher

IC Engine:

    Power rating = 34.6 kW   37.6 kW

    Speed = 5,000 rpm   "

    Weight = 34.6 kg   10% higher

    Cost = $519   10%higher

Generator:

    Machine = Induction   "

    Power rating = 32.9 kW or 38.7 KVA   35.7 kW or 42 KVA

    Power factor = 0.85   "

    Speed = 5,000 rpm   "

    Poles = 4   "

    Frequency = 166.7 Hz   "

    Voltage rating = 250 V   130 V

    Rated line current = 89.4 A   186.7 A

    Efficiency = 0.95   "

    Rated torque = 62.8 Nm   -

    Weight = 23.2 kg   20% higher

    Cost = $123   20% higher

Converter for Generator:

No. of devices = 12 IGBTs	6
= 12 diodes	6
Device rating = 1000 V, 200 A	600 V, 300 A
Power rating = 31.6 kW or 39.5 KVA	35.7 Kw or 42 KVA
Efficiency = 0.96	0.94
Weight = 9.9 kg	20% lower
Cost = $790	20% lower

Battery:

Power rating = 79.1 kW	"
Nominal voltage = 300 V (210 - 390 V)	"
Energy storage = 7.92 kWh	"
Equivalent R = 0.1 Ohm	"
Equivalent L = 100 uH	"
Weight = 176 kg	"
Cost = $3,168	"

Filter Capacitor = 1.74 uF, 500 V   4,314 uF, 500 V

Resonant Inverter:

No. of devices = 4 IGBTs

= 4 diodes

Device ratings = 600 V, 600 A

Power rating = 77.5 kW or 96.9 KVA

Efficiency = 0.98

Weight = 14.5 kg

Cost = $969

HF Transformer:

Material = Ferrite

Capacity = 106.6 KVA

Turns ratio = 184.6 : 44 = 1 : 2.38 (primary : secondary)

Weight = 21.3 kg

Cost = $533

Precise quantitative comparison between HFAC and DC systems is difficult but the following points can be highlighted:

- HFAC system needs 28 IGBTs whereas DC system needs 18 IGBTs. However, availability of integral ac switches will shrink the device count to 16, for HFAC system.

- The devices in HFAC system are soft-switched giving advantages of higher converter efficiency, improved reliability, and no snubbers are required. Of course, converter conduction losses will be higher.

- The transformer in HFAC system permits isolation and higher machine voltage rating making them more economical.

- The machine harmonic voltages are higher tending to give higher harmonic currents. Therefore, machines are to be designed with higher leakage inductances.

- The filter capacitor in HFAC system is extremely small compared to DC system. A more reliable ac capacitor can be used.

- With higher speed power devices in the next generation, voltage and frequency can be boosted further to shrink the size and cost of the power circuit components.

- Auxiliary power supply is very economical in HFAC system

15. Control Development of HFAC System

In this section, a preliminary control development of the HFAC system is described. The control development was needed for the system simulation study.

15.1. Control of Converter - Motor

The drive motor was controlled by indirect vector control (or field-orientation control) method, as shown in Fig. 26. With vector control, the induction motor drive
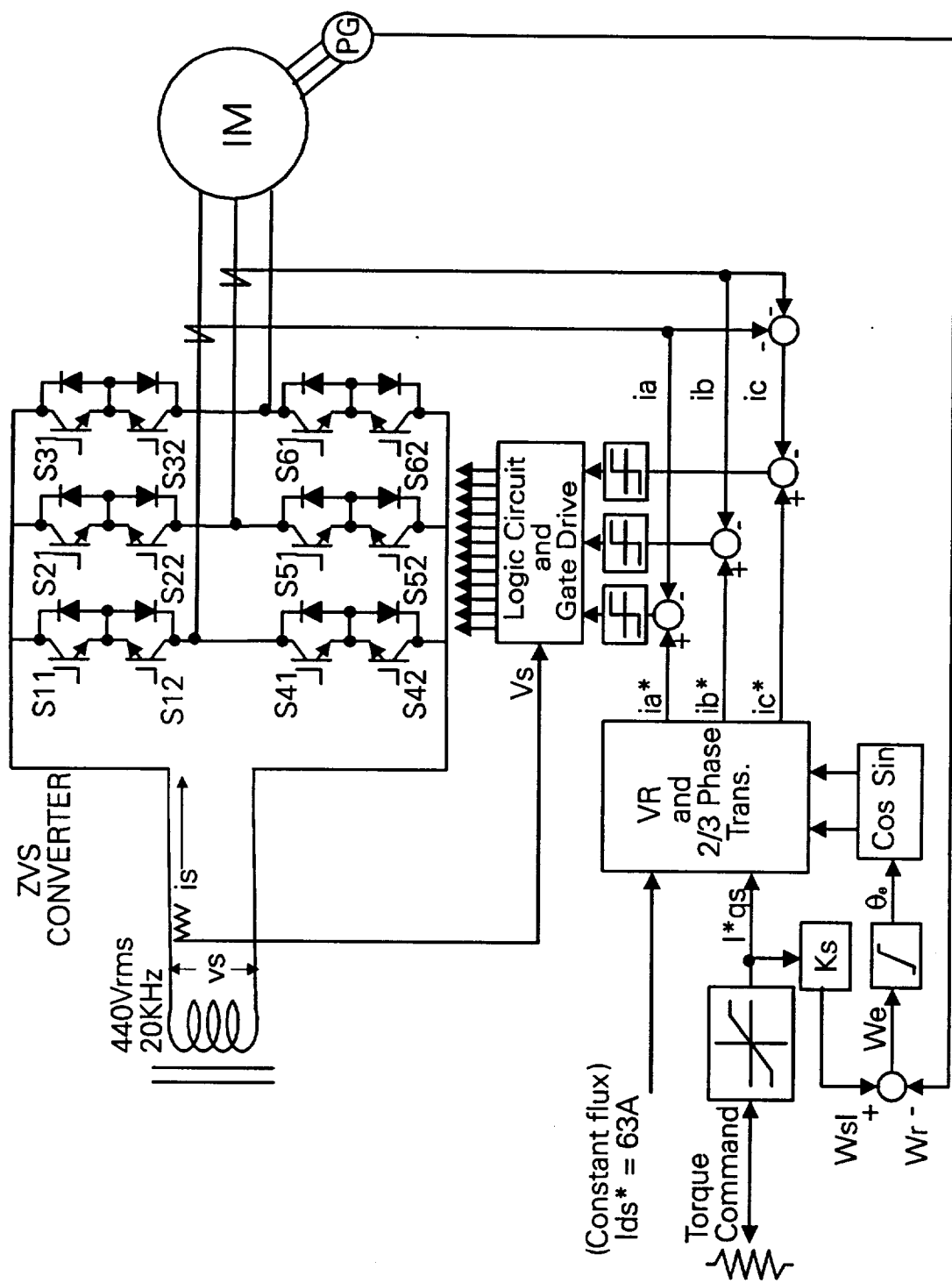
FIG. 26: CONTROL BLOCK DIAGRAM OF DRIVE MOTOR

110

behaves like a separately excited dc motor drive, i.e., the transient response is very fast, and there is no usual stability problem of the drive. In the outer loop, it is a torque-controlled system where the torque component of current I_{qs}^* (proportional to torque) is controlled by the potentiometer. The rotor flux is constant in the constant torque region, and it is controlled by the flux component of current I_{ds}^*, as shown. The Delco Remy 100 kW (peak power) machine (see Table 17) has been considered in the control development and simulation study. The slip frequency signal W_{sl} is proportional to I_{qs}^* by the slip gain factor K_s. The speed signal W_r is added to the slip signal W_{sl} to generate the frequency command W_e which is then integrated to generate the unit vector signals through the function generators. Both the signals I_{qs}^* and I_{ds}^* are then vector-rotated and converted to three-phase current command, as shown.

The phase currents are controlled independently by discrete half-cycle pulsewidth modulation (also known as Delta modulation), as shown in Fig.27. As the polarity of phase current error (err) changes and exceeds a threshold value, the converter is ready to change the switching pattern. However, since the converter is constrained to have zero voltage switching (ZVS), it waits until the next zero crossing interval is identified. The resonance pulse hold (RPH) produces half-cycles of resonant pulses which have periodic zero crossing. Fig. 28 shows the equivalent half-bridge converter with respect to the hypothetical center-point of HFAC voltage V_s. Table 16 shows the switching control strategy and Fig. 29 explains the control principle in detail. In Fig. 29, the HFAC voltage wave V_s is processed and logic pulse train (L)

111
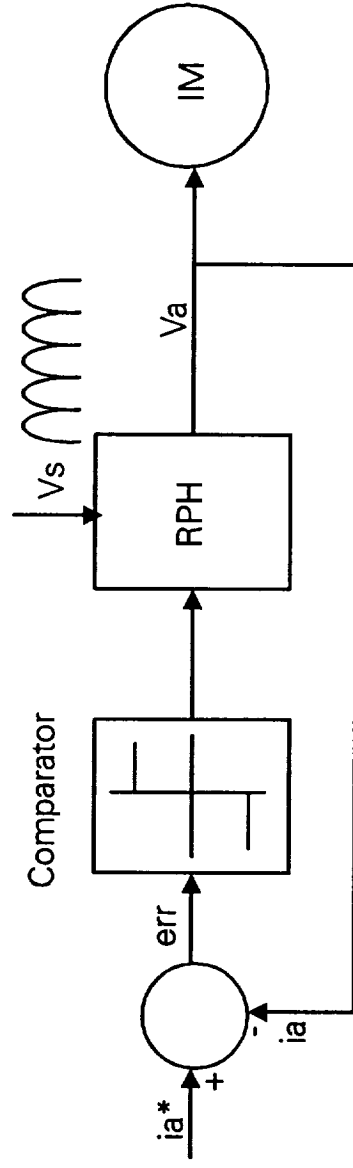
FIG. 27: BLOCK DIAGRAM FOR CURRENT REGULATED DELTA MODULATION (CRDM)

112
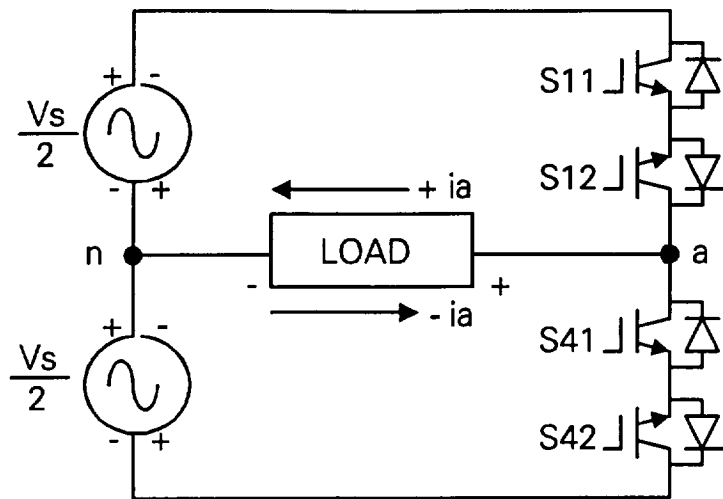
FIG. 28: EQUIVALENT HALF-BRIDGE INVERTER

Table 16 : Switching Modes of Half-Bridge Inverter

MODE	ia	err	Vs	SW
1	+	+	+	S11
2	+	+	-	S42
3	+	-	+	S41
4	+	-	-	S12
5	-	+	+	S41
6	-	+	-	S12
7	-	-	+	S11
8	-	-	-	S42
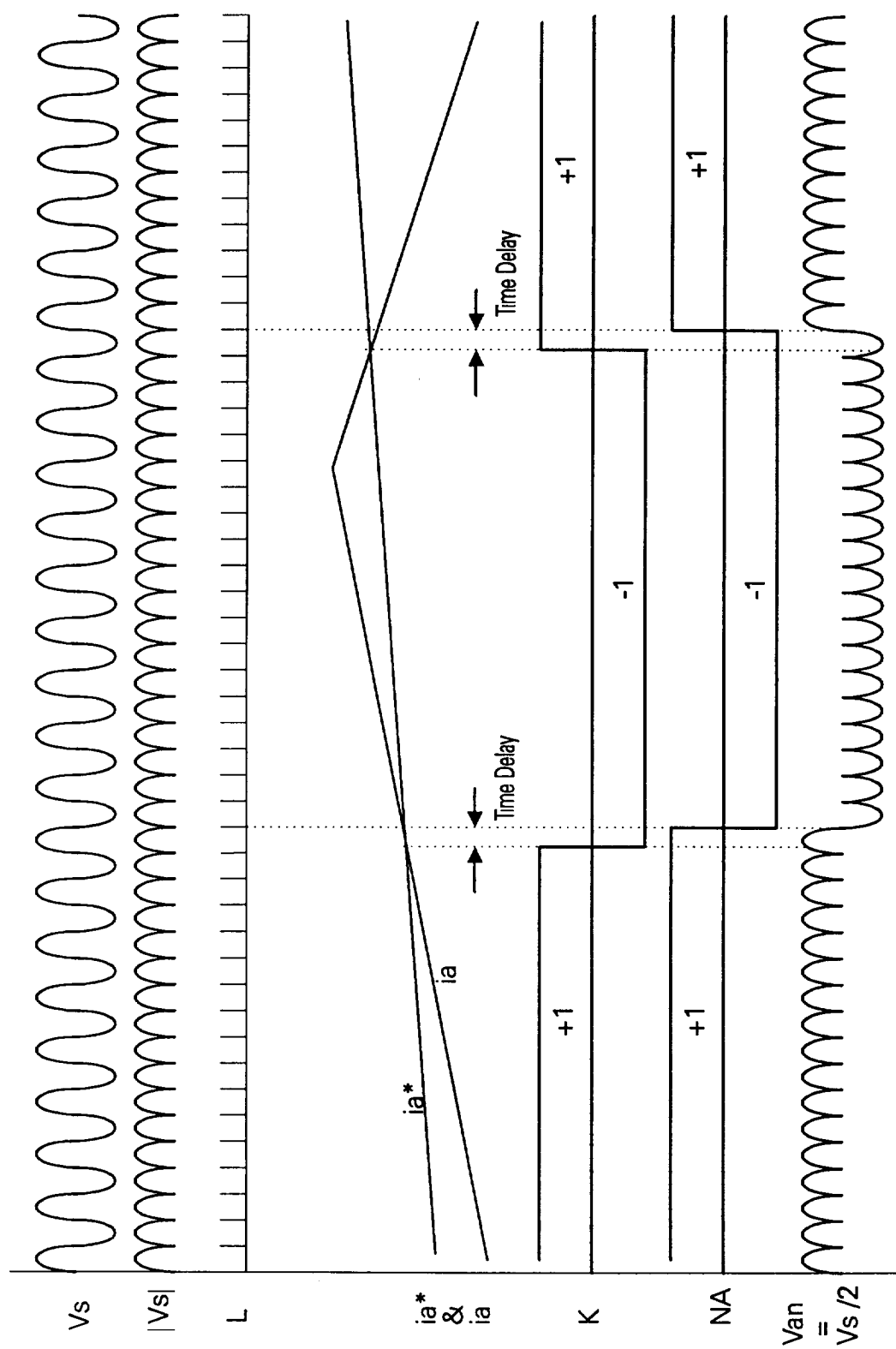
FIG. 29: OPERATION OF ONE PHASE OF CONVERTER

114

generated which gives the permissible window time for switching of the devices. The logic signal K corresponds to the polarity of err signal and NA is the logical interval for switching. Note that NA wave is delayed because of the time delay for zero voltage switching. The phase voltage V_{an} (with respect to the center-point) appears like a "square wave", but it is further dictated by the polarity of V_s signal , as indicated in Table 16. For example, in mode 4, i_a is positive, err is negative, V_s polarity is negative, and therefore, the switch S_{12} should be on to force the decrease of $+i_a$. The motor phase voltage will be the same as V_{an} wave if the motor neutral is tied to the supply center point. For isolated neutral machine , the machine phase voltage may be zero, $\pm 1/3\ V_s$ or $\pm 2/3\ V_s$ in any HFAC half-cycle period.

15.2. Control of Converter - Generator

The control principle of converter-generator is essentially similar to the converter-motor system, and is shown in Fig. 30. The same induction machine, as shown in Table 17, is considered for control development and simulation study. The ICE is initially started with the generator operating in motoring mode. As the ICE starts, its speed is raised and locked to the constant speed of 5000 rpm. The programmable speed control for optimization of ICE efficiency is also possible. The speed loop operates independently with the control of throttle angle, as indicated in the figure. Once in generating mode at constant speed, the variable power of the generator is controlled by variable torque by manipulation of I_{qs} (negative). In actual system, feedforward power

115
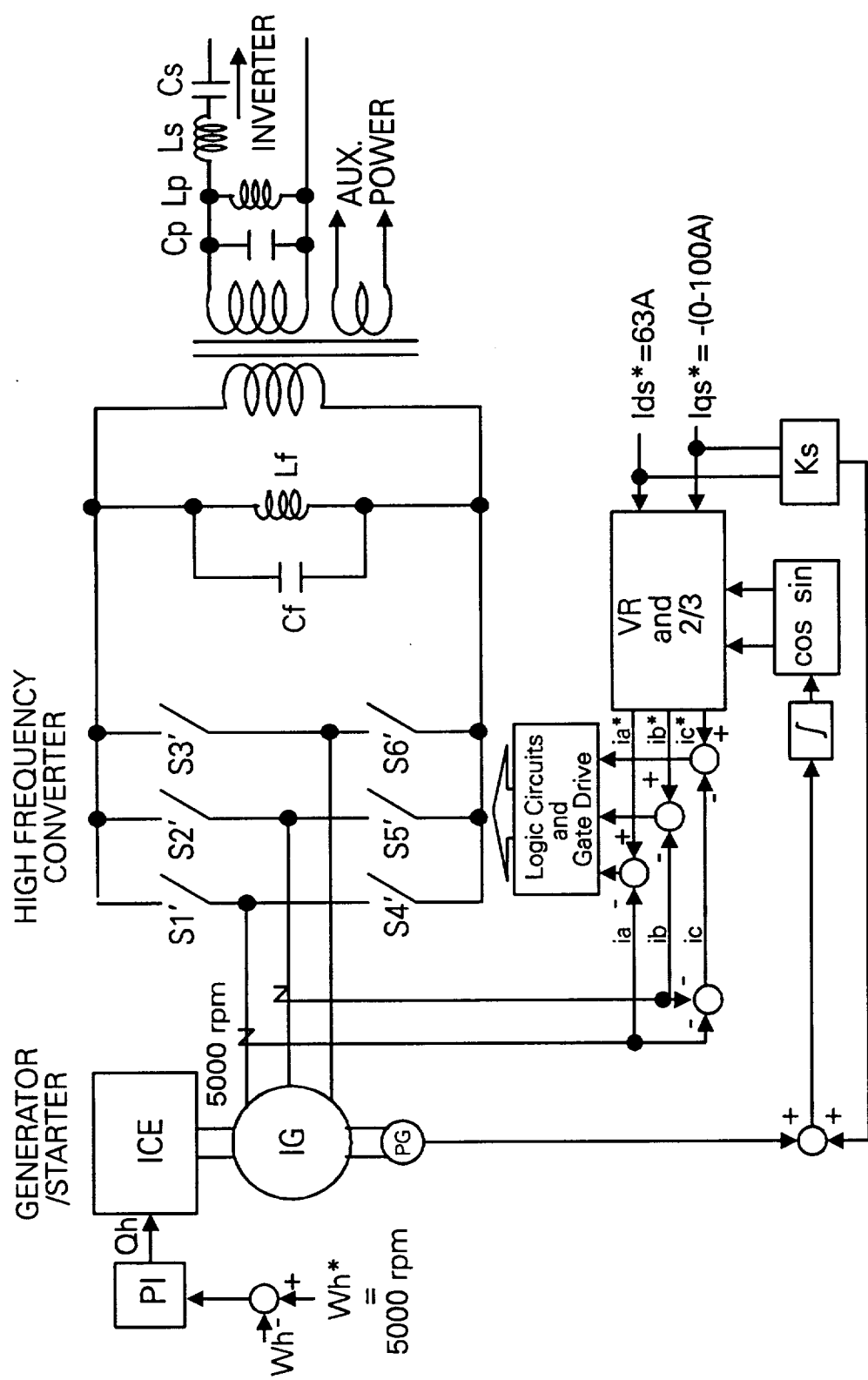
FIG. 30: CONTROL BLOCK DIAGRAM OF ICE AND GENERATOR

116

injection will be needed to minimize fluctuation of HFAC voltage.

15.3. Control of Resonant Inverter

Fig. 31 shows the control block diagram of the resonant inverter, and Fig. 32 shows the explanatory waves. As indicated before, the two legs of the H-bridge are controlled at variable phase angle to generate the quasi-square wave so as to regulate the output fundamental voltage irrespective of the battery voltage and load variation. The inverter operates with close loop voltage control with the feedback voltage signal derived from the HFAC link through a rectifier and lowpass filter. The error voltage through a PI (proportional - integral) controller is added to the bias voltage signal to constitute the $V_{cr}*$ signal , as shown. Since the inverter is to operate at slightly lagging power factor, the ideal HFAC frequency (20kHz) is added with f_{rr} (400Hz) to generate the actual frequency command (f_r). A control sawtooth wave is generated at frequency f_r, as shown. The bias voltage signal is generated such that the inverter operates at delta angle of 120 deg. at 300 V battery voltage. The angle will increase at lower voltage whereas it will decrease at higher voltage. The generation of IGBT gate drive signals for generation of quasi-square wave is indicated in the figure. The control circuit was valid for motoring mode of the drive system.

The developed control of the total system is shown in Fig. 33. Fig. 34 shows the conceptual digital signal processor based control where optimal power distribution
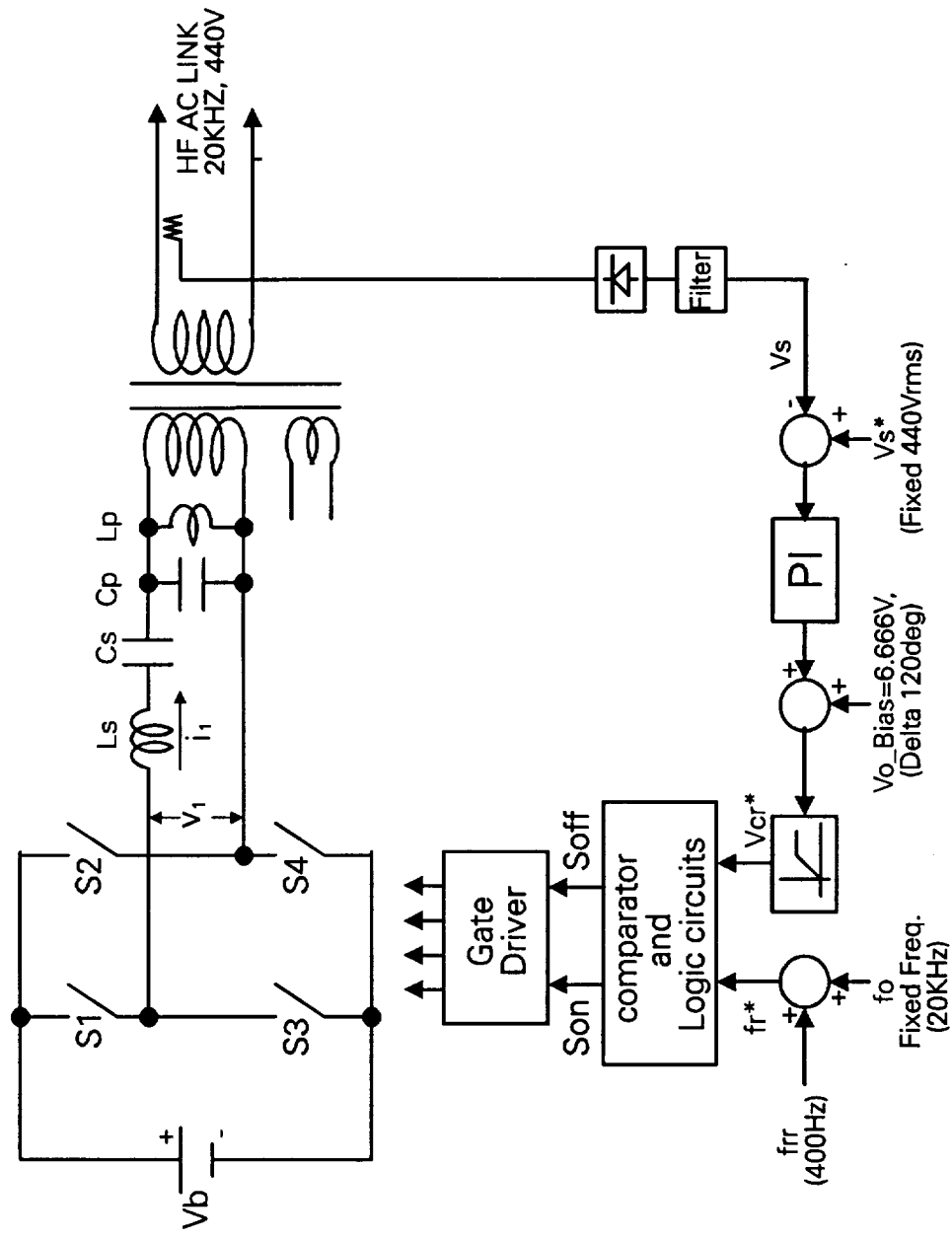
FIG. 31: CONTROL BLOCK DIAGRAM OF RESONANT INVERTER

118
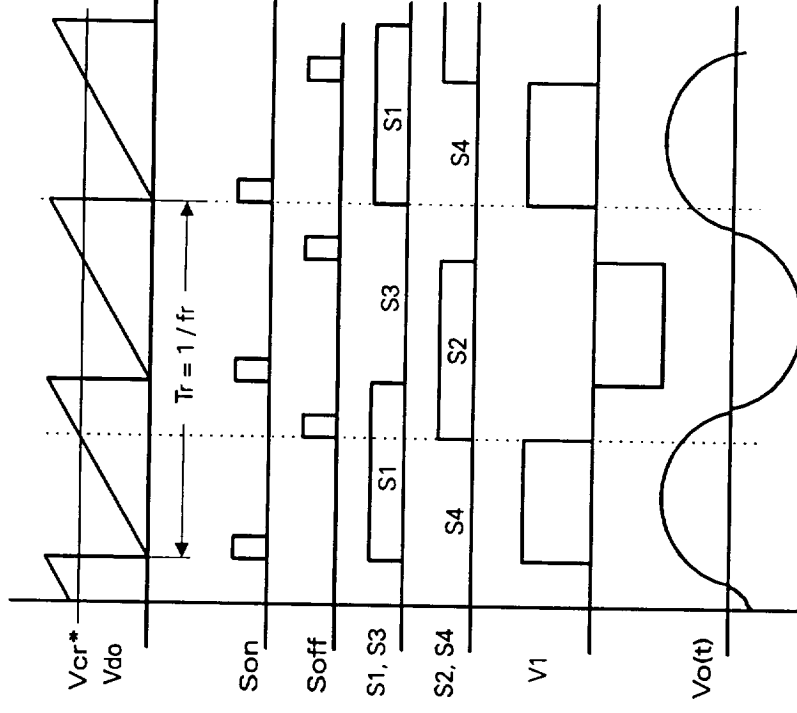
FIG. 32: CONTROL WAVES OF RESONANT INVERTER

119
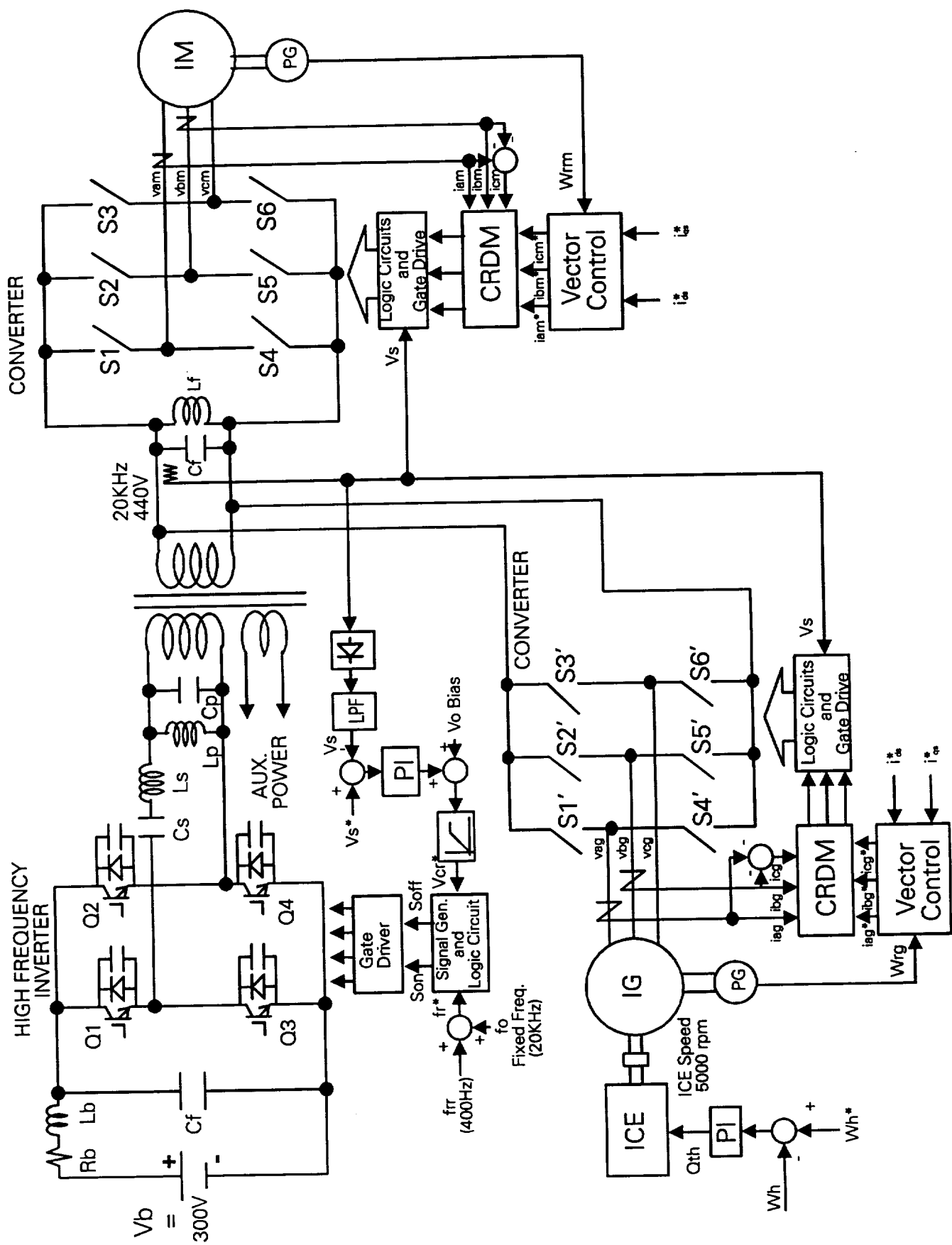
FIG. 33: CONTROL BLOCK DIAGRAM OF THE TOTAL
SYSTEM

120
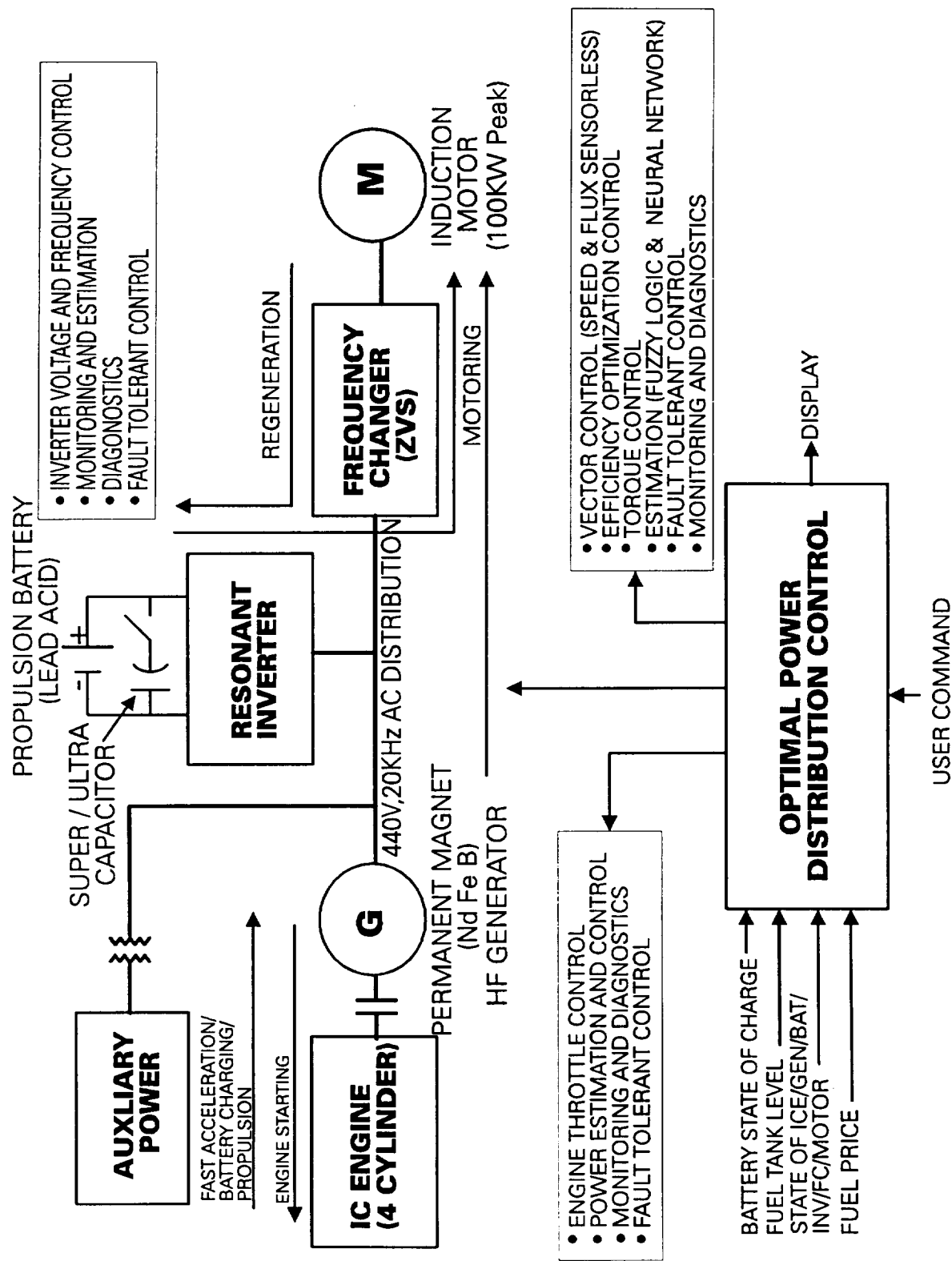
FIG. 34: CONCEPTUAL HFAC POWER DISTRIBUTION SYSTEM WITH DIGITAL SIGNAL PROCESSOR BASED CONTROL

121

control block has been added. Note that an ultracapacitor has been added in parallel with the battery to supplement its power capability.

16. Modeling and Simulation Study of the Candidate HFAC System

A preliminary modeling and simulation study of the candidate HFAC system given in Fig. 13 has been described in this section. The study is based on the numerical component sizing and control development described before. The performance of the system could be improved significantly by improvement of the control strategy but it could not be possible within the time constraint of the project. The language SIMNON (Engineering Software Concepts) was used for simulation. Initially, the total system was subdivided into several sub-systems, and modeling and simulation study was made on each sub-system. Finally, when each sub-system was operating successfully, the total system simulation was studied.

16.1. Battery - Resonant Inverter (Sub-System - 1)

The sub-system 1, as shown in Fig. 35, was first taken into consideration. The HFAC link supply (440 V, 20kHz) was generated by the open-loop voltage control of the resonant inverter, and was terminated by passive RL load. Only nominal battery voltage (300 V) that generates a quasi-square wave voltage at delta angle of 120 deg. was
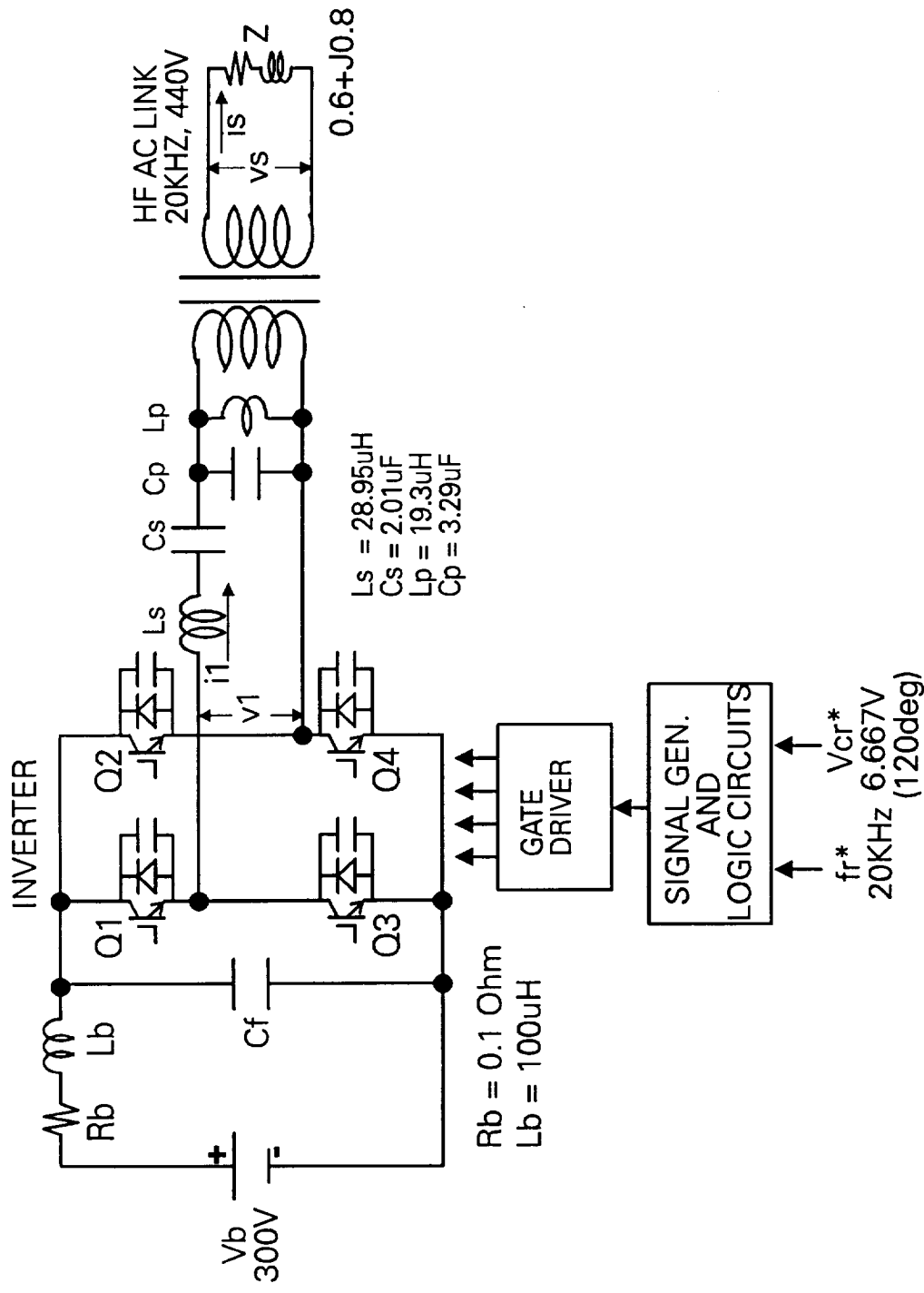
FIG. 35: SIMULATION BLOCK DIAGRAM FOR SUB-SYSTEM 1

123
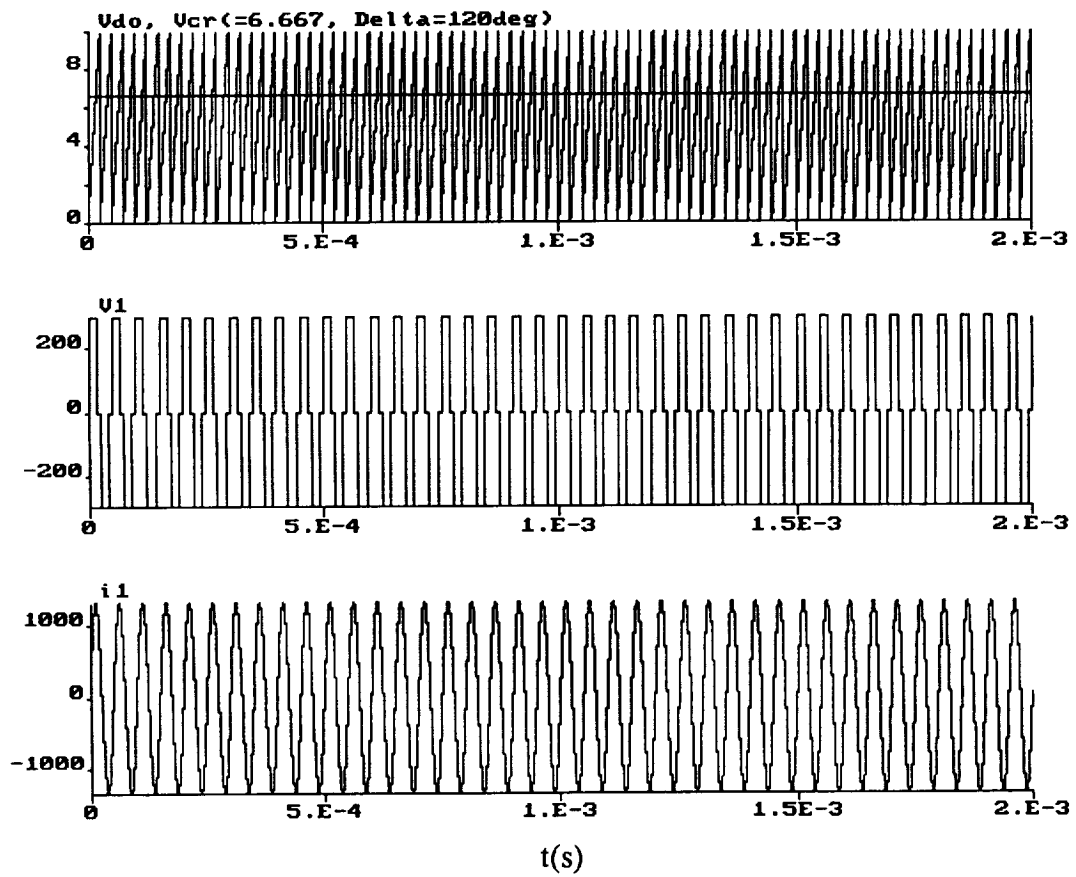
FIG. 36: WAVEFORMS OF Vdo, Vcr, V1 AND i1 (SUB-SYSTEM 1)

124
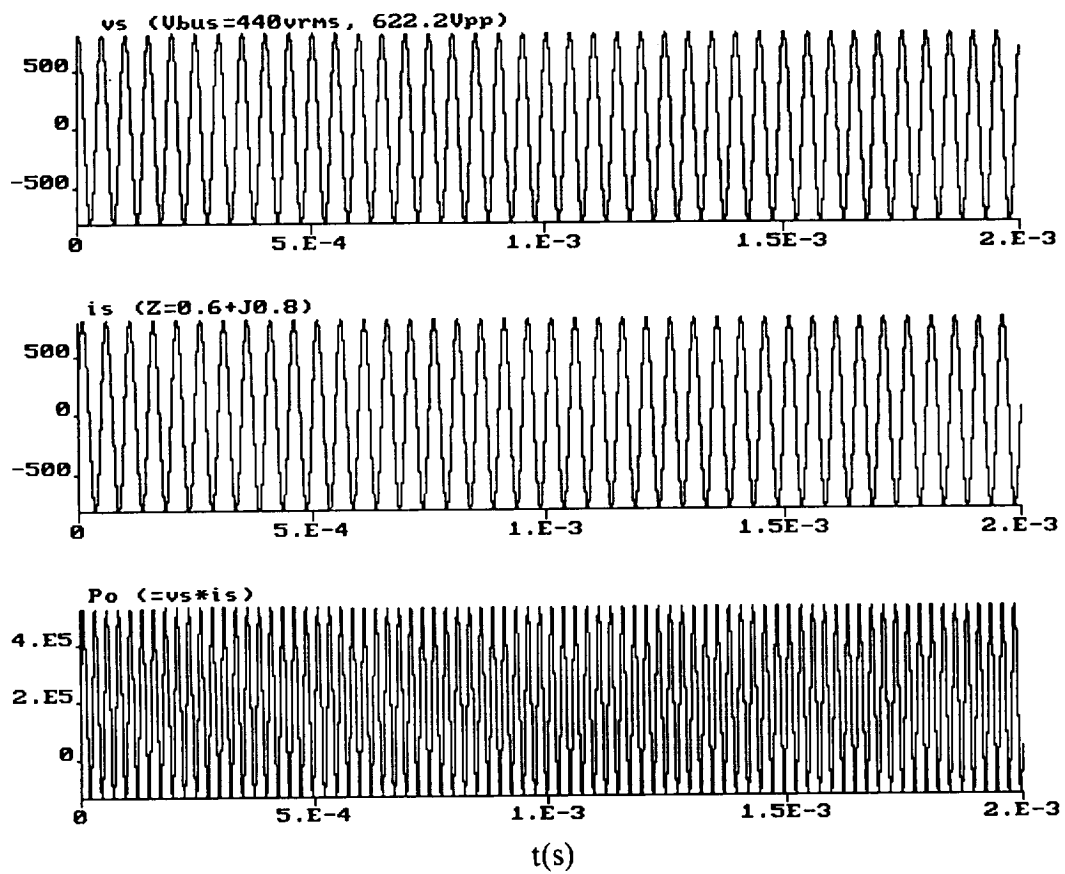
FIG. 37: WAVEFORMS OF vs, is AND P0 (SUB-SYSTEM 1)

125
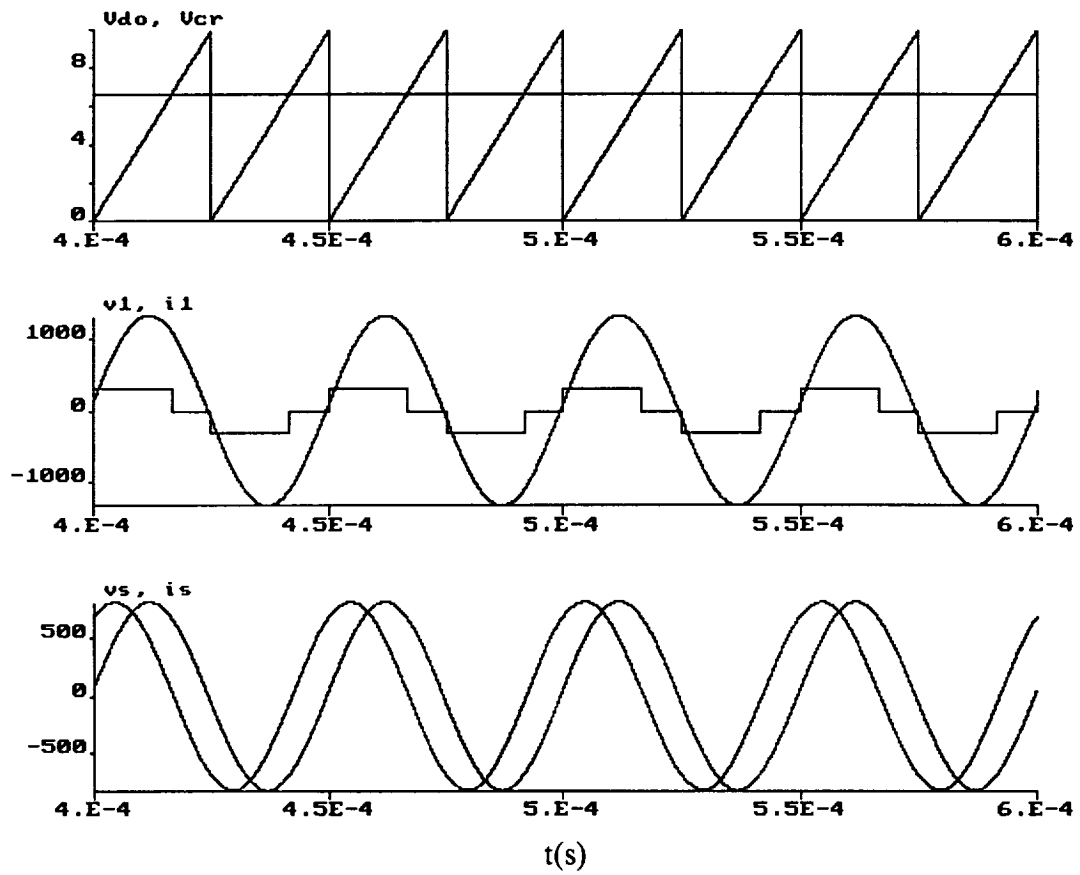
FIG. 38: EXPANDED WAVEFORMS OF Vdo, Vcr, v1, i1, vs AND is (SUB-SYSTEM 1)

126
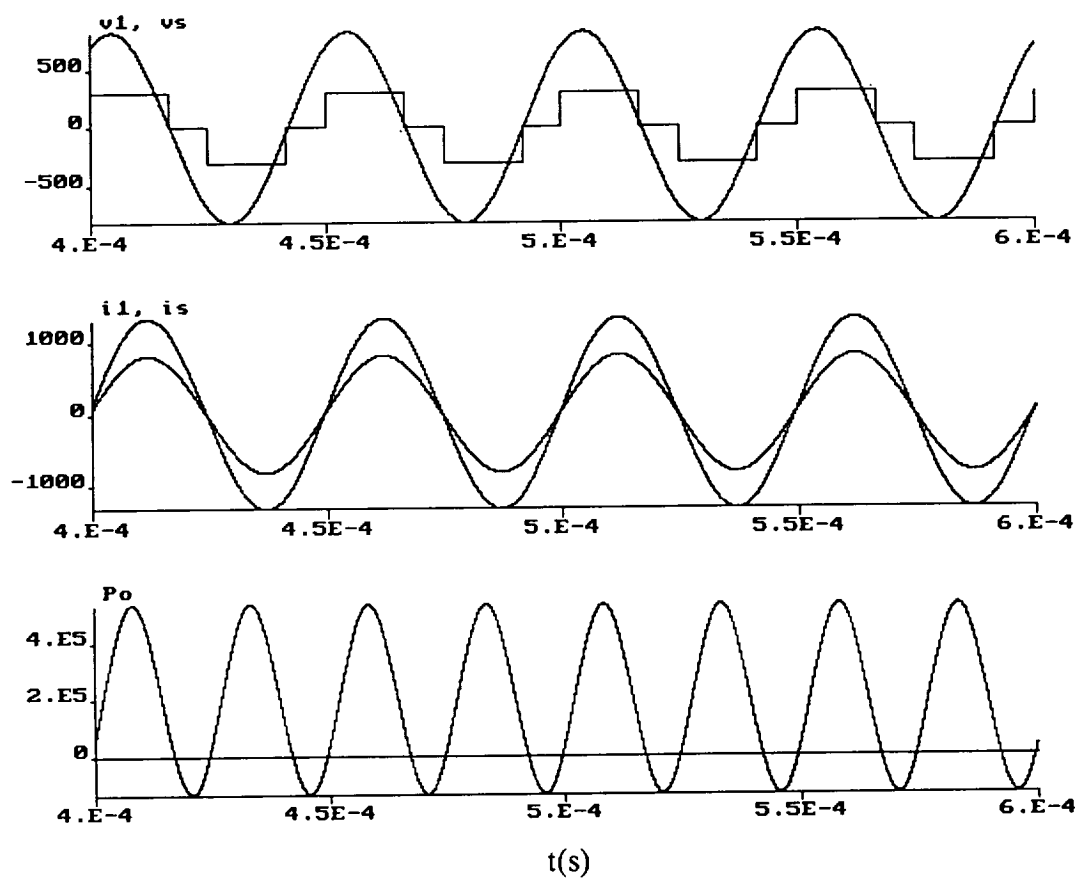
FIG. 39: EXPANDED WAVEFORMS OF v1, vs, i1, is AND P0 (SUB-SYSTEM 1)

127

considered. Fig. 36 shows the Vdo, Vcr*, v1 and i1 waves at ideal 20 kHz frequency with δ = 120 deg. (i.e. Vcr = 6.667 V). Fig. 37 shows the corresponding waveforms of Vs, is and instantaneous power P0 waves for load impedance of Z = 0.6 + J0.8 Ohms. Figs. 38 and 39 show the expanded view of these waves. The currents i1and is lag with respect to their fundamental components of voltage. Both the current waves i 1 and is are in phase except the amplitude difference because of the transformer.

16.2. HFAC - Converter - Induction Motor (Sub-System - 2)

The configuration for this sub-system is shown in Fig. 40. An ideal HFAC source was considered for this study. The induction motor was represented by dynamic d -q model (synchronously rotating reference frame). A Delco Remy 100 kW (peak power) machine designed for EV drive was taken for the simulation study. The machine parameters are shown in Table 17.

Table 17: Parameters for 100 kW (Peak Power) Machine

==

Line Voltage = 240 V

Poles = 4

Rated i_{ds} = 63 A

Rated i_{qs} = 278 A (50 kW)

Peak i_{qs} = 556 A

Rated Stator Current = 202 A

Maximum Speed = 14,000 rpm

Power Factor = 0.8

Stator Resistance (R_s) = 0.01121 Ohm

Rotor Resistance (R_r) = 0.01243 Ohm

Stator Leakage Inductance (L_{ls}) = 0.001314 mH *

Rotor Leakage Inductance (L_{lr}) = 0.001314 mH*

Magnetizing Inductance (L_m) = 2.13 mH

==

* Leakage inductances were multiplied by 3 for the simulation study

As mentioned before, the EV drive is essentially a torque-controlled system. But, for the convenience of simulation study, a speed-controlled system was considered. Fig. 40 shows the sub-system for simulation study. Fig. 41 shows the speed loop response, vs and is waves, and Fig. 42 shows the corresponding current and torque responses. The torque component of current iqs remains saturated (500 A) during accleration, and then falls to the steady state value as demanded by the steady state load torque (Tl), but the magnetizing current ids always remains constant at 63 A. Fig. 43 shows the machine phase voltages, and Fig. 44 shows the corresponding waveforms at expanded scale. Fig. 45 shows the expanded view of HFAC voltage, current and instantaneous power waves. The current is flat-topped and highly distorted which has low distortion factor but near unity displacement factor. It also contains small amount of subharmonics. The

FIG. 40: SIMULATION BLOCK DIAGRAM FOR SUB-SYSTEM 2

130
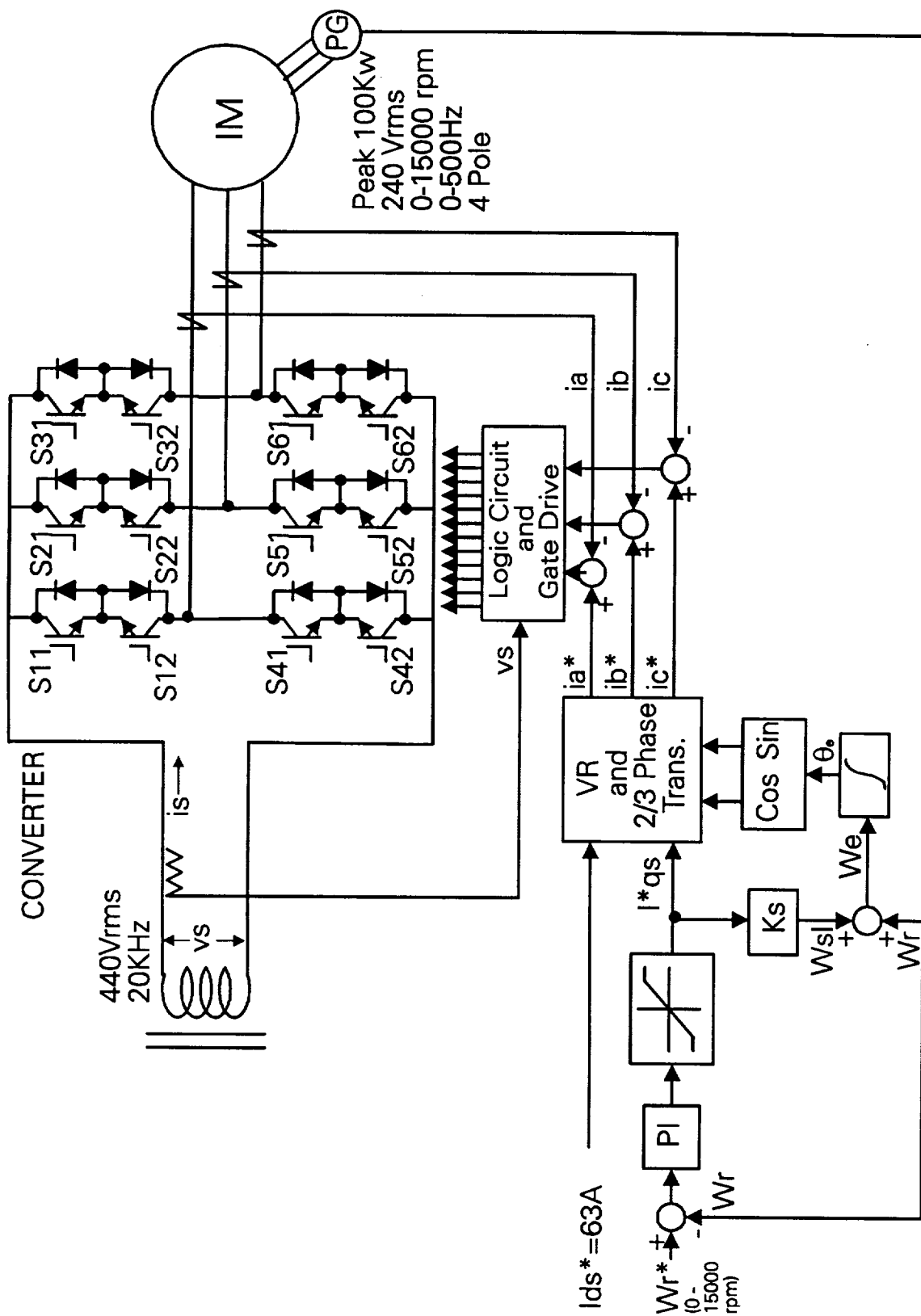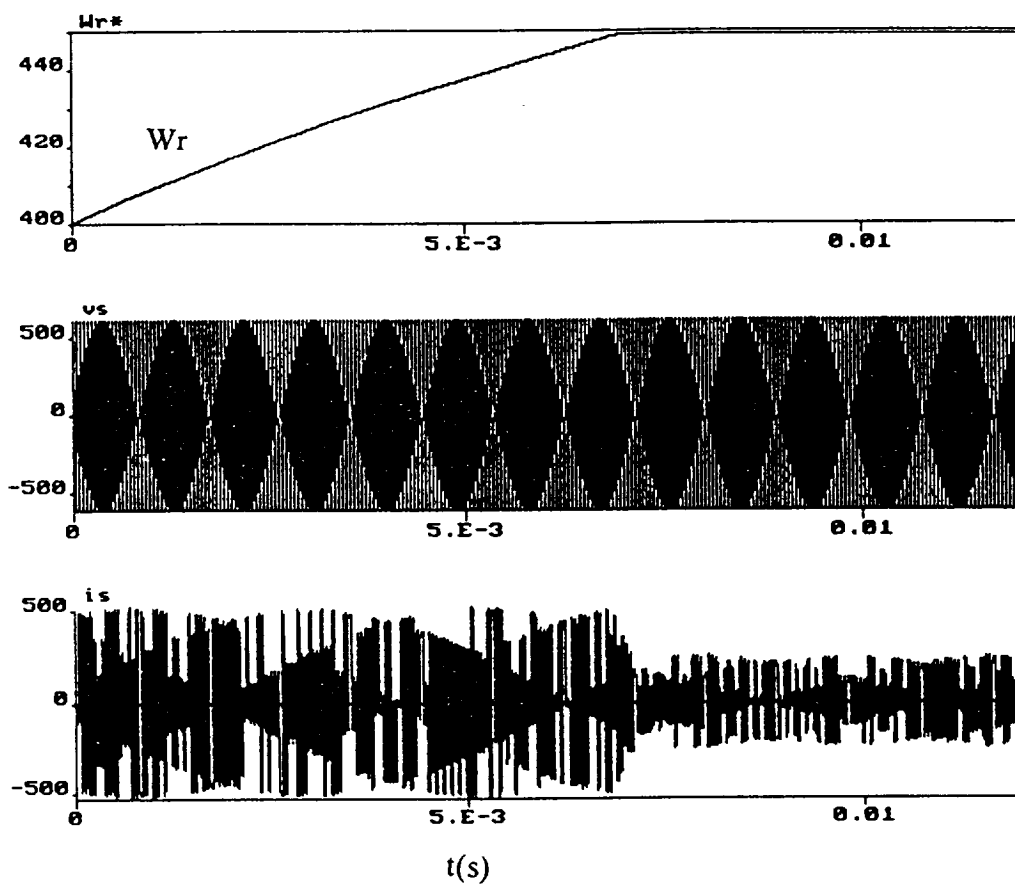
FIG. 41: WAVEFORMS OF Wr*- Wr, vs AND is (SUB-SYSTEM 2)

131
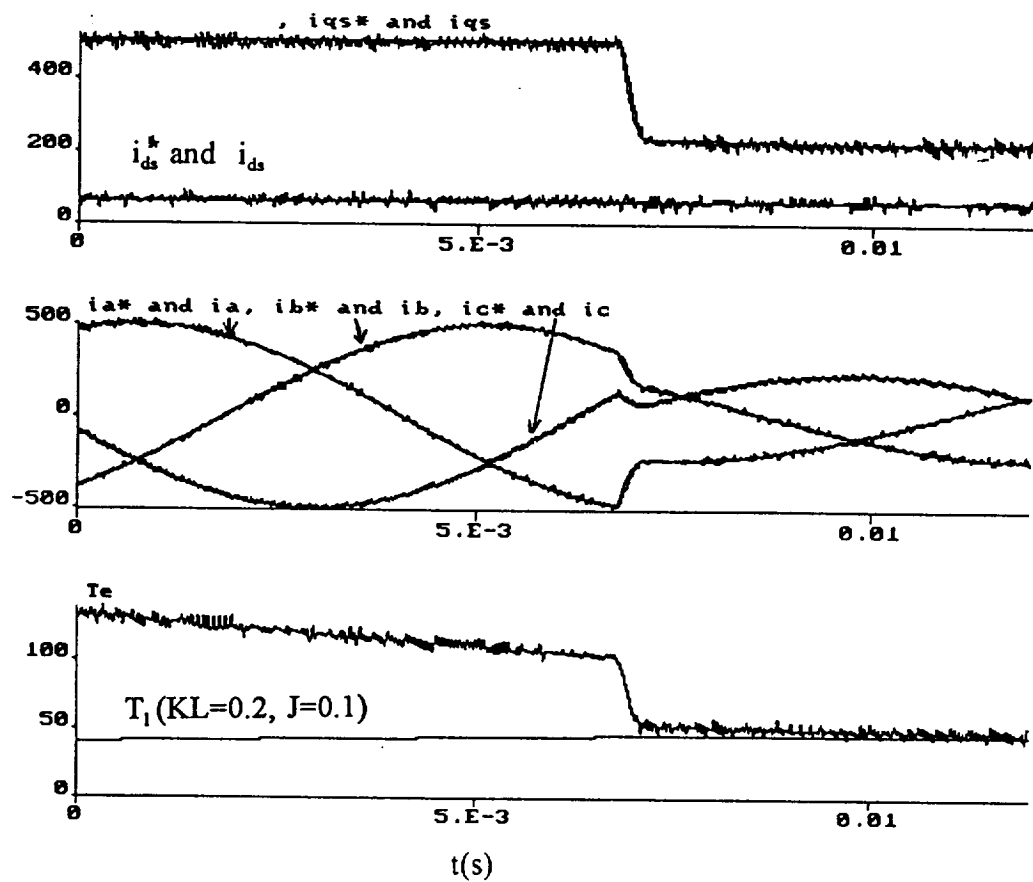
FIG. 42: WAVEFORMS OF ids, iqs, ia*-ia, ib*-ib, ic*-ic, Te AND Tl
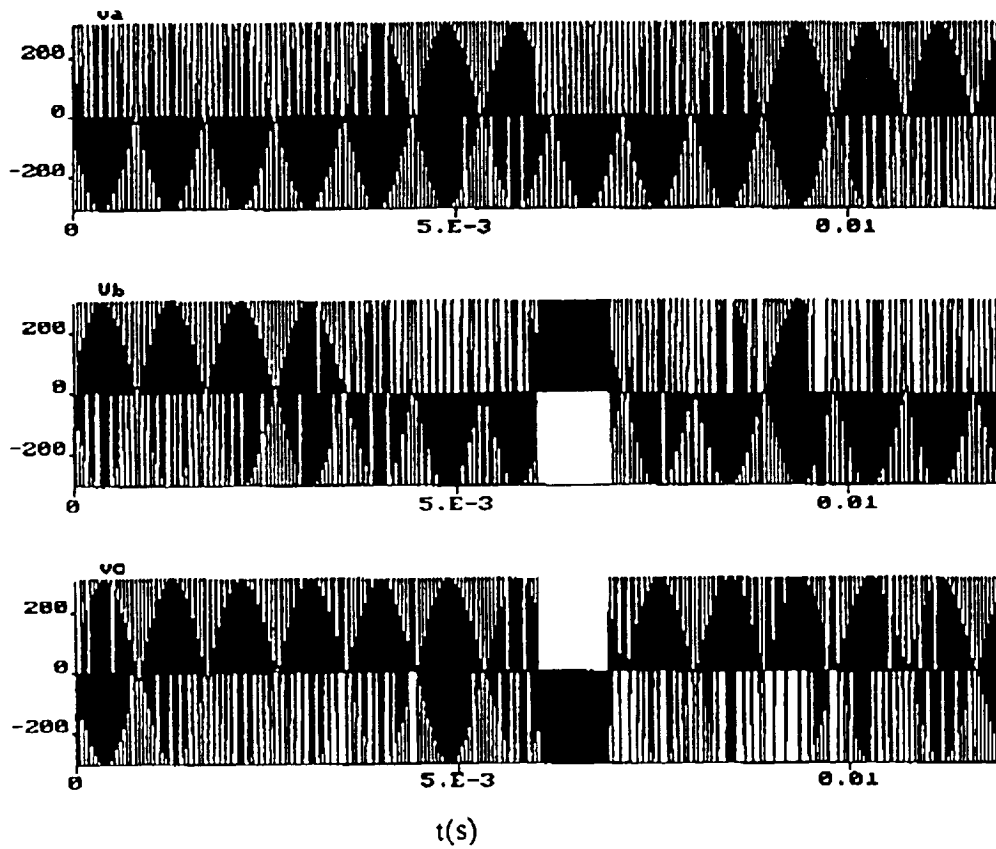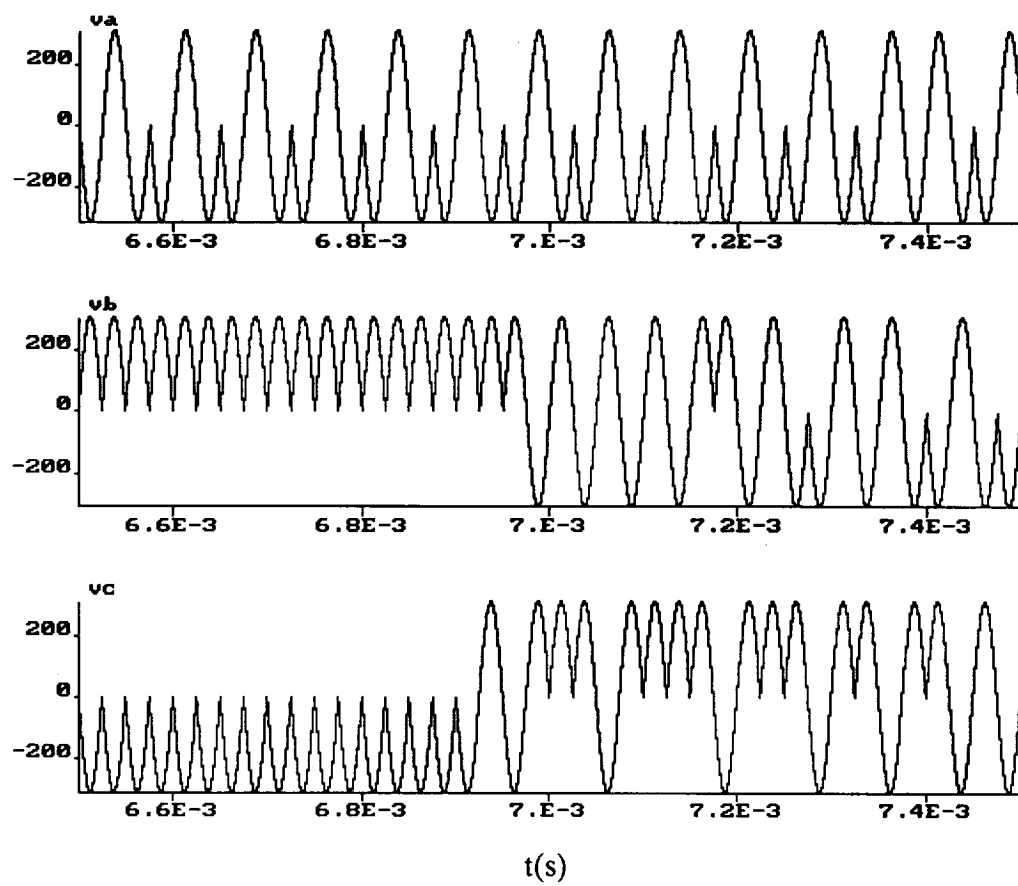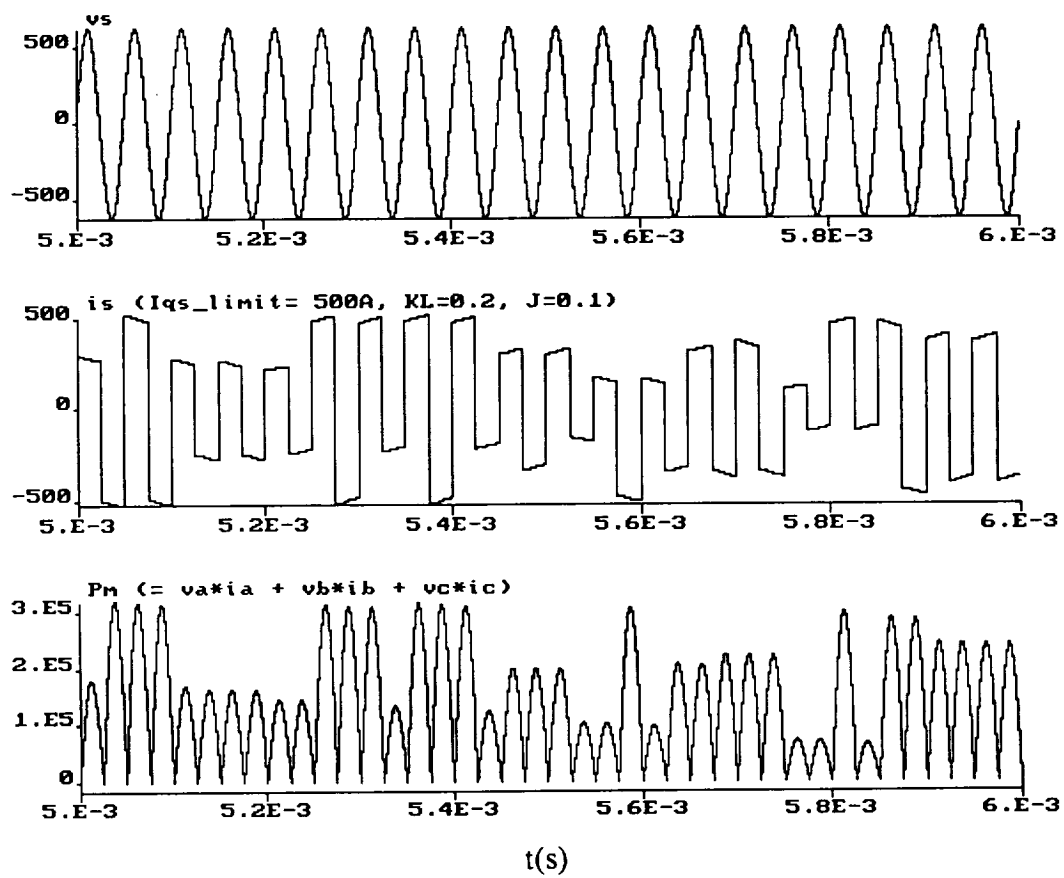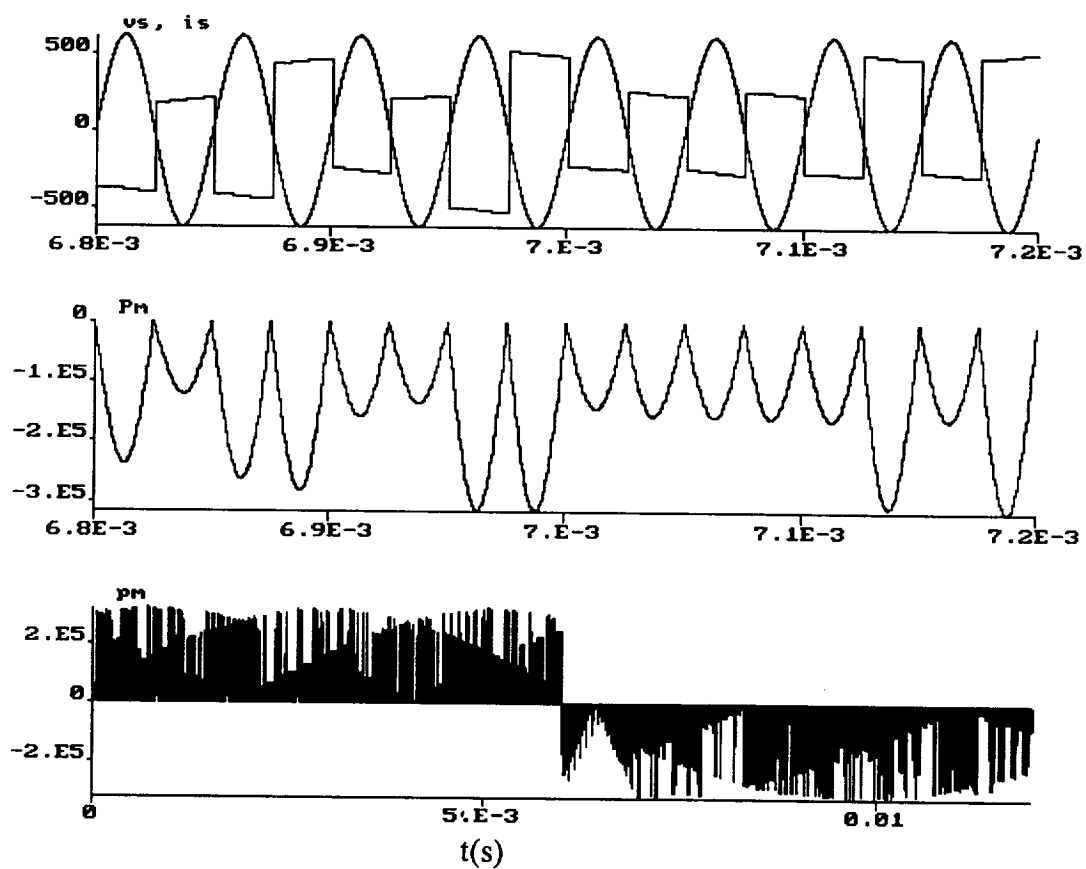**(SUB-SYSTEM 2)**

132
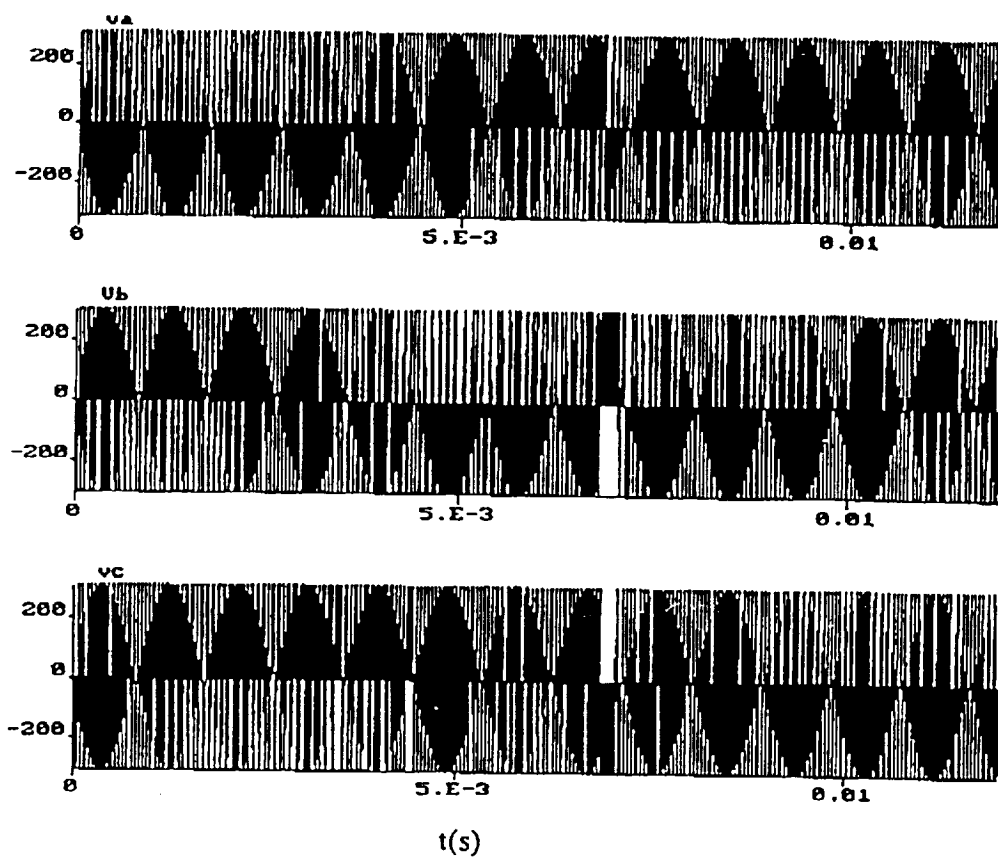
FIG. 43: WAVEFORMS OF va, vb AND vc (SUB-SYSTEM 2)

133
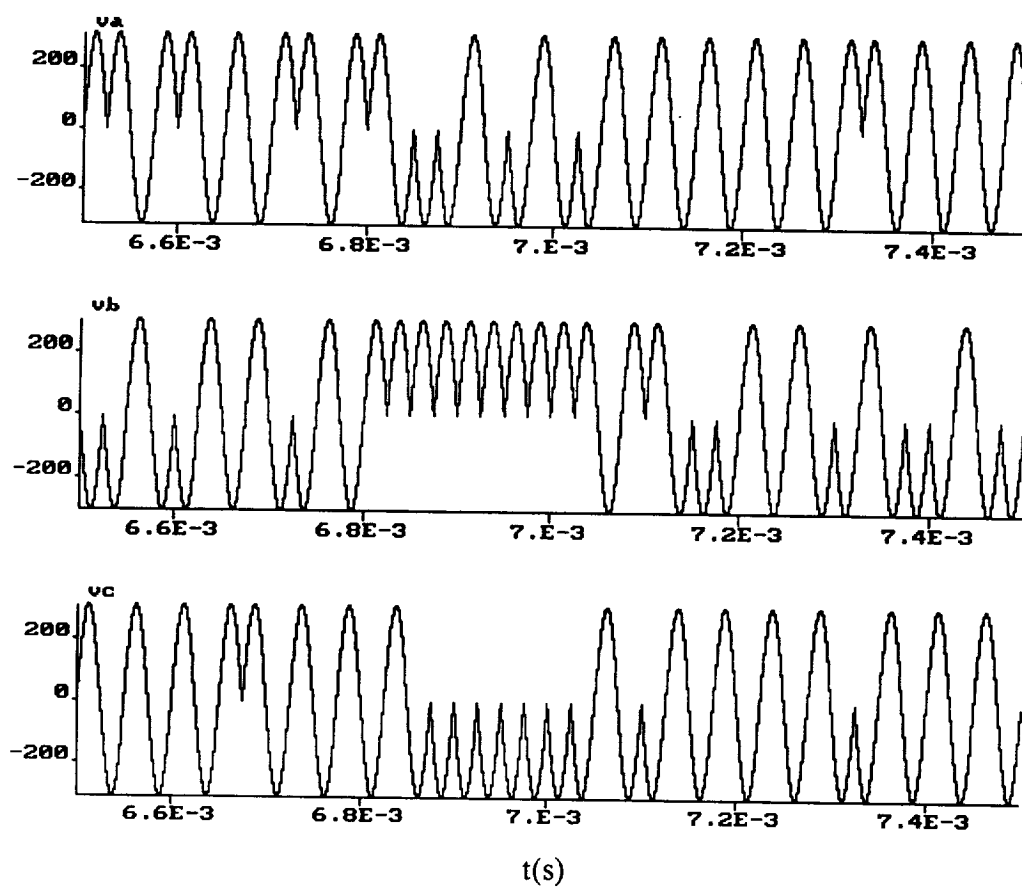
**FIG. 44: EXPANDED WAVEFORMS OF va, vb AND vc
(SUB-SYSTEM 2)**

134
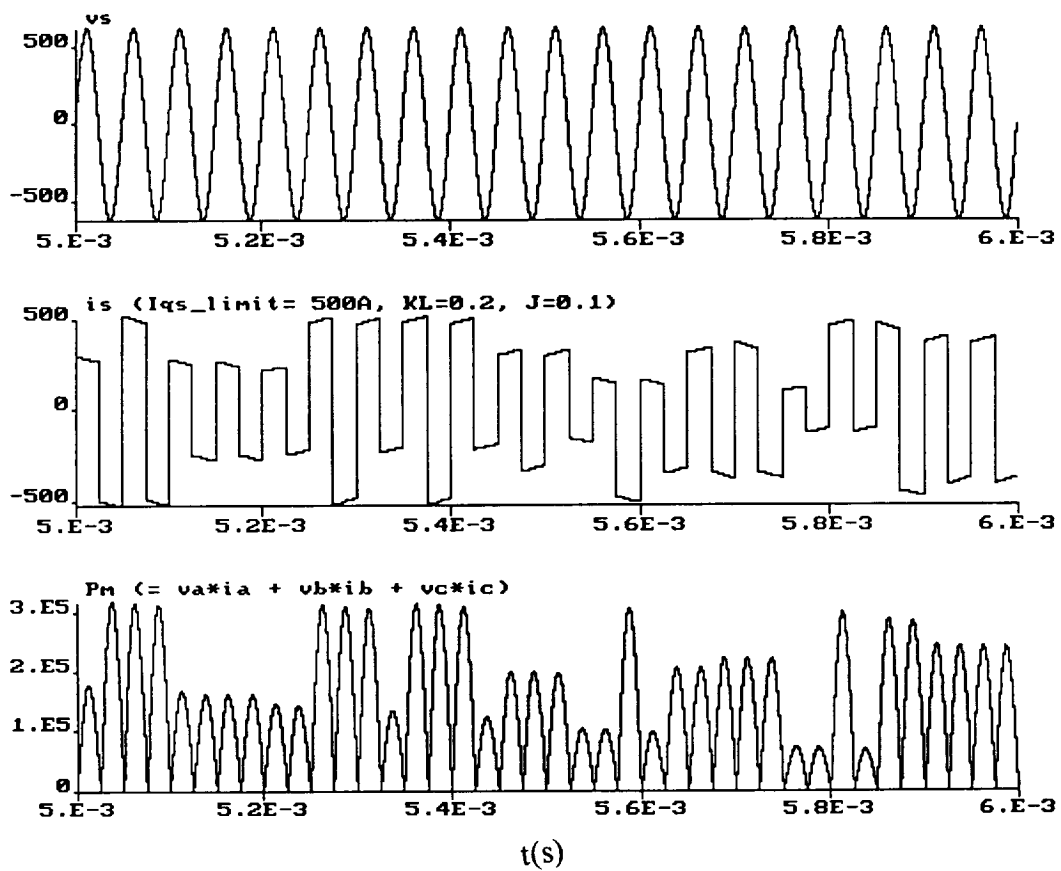
FIG. 45: EXPANDED WAVEFORMS OF vs, is AND Pm (SUB-SYSTEM 2)
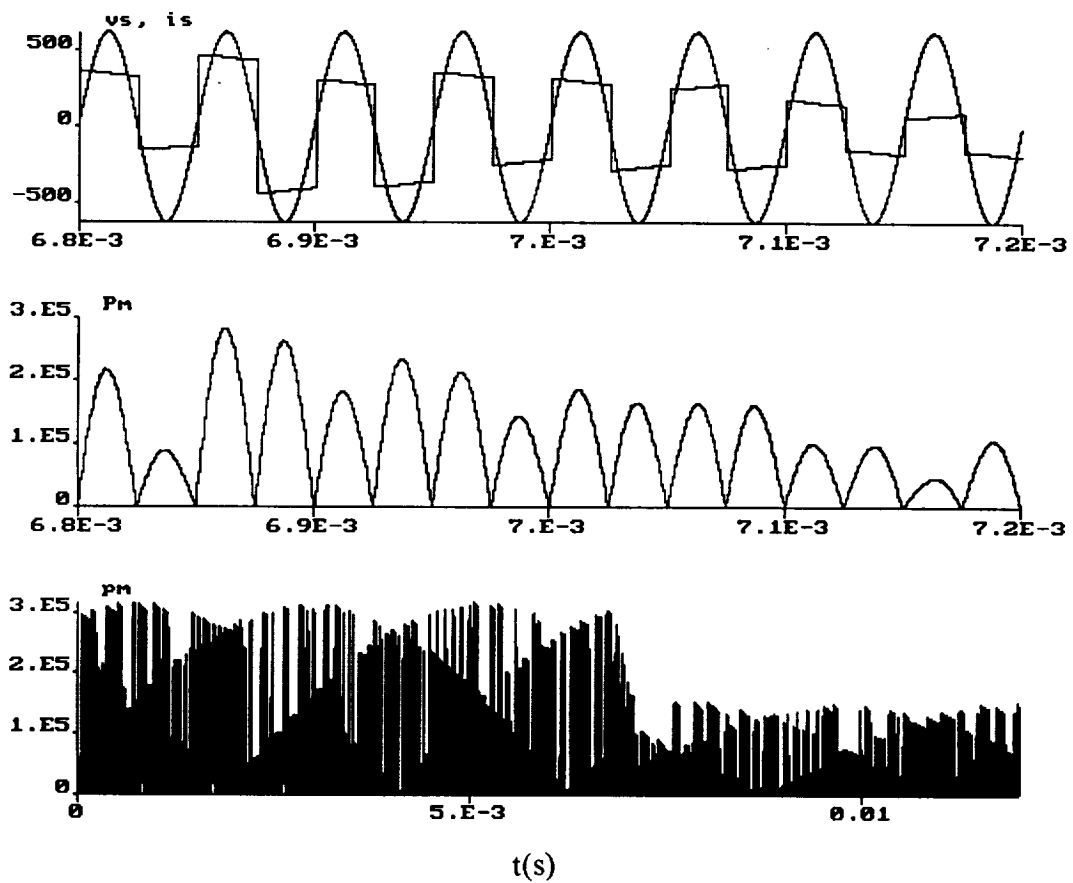
FIG. 46: EXPANDED WAVEFORMS OF vs, is AND Pm
(SUB-SYSTEM 2)

136
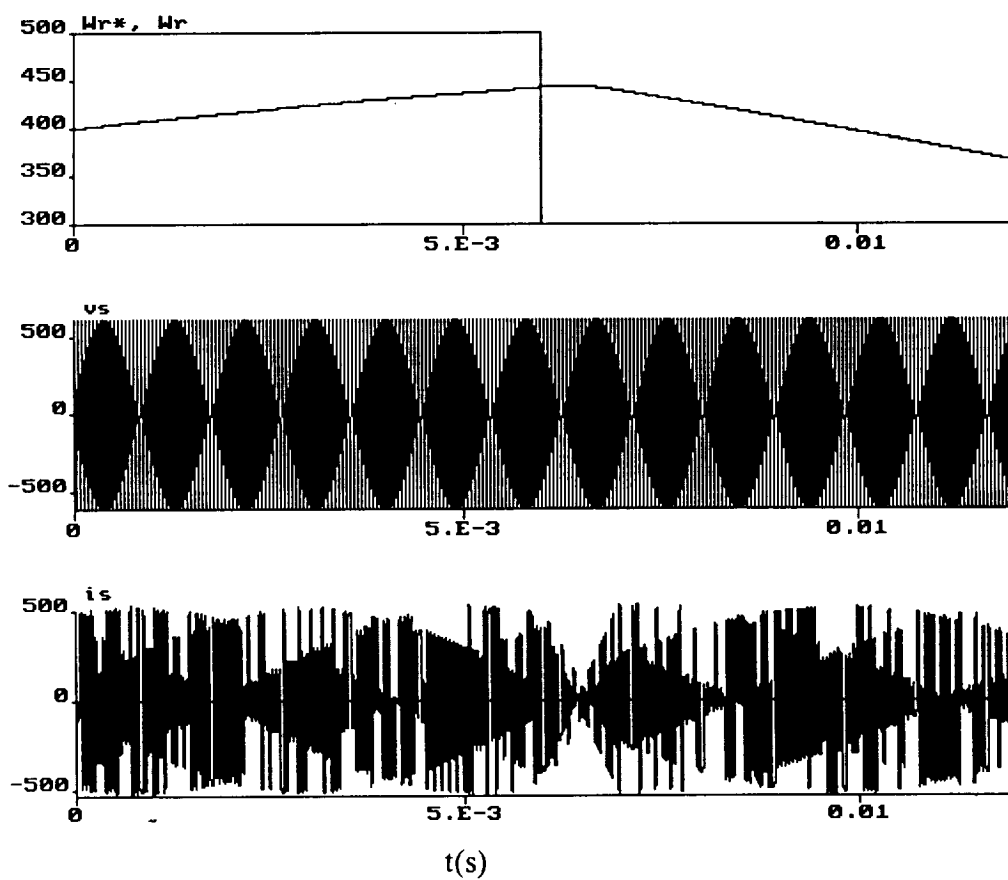
**FIG. 47: WAVEFORMS OF Wr*-Wr, vs AND is
(SUB-SYSTEM 2)**

137
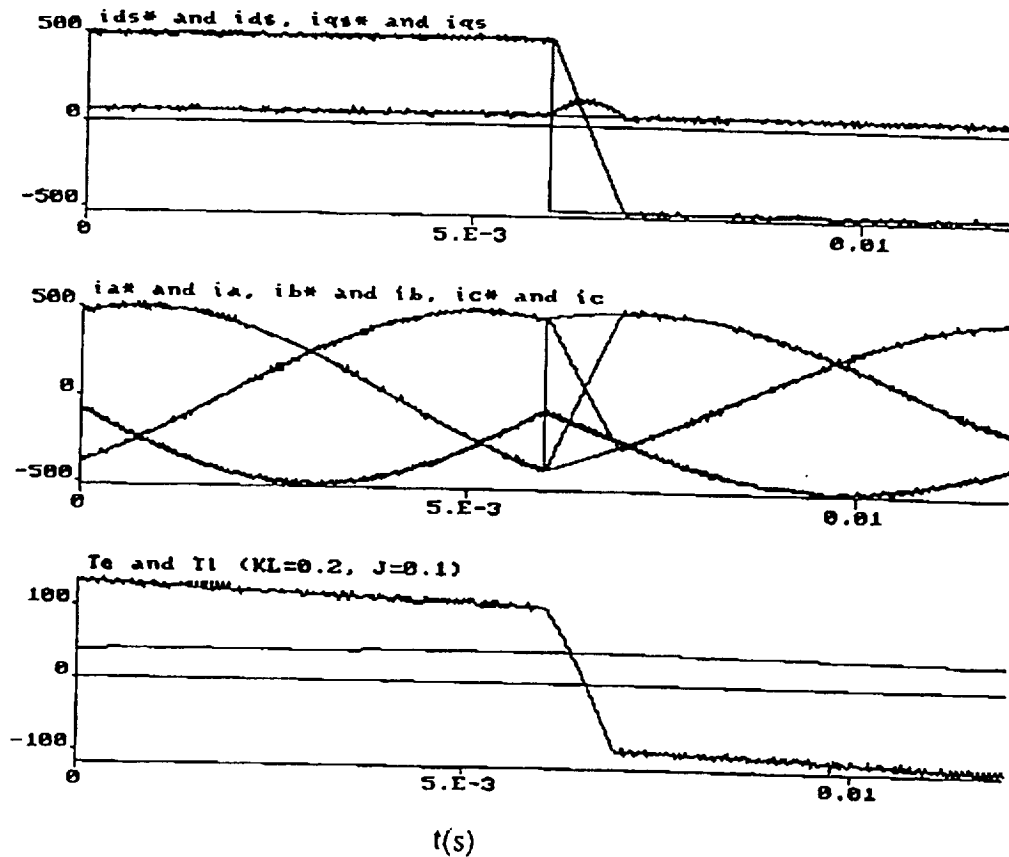
FIG. 48: WAVEFORMS OF ids*-ids, iqs*-iqs, ia*-ia, ib*-ib, ic*-ic, Te AND Tl   (SUB-SYSTEM 2)

FIG. 49: WAVEFORMS OF va, vb AND vc (SUB-SYSTEM 2)

139

**FIG. 50: EXPANDEDWAVEFORMS of va, vb AND vc
(SUB-SYSTEM 2)**

FIG. 51: EXPANDED WAVEFORMS OF vs, is AND Pm
(SUB-SYSTEM 2)

141

**FIG. 52: EXPANDED WAVEFORMS OF vs, is AND Pm
(SUB-SYSTEM 2)**

142

instantaneous power wave is fluctuating, as expected. In Fig. 46, the vs and is waves are superimposed . Fig. 47 demonstrates motoring and regeneration mode of operation of the drive. The corresponding waveforms are shown in detail in Figs. 48- 52. The phase of is changes from motoring to regeneration, and the corresponding average power becomes negative.

16.3. Battery - Inverter - Converter - Induction Motor (Sub-System 3)

The sub-systems 1 and 2 are cascaded to constitute the sub-system 3, as shown in Fig. 53. It is definitely a more complex system demanding sophisticated control. Note that the resonant inverter has been controlled with close loop voltage control and a resonant filter has been added at the input of the motor converter to trap the current harmonics. The system has been studied only for steady state condition. Fig. 54 shows the speed, voltage vcr and the inverter voltage loop response. The machine shaft has high inertia, and therefore, the speed change from initial speed is minimal within 10 ms
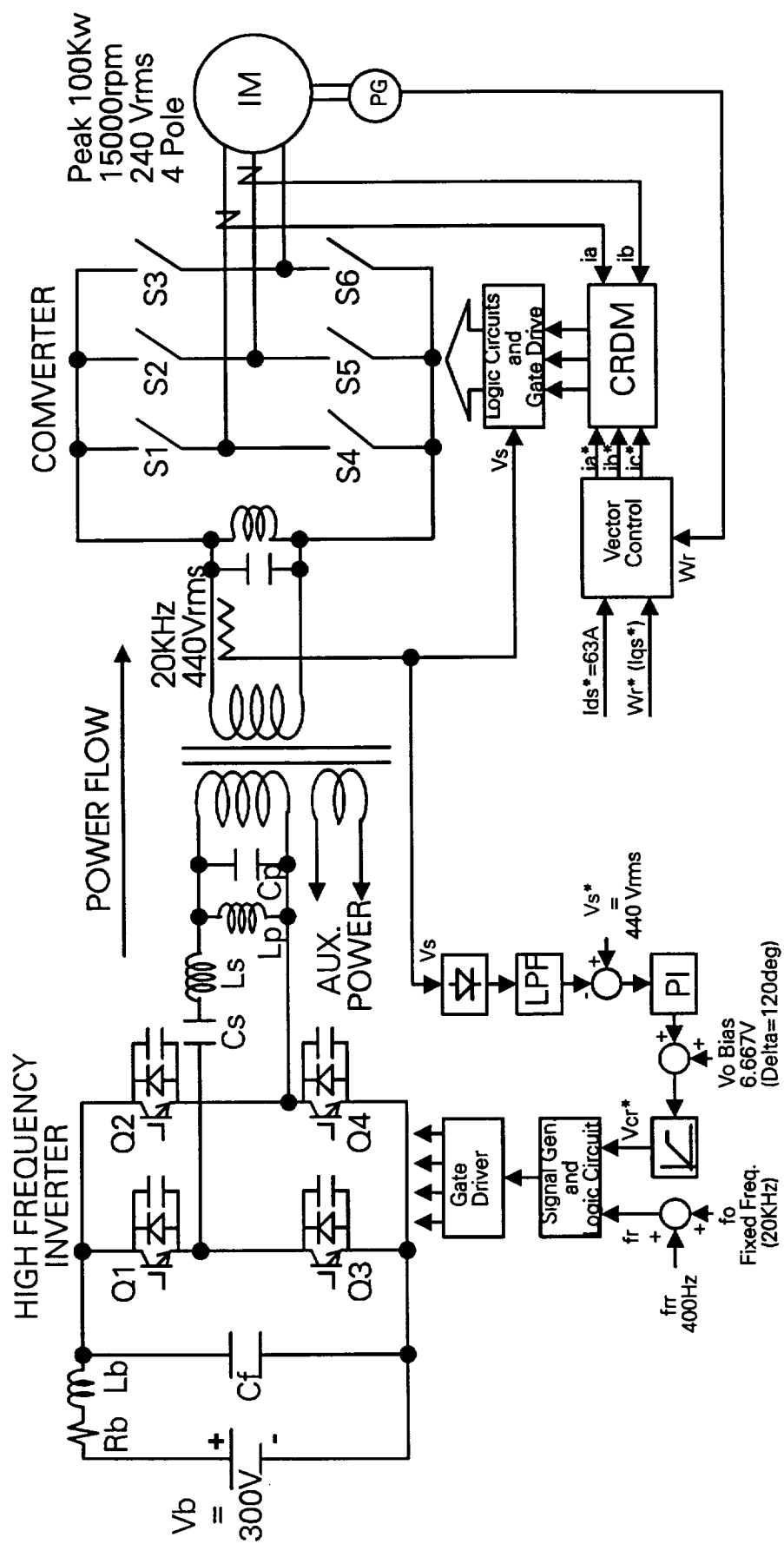
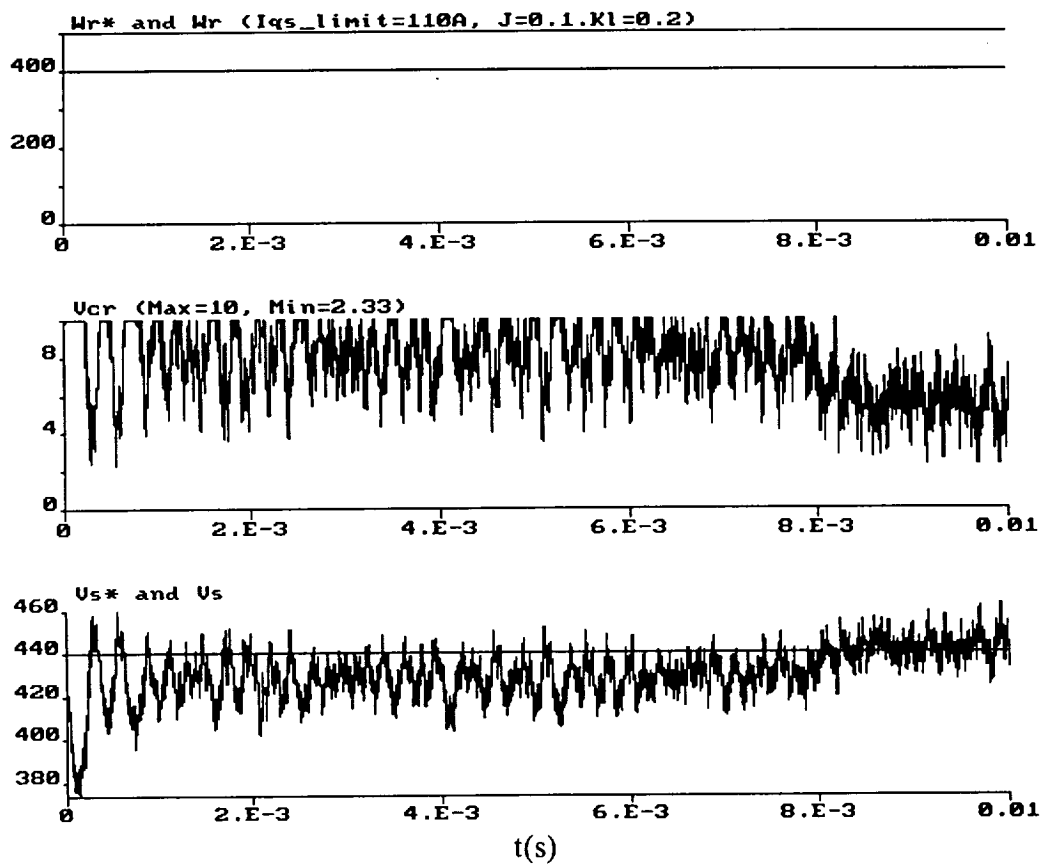**FIG. 53: SIMULATION BLOCK DISGRAM FOR SUB-SYSTEM 3**

144

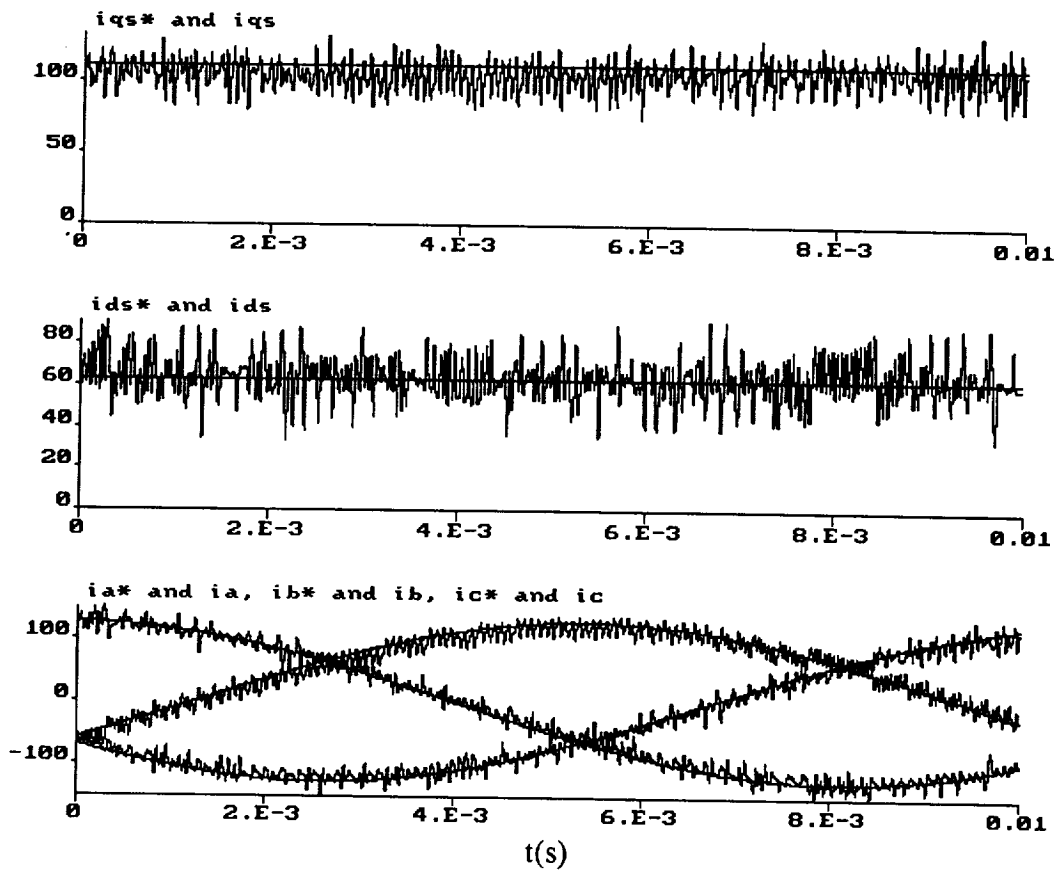**FIG. 54: WAVEFORMS OF Wr*- Wr, Vcr AND Vs*-Vs
(SUB-SYSTEM 3)**

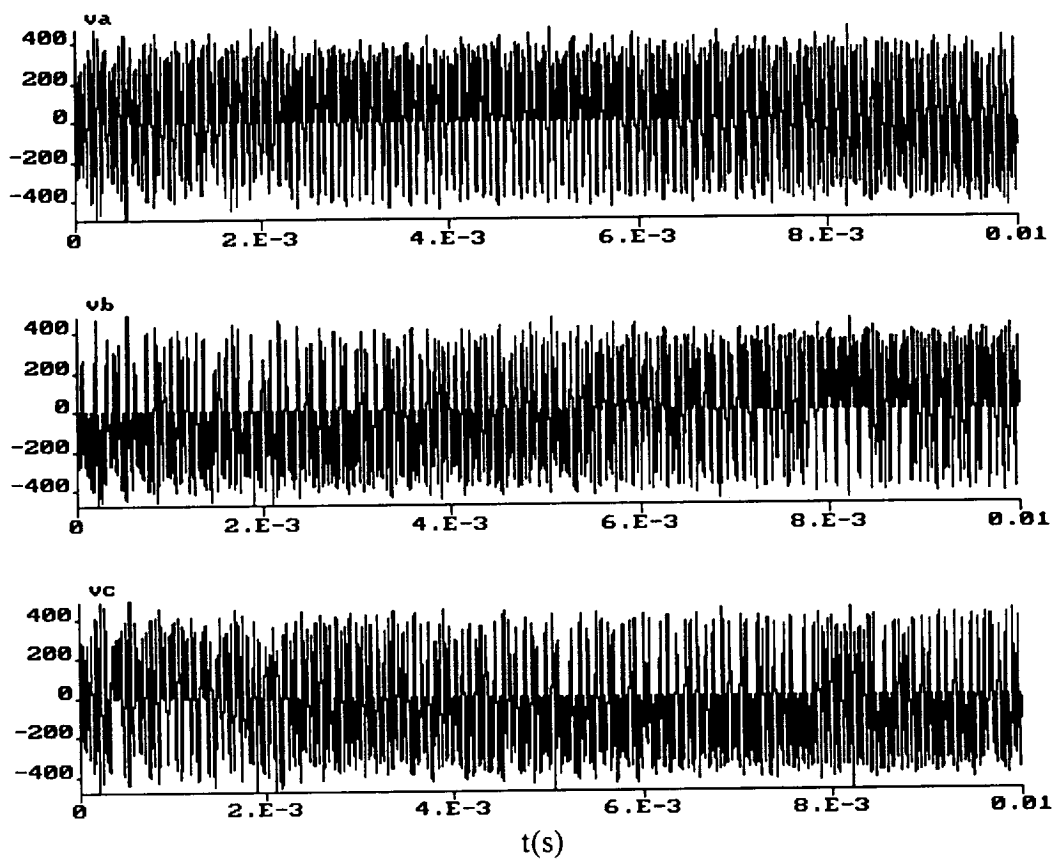**FIG. 55: WAVEFORMS OF iqs*-iqs, ids*-ids, ia*-ia, ib*-ib AND ic*-ic (SUB-SYSTEM 3)**

146

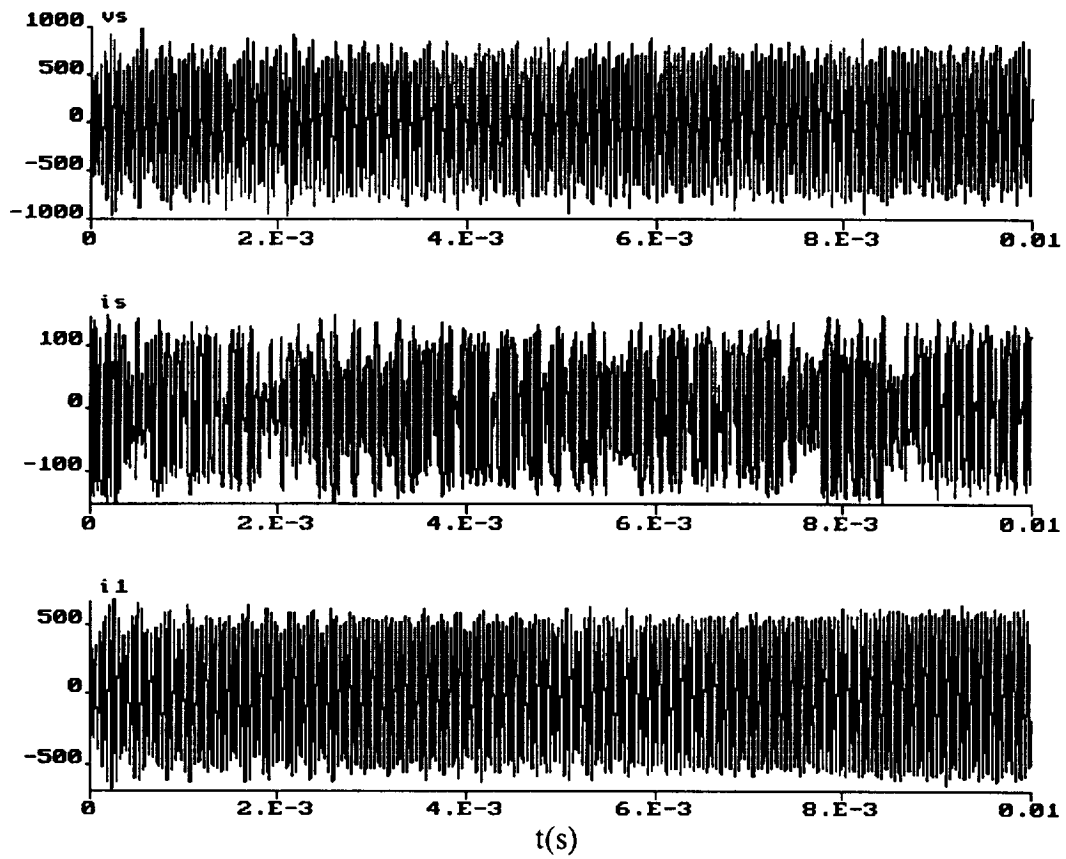FIG. 56: WAVEFORMS OF va, vb AND vc (SUB-system 3)

147

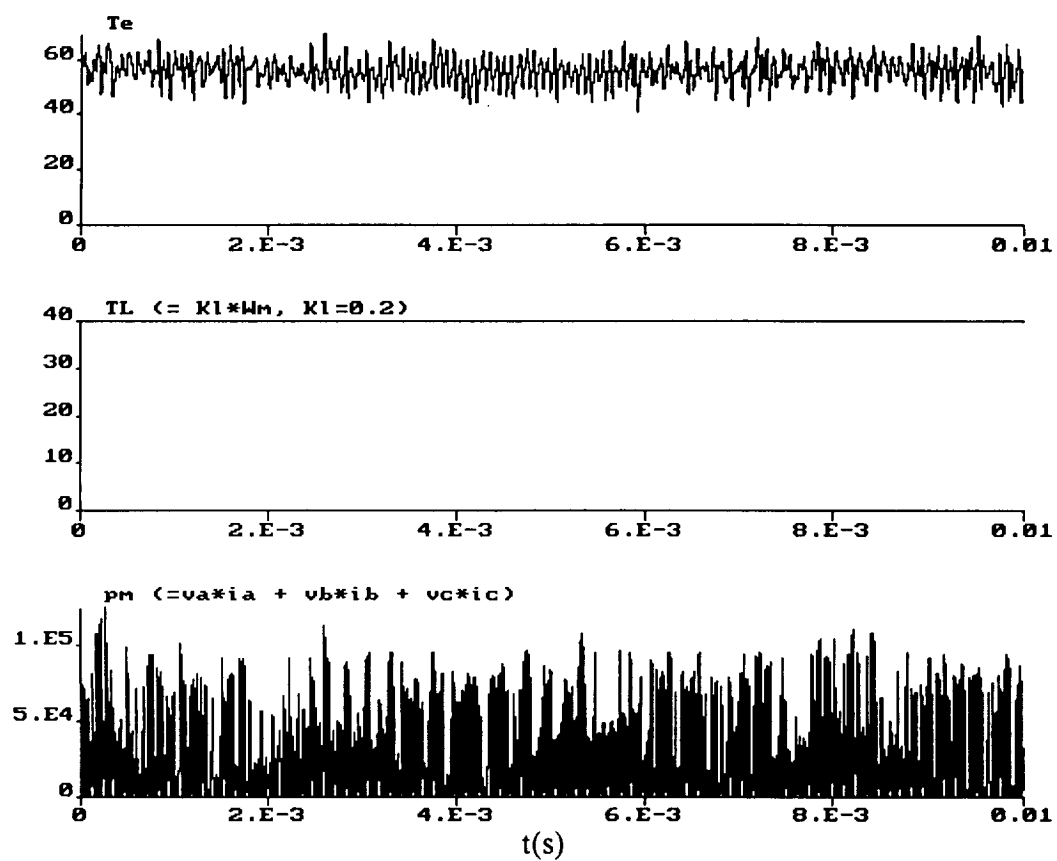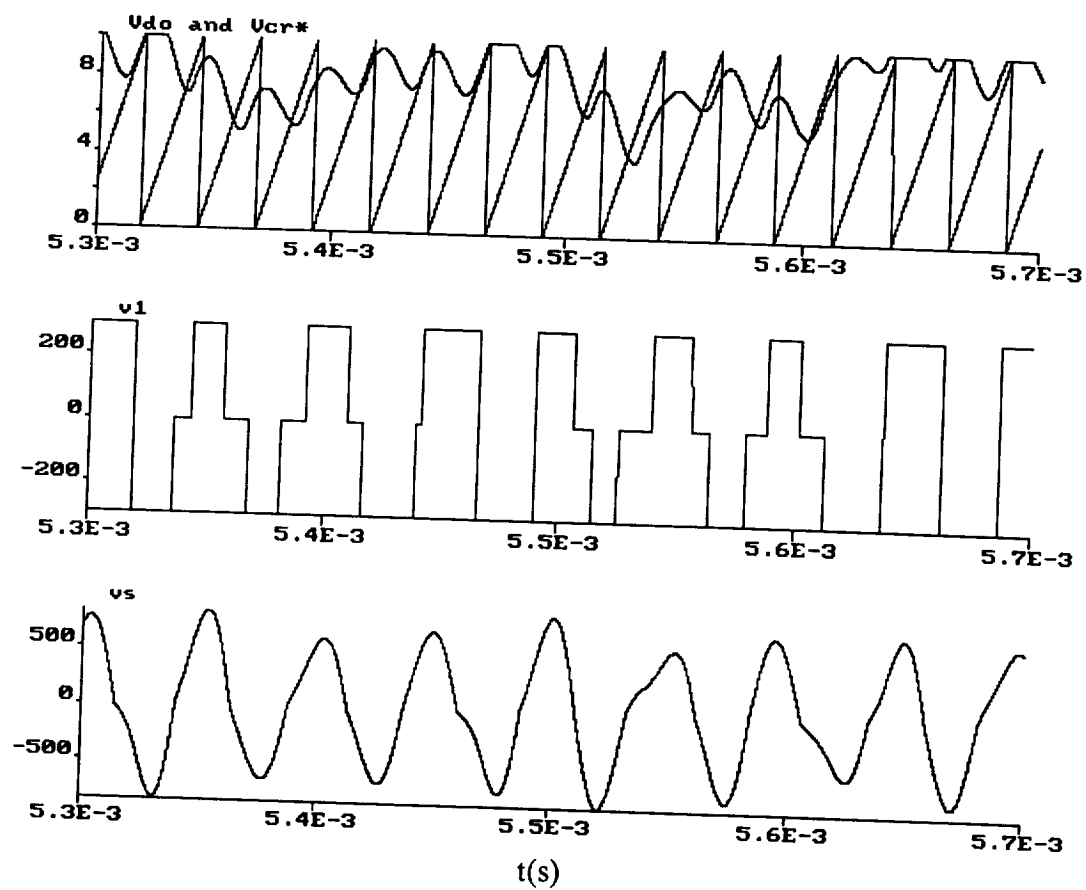FIG. 57: WAVEFORMS OF vs, is AND i1 (SUB-SYSTEM 3)

148

FIG. 58: WAVEFORMS OF Te, Tl AND Pm (SUB-SYSTEM 3)

149

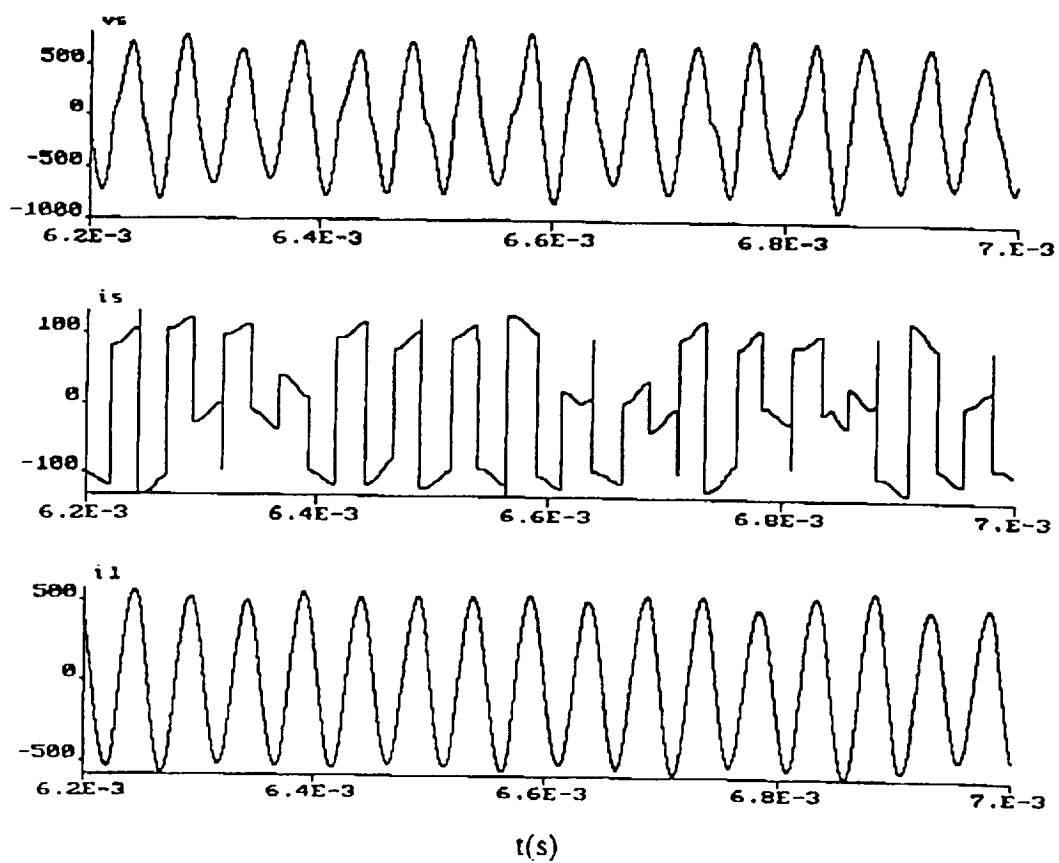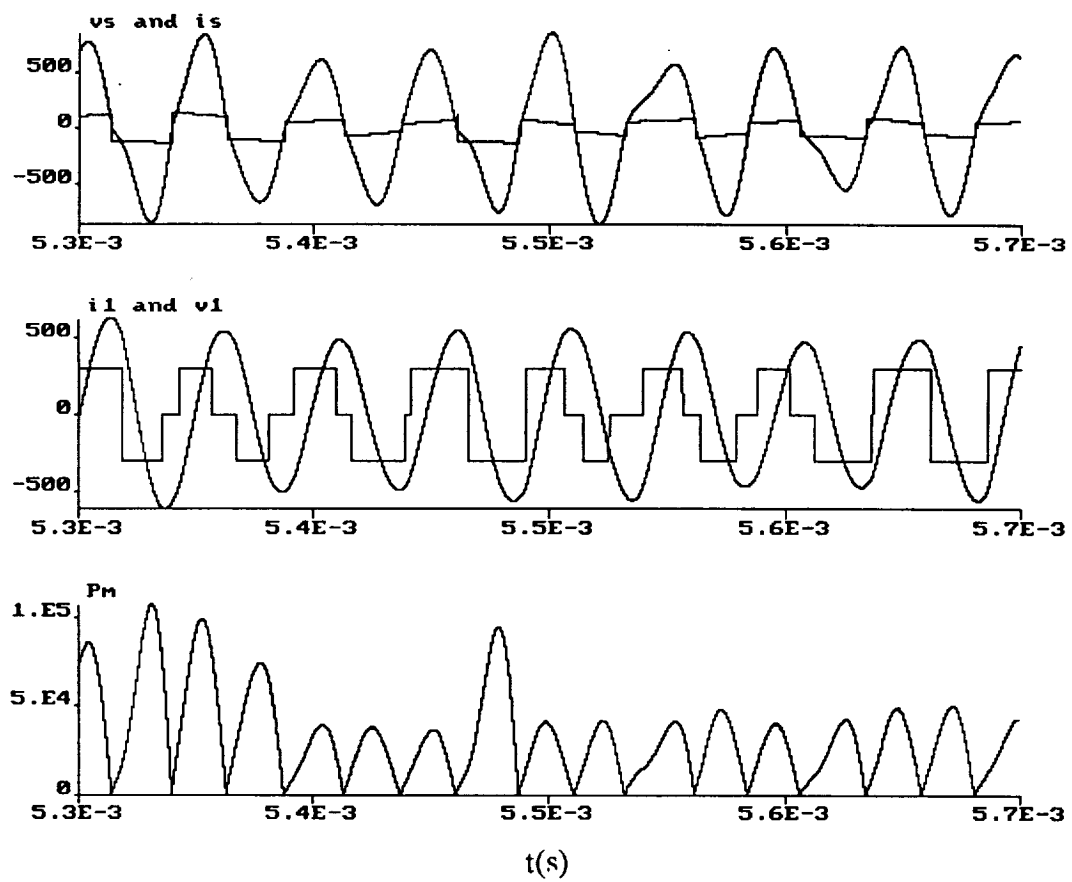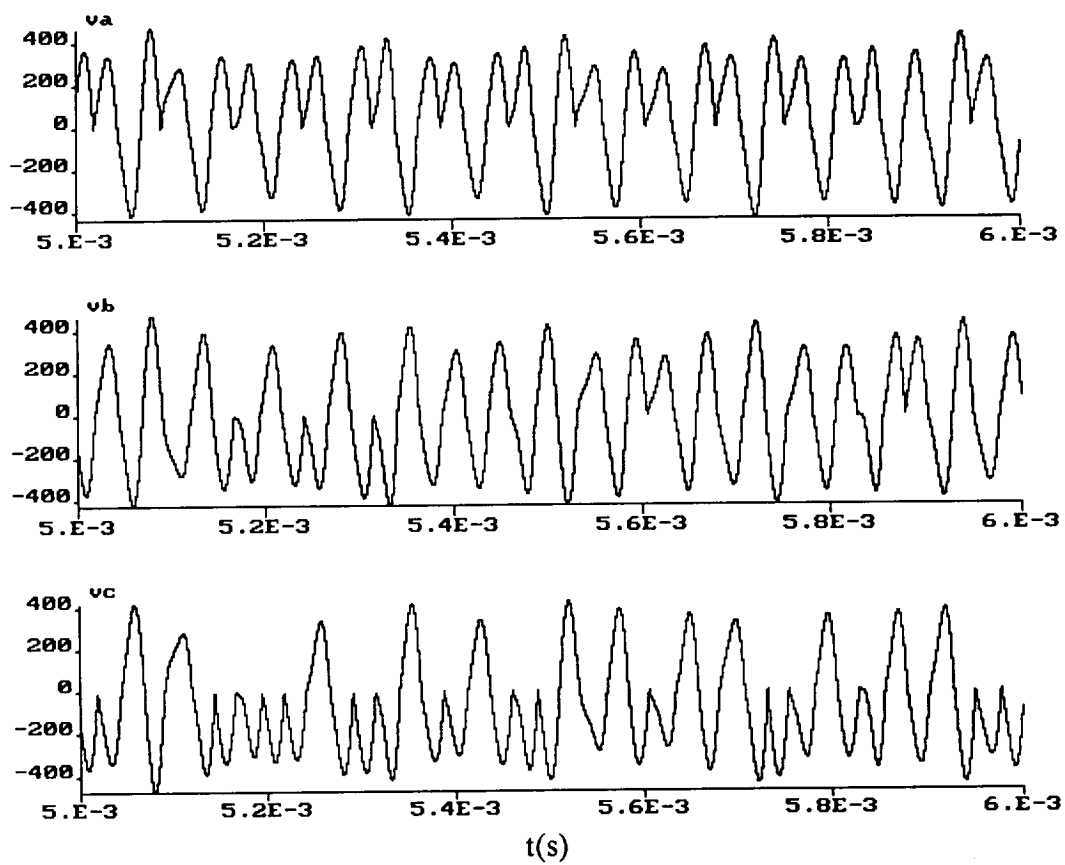**FIG. 59: EXPANDED WAVEFORMS OF Vdo, Vcr, v1 AND vs (SUB-SYSTEM 3)**

FIG. 60: EXPANDED WAVEFORMS OF vs, is AND il
(SUB-SYSTEM 3)

151

FIG, 61: EXPANDED WAVEFORMS OF vs, is, v1, i1 AND Pm (SUB-SYSTEM 3)

152

**FIG. 62: EXPANDED WAVEFORMS OF va, vb AND vc
(SUB-SYSTEM 3)**

153

time interval. Figs. 55-58 show the corresponding currents, phase voltages , HFAC link voltages and currents, torque and power waves. The corresponding expanded waves are shown in Figs. 59-62. In the absence of any control sophistication, the HFAC voltage wave is distorted and varies widely, but it does not affect the motor performance and does not exceed the safe limit. A feedforward instantaneous power control will alleviate this condition. Again, near-unity displacement factor condition has been demonstrated by the vs and is waves.

16.4. Total System

The total system under simulation study is shown in Fig. 63. It consists of sub-system 3 added with the ICE-generator-converter sub-system (sub-system 4). The sub-system 4 is essentially the same as that of sub-system 2, and therefore, it will not be discussed separately. The total system was studied at steady state condition for the ICE speed of 5,000 rpm and the motor speed of 2000 rpm (about) with both under feedback control. Fig. 64 shows the speeds, vcr* wave and the inverter voltage loop performance. Figs. 65 and 66 show the motor currents and the phase voltage waves, respectively. The corresponding waves for the generator are shown in Figs. 67 and 68. Fig. 69 shows the motor and generator torques indicating that the motor torque is positive but the generator torque is negative. Fig. 70 shows the HFAC link voltage and current waves. Figs. 71 and 72 show the expanded view of phase voltages at the motor and generator

154

FIG. 63: SIMULATION BLOCK DIAGRAM OF TOTAL SYSTEM

155

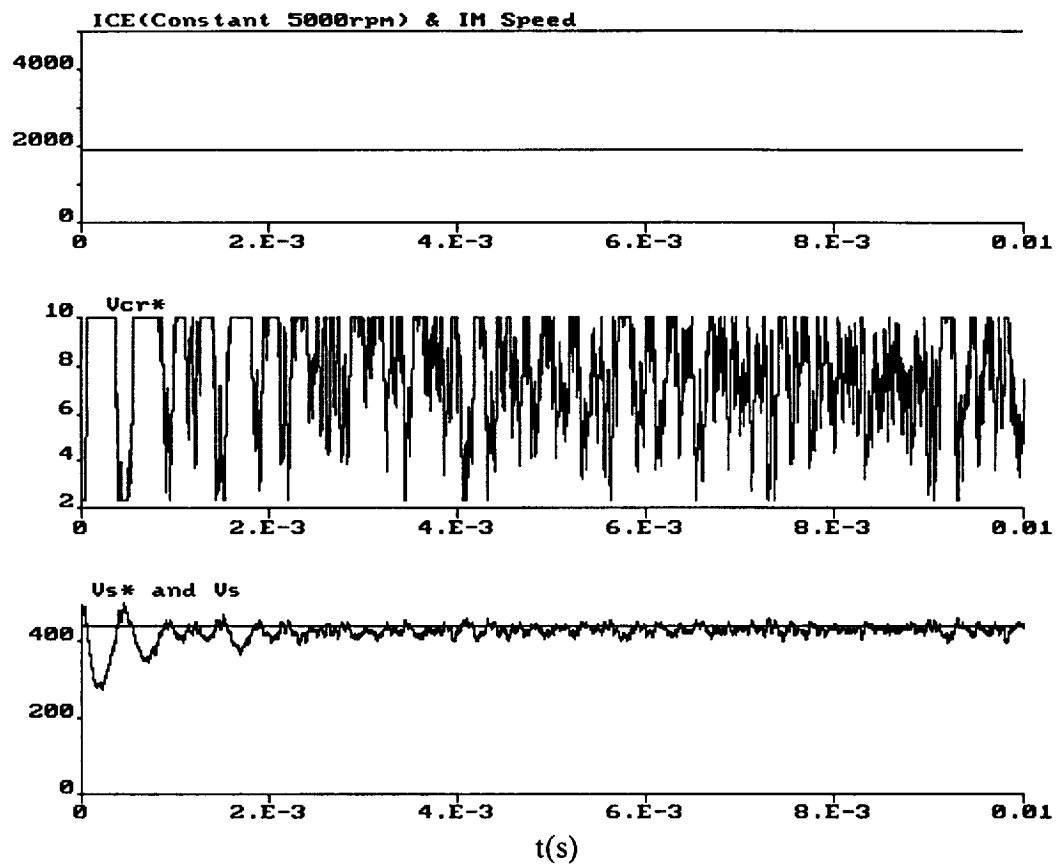**FIG. 64: WAVEFORMS OF ICE SPEED, IM SPEED AND Vs*-Vs (TOTAL SYSTEM)**
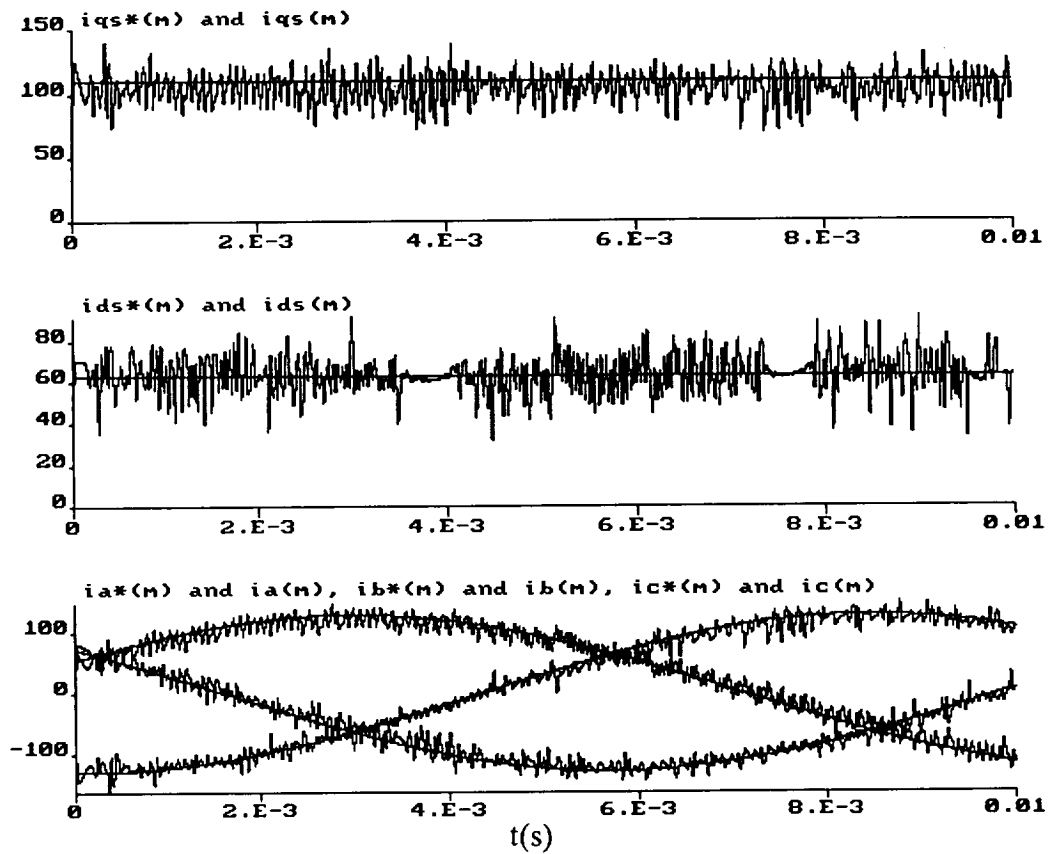
FIG. 65: WAVEFORMS OF iqs*-iqs, ids*-ids, ia*-ia, ib*-ib AND ic*-ic
FOR MOTOR (TOTAL SYSTEM)

157
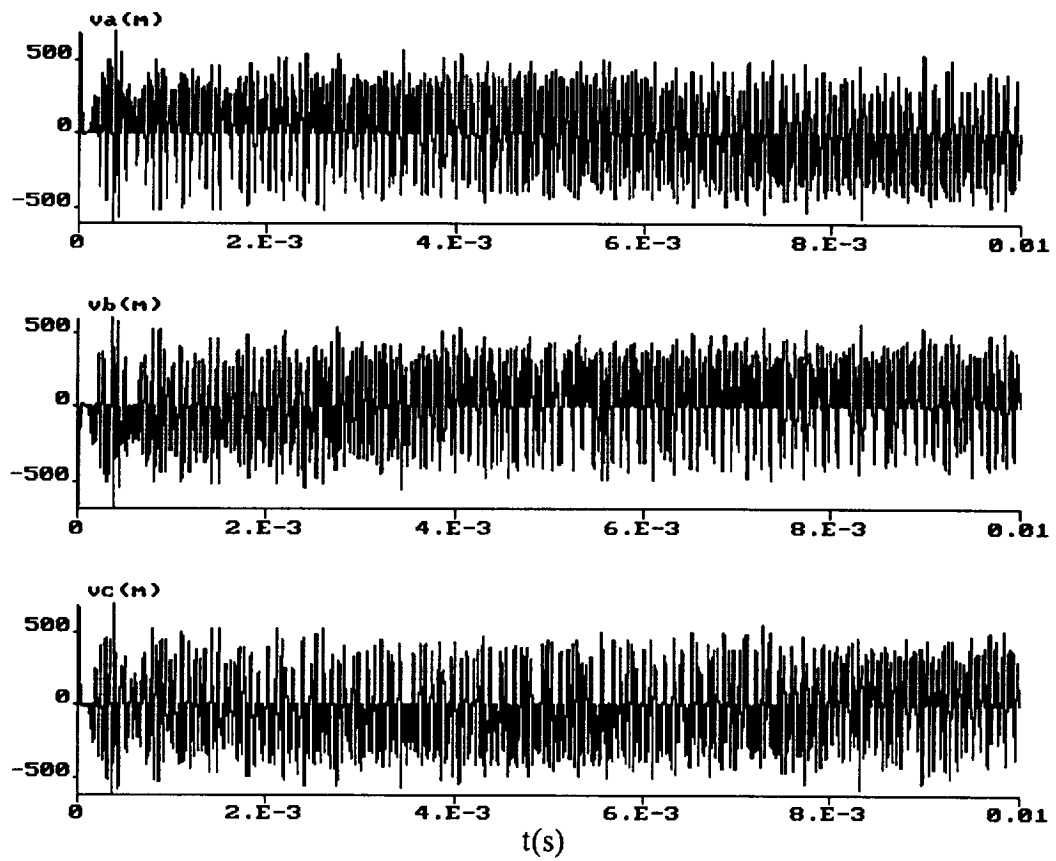
FIG. 66: WAVEFORMS OF va, vb AND vc FOR MOTOR (TOTAL SYSTEM)
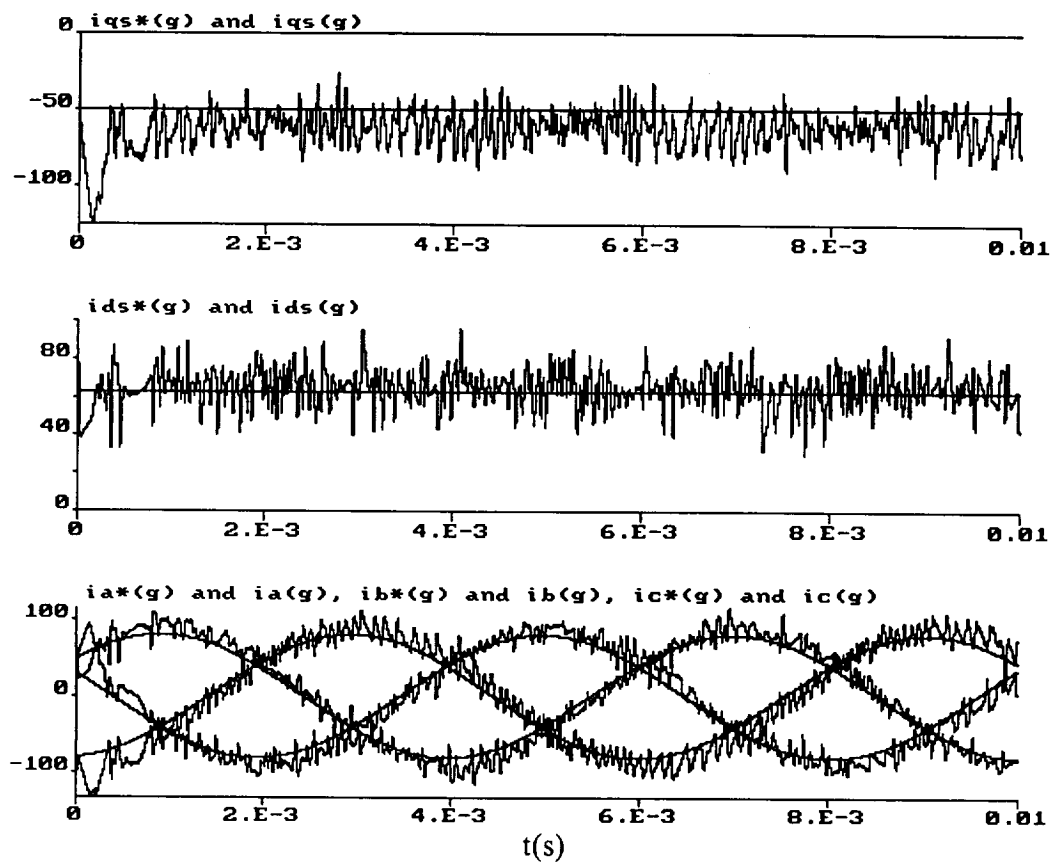
FIG. 67: WAVEFORMS OF iqs*-iqs, ids*-ids, ia*-ia, ib*-ib AND ic*-ic FOR GENERATOR (TOTAL SYSTEM)

159
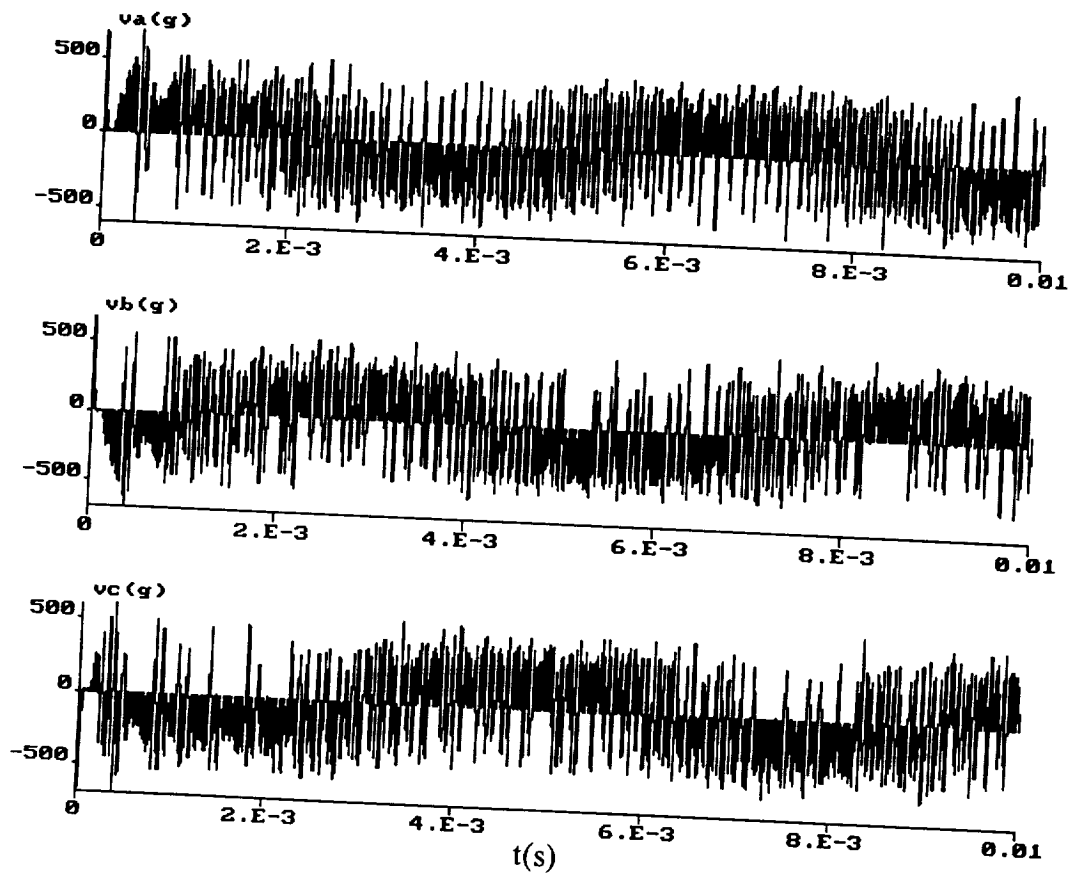
FIG. 68: WAVEFORMS of va, vb AND vc FOR GENERATOR
(TOTAL SYSTEM)
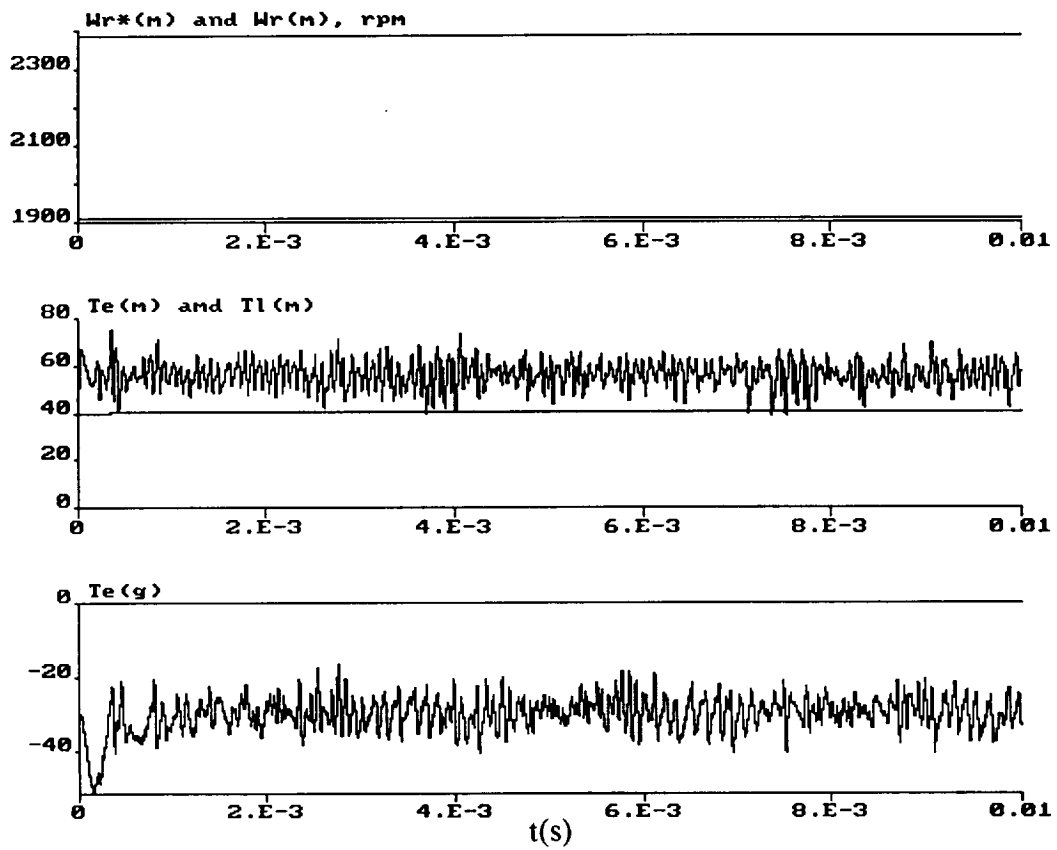
FIG. 69 WAVEFORMS OF Wr*-Wr, Te AND Tl (MOTOR) AND Te (GENERATOR) (TOTAL SYSTEM)

161
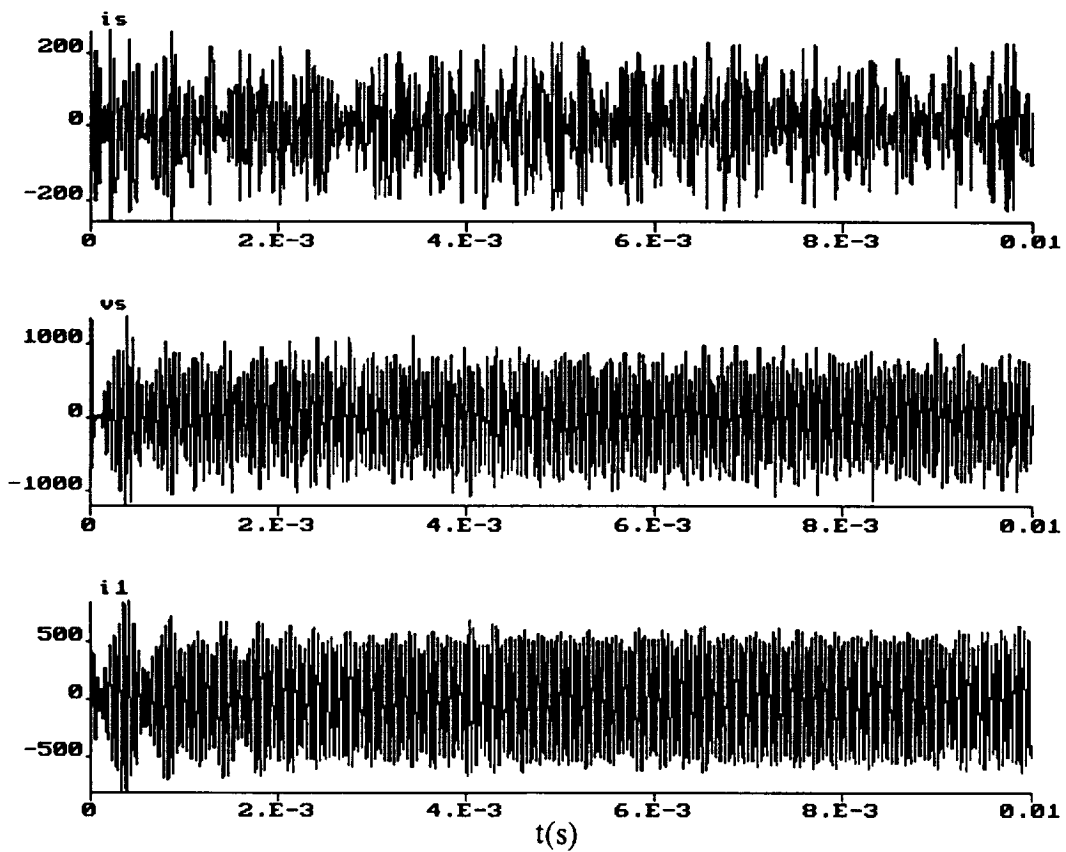
FIG. 70: WAVEFORMS OF is, vs AND i1 (TOTAL SYSTEM)

162
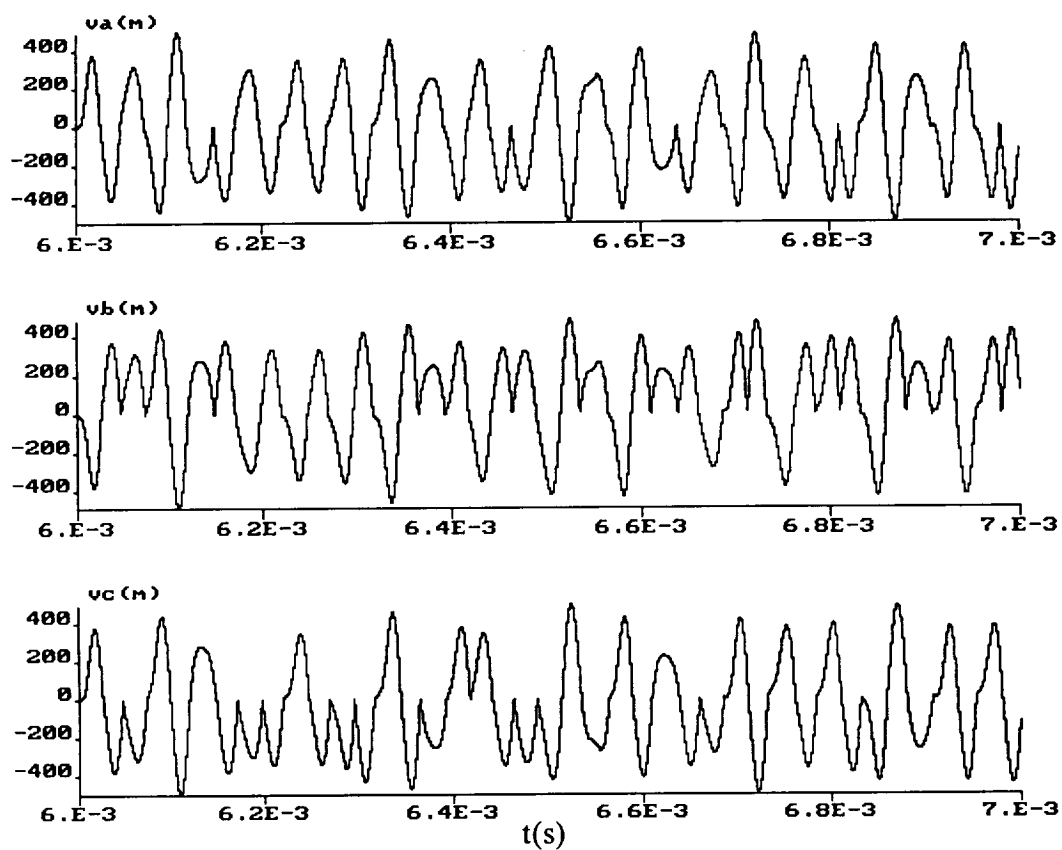
FIG. 71: EXPANDED WAVEFORMS OF va, vb AND vc (MOTOR)
(TOTAL SYSTEM)

163
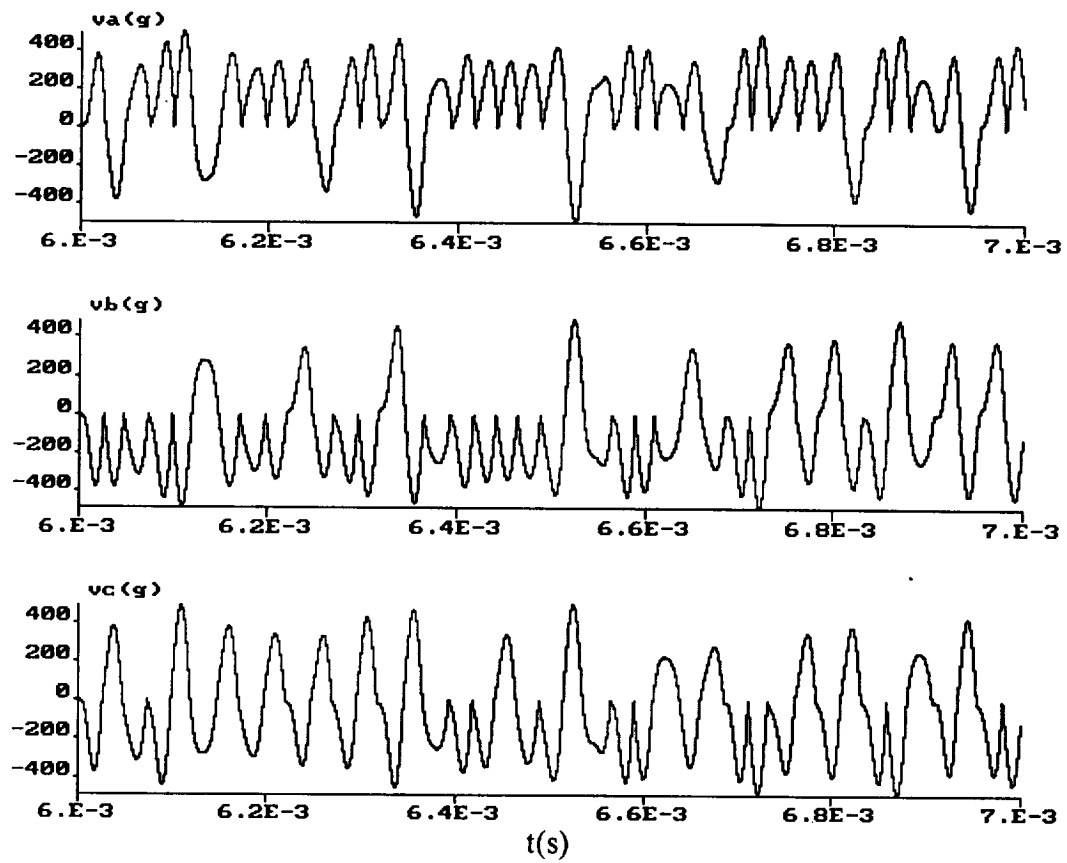
FIG. 72: EXPANDED WAVEFORMS OF va, vb AND vc (GENERATOR) (TOTAL SYSTEM)
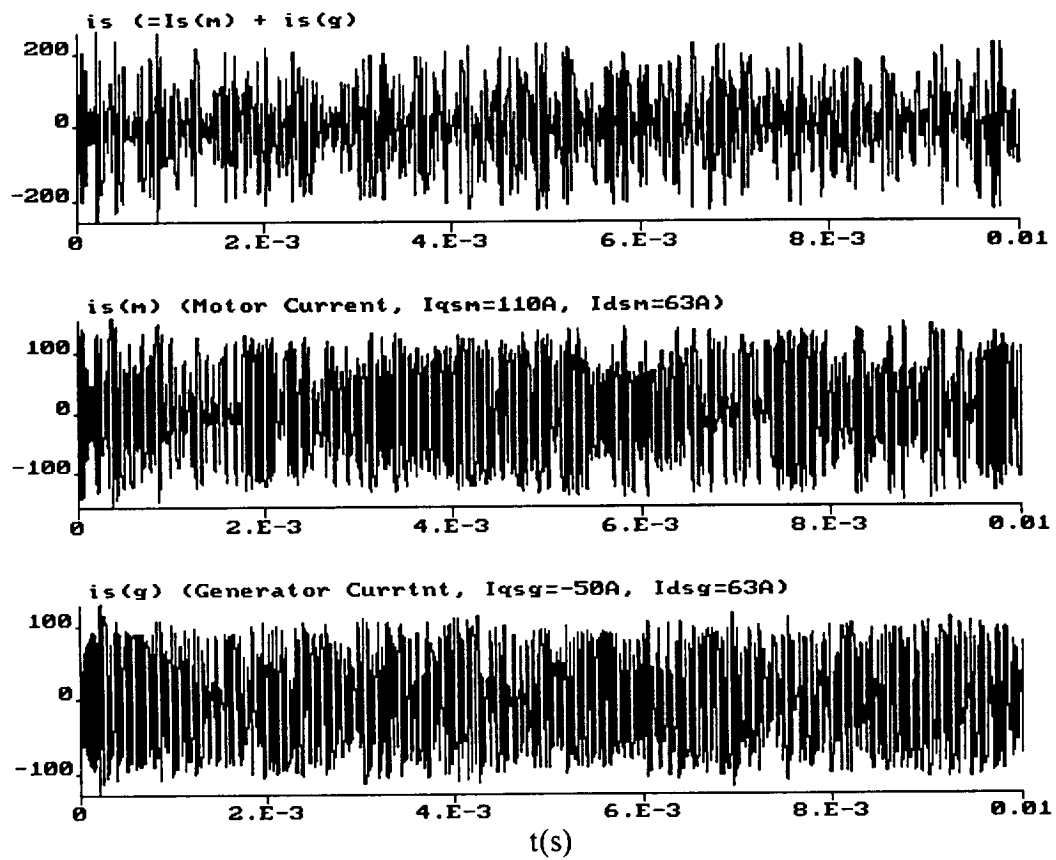
FIG. 73: WAVEFORMS OF is, is (MOTOR) AND is (GENERATOR)
(TOTAL SYSTEM)

165
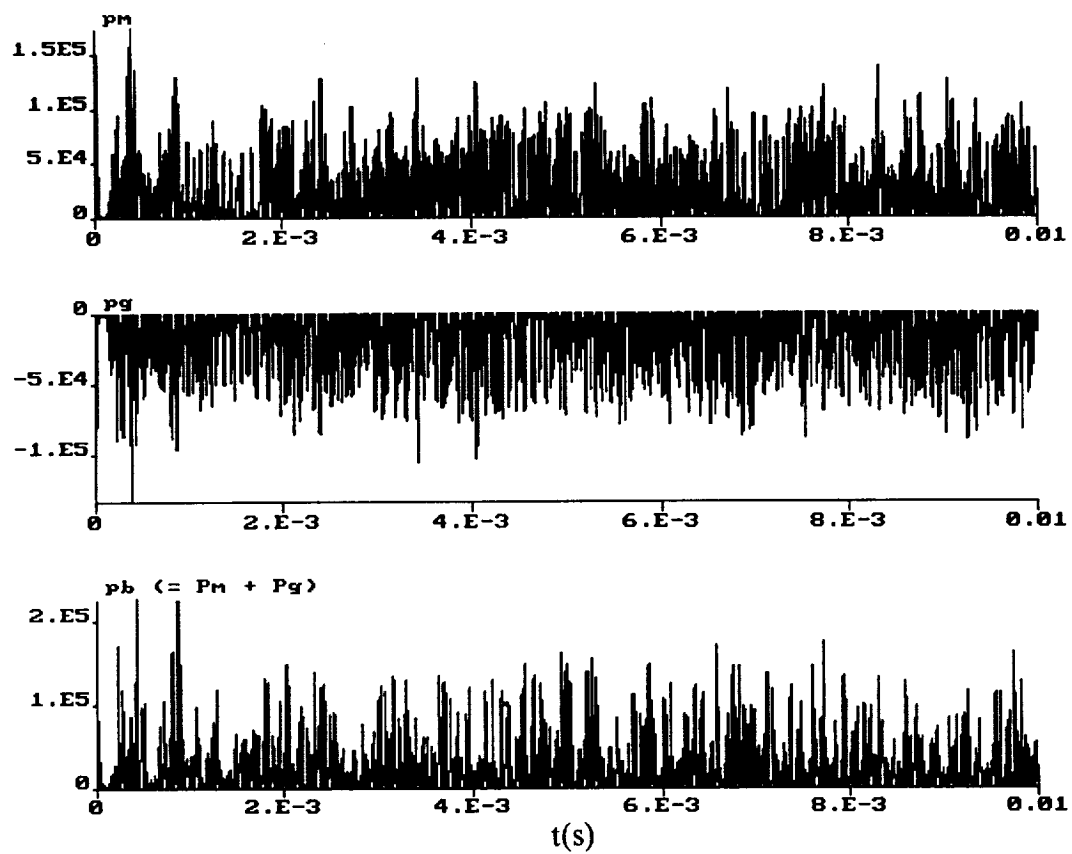
FIG. 74: WAVEFORMS OF Pm (MOTOR), Pg (GENERATOR) AND
Pb (TOTAL) (TOTAL SYSTEM)

166
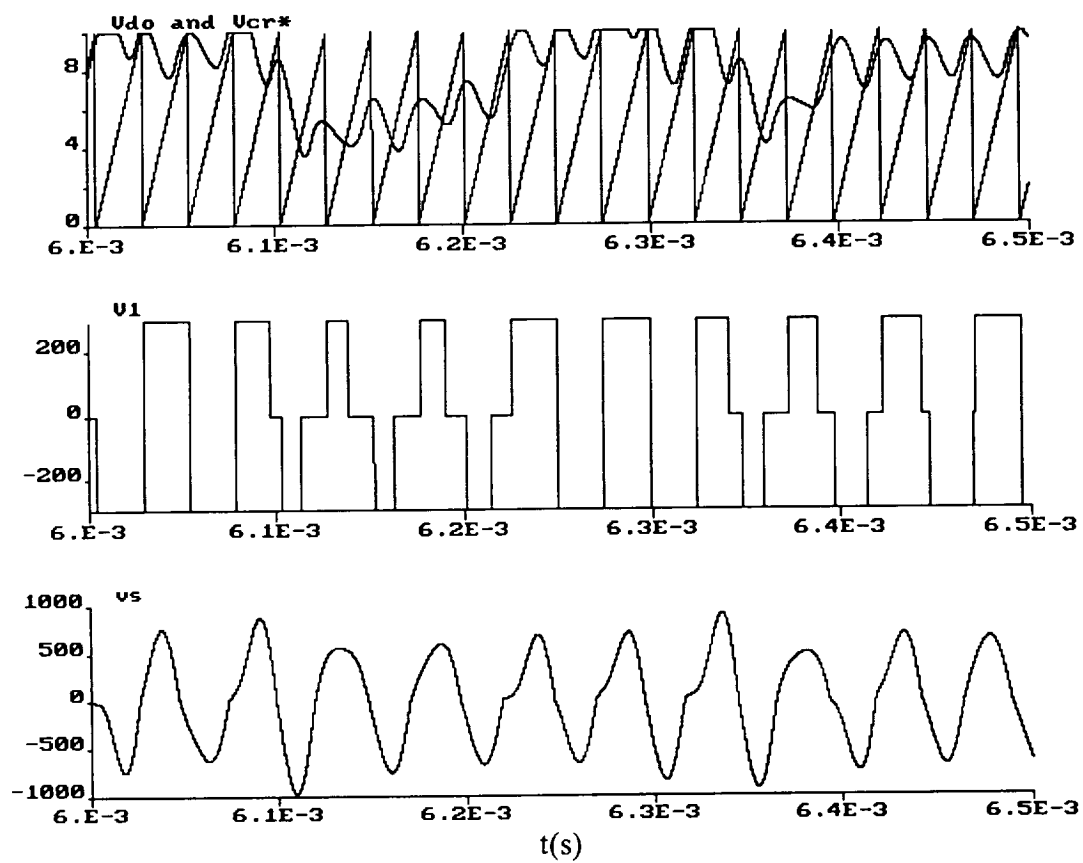
**FIG. 75: EXPANDED WAVEFORMS OF Vdo, Vcr*, V1 AND vs
(TOTAL SYSTEM)**

167
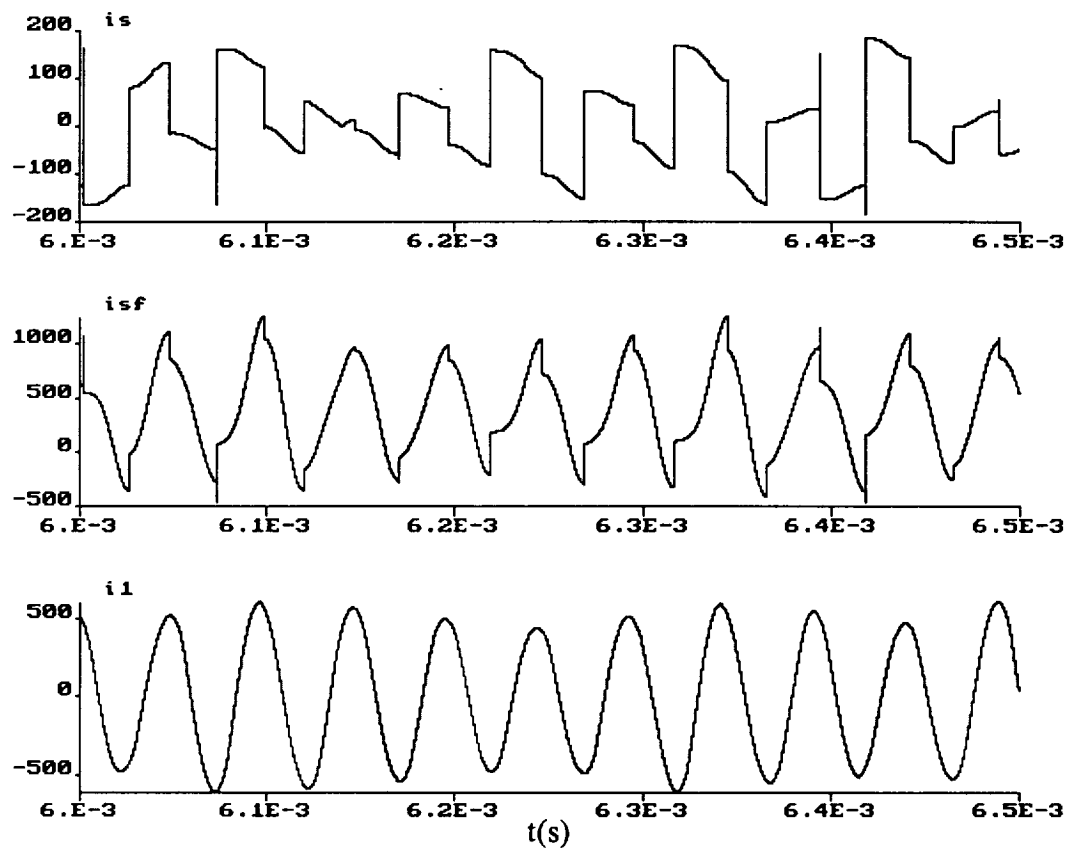
**FIG. 76: EXPANDED WAVEFORMS OF is, isf(FILTERED) AND i1
(TOTAL SYSTEM)**
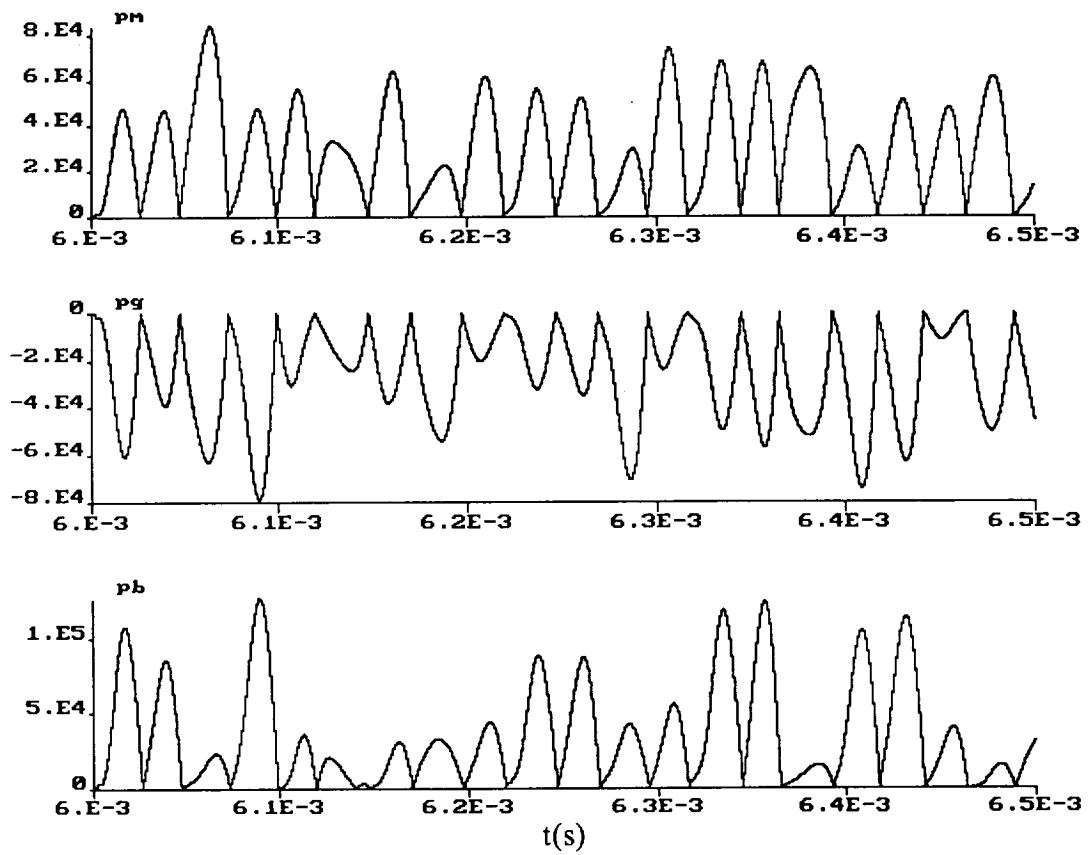
FIG. 77: EXPANDED WAVEFORMS OF Pm (MOTOR), Pg(GENERATOR)
AND Pb (TOTAL) (TOTAL SYSTEM)

169
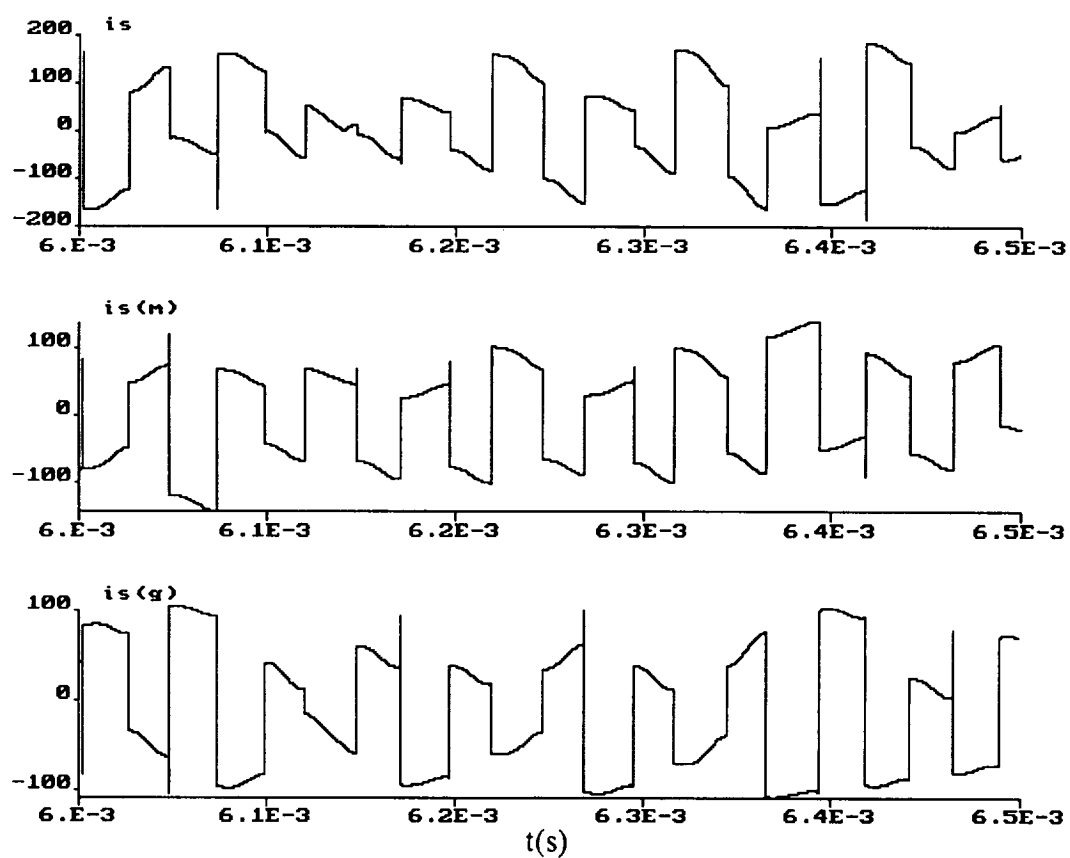
**FIG. 78: EXPANDED WAVEFORMS OF is, is(MOTOR) AND is (GENERATOR)
(TOTAL SYSTEM)**

terminals, respectively. Fig. 73 shows the distribution of HFAC link currents between the motor and the generator, and Fig. 74 shows the corresponding distribution of HFAC link powers. Figs. 75-78 show expanded view of some of the waves in the total system. The satisfactory operation of the system is obvious inspite of the modulation of HFAC voltage, current and power waves.

17. Conclusion

The report on this preliminary system study tends to establish the superiority of high frequency ac (HFAC) for propulsion power distribution system in the next generation advanced electric/hybrid vehicles that tends to satisfy the PNGV (Partnership for Next Generation) goals.

In the beginning of the study, the need for EV/HEV in replacement of the conventional IC engine vehicle has been broadly discussed from the viewpoint of fuel economy, air pollution and dependence on imported oil. The different modes of operation of a standard HEV system have been reviewed. A number of possible energy storage devices in the HEV system, such as battery, flywheel, ultracapacitor and superconducting magnet have been reviewed and compared. The superconducting magnet can be ruled out in the foreseeable future. The ultracapacitor has some good features. However, the technology is not available in near term, and requires a lot of R & D in materials. The flywheel is expensive and has safety problem. Of all the storage

devices, the battery appears to be the most viable. Again, in near term technology, the lead-acid battery is the best compromise in energy density, power density, life-cycle, cost and other criteria.

Then, various power devices, such as IC engine, diesel engine, Stirling engine, gas turbine and fuel cell have been reviewed and compared. Although fuel cell is a static device and is very attractive from the viewpoint of efficiency and emission, the technology yet needs extensive R & D for HEV application. Automotive gas turbine has several attractive features, but because of the need for structural ceramic, it can be ruled out from the near term. The Stirling engine is a far-off technology. Diesel engine has improved efficiency, but because of high noise level and exhaust fumes, its consumer acceptance will be poor. This leaves the present IC engine as the best candidate at least up to the early part of the next century.

The discussion on drive motor /engine generator indicates the superiority of induction machine. At present, IGBT appears to be the best power semiconductor device, although MCT (MOS-controlled thyristor) appears to be a viable candidate in the next generation.

Altogether nine candidate propulsion power distribution systems have been identified with various combination of power and energy storage devices and comparison have been made on their features. The features of the distribution systems

are dictated by the characteristics of the respective power and energy sources. In near term technology, the battery-IC engine system appears to be most viable.

Next, the traditional dc distribution system and HFAC system have been described. The HFAC system has been classified as biased ac, single-phase ac, two-phase ac and three-phase ac. The biased ac is defined as resonant link dc (RLDC) system which uses the soft switching converters using unidirectional power semiconductor devices. Any other biased ac system will not satisfy all the operation modes of HEV. The RLDC system uses additional circuit components, has penalty of over-voltages and somewhat degraded harmonic current on the machine side inspite of the advantages of soft switching. The experience in their applications in HEV power range is not yet adequate . For polyphase HFAC systems, conceptual converter configurations have been described, but they appear to be too complex and expensive compared to single-phase HFAC system. A numerical component sizing has been made in detail for the most competitive distribution systems, i.e., conventional dc and single-phase HFAC systems. Although the HFAC system uses additional components, such as resonant inverter and HF transformer, its advantages can be summarized as follows:

- The power devices of converters use soft or zero voltage switching(ZVS) giving the advantages of (1) elimination of switching loss, (2) elimination of dissipative snubber, (3) attenuation of acoustic noise, (4) improvement of device MTBF, (5) attenuation of EMI problem, (6) improved dv/dt and di/dt for devices and machine insulation. The result is a more reliable and efficient converter that can

possibly be integrated in a lower mass and volume which are extremely important for HEV application.

- The HFAC distribution voltage and the corresponding machine voltages are independent of battery voltage. Therefore, the battery voltage can be selected on the optimum cost and weight basis. Higher HFAC voltage permits higher machine voltage which makes the machine size smaller and more economical compared to dc system

- Higher HFAC voltage also makes the converter economical. Besides, lower current rating eliminates the need for complex parallel operation of the devices as in a low voltage dc system.

- The auxiliary power for HEV can be directly tapped from the HF transformer. The secondary voltage for each auxiliary power (dc or ac) can be directly tapped by appropriate turns ratio transformer. This provides component saving, reduced size and higher efficiency compared to dc system. This advantage offsets the disadvantage of additional components (inverter and transformer) in HFAC system.

- The size of battery terminal filter is smaller by three orders of magnitude compared to dc system giving improved reliability, cost and size benefits.

Inspite of all the above advantages, there are a few disadvantages of HAFC system which can be summarized as follows:

- The HFAC converters that handle ac-to-ac conversion must use ac switches that can handle bi-directional voltages and currents. The ac switches constituted of unidirectional devices are more expensive and have higher conduction losses. However, when the HEV need is established, more efficient and inexpensive ac switches with monolithic integration may be available in the market. Note that the device count remains the same as in a converter in dc system where the devices are paralleled.

- Discrete PWM operation of converter will tend to increase harmonic current in machine unless compensated by higher leakage inductance of machine.

After justifying the superiority of HFAC system over the dc system, a preliminary control strategy has been developed for the resonant inverter, converter-motor, converter-generator and the IC engine. Finally, the components of the system have been modeled and studied by simulation. The simulation study has been made initially on the component sub-systems, and then finally on the total system. As usual, the injected converter current in HFAC link are flat-topped which are rich in harmonic content. In single-phase system, power flow is fluctuating and the mismatch of generated power

175

with consumed power tends to cause fluctuation of link voltage with added distortion. Feedforward power compensation is needed to alleviate this condition. However, inspite of distortion and modulation of HFAC voltage, the converters were functioning satisfactorily generating good quality current-controlled PWM waves. In single-phase HFAC, the distribution circuit is simple with minimum wiring length, and possibly the ground return can be used. Unlike long distribution length in aerospace application, the short run can permit modular construction of the total propulsion system.

Although 20kHz, 400V system was considered for the study, it appears that there are additional advantages for selecting higher voltage and higher frequency. Higher link voltage with higher frequency, will make both converter and machine more economical, improve efficiency, and filter size becomes more economical. However, the zero voltage switching of the devices becomes more demanding within a short window-time which will be hopefully met by the next generation high speed devices.

18. Selected References

(Not in a particular order)

1. Partnership for Next Generation of Vehicles (PNGV) Program Plan, July 1994.

2. I. G. Hansen and G. R. Sundberg, "Space station 20-kHz power management and distribution system ", IEEE PESC Conf., pp. 676 - 683, 1986.

3. I. G. Hansen, "Description of a 20 kHz power distribution system", 21st Intersociety energy Conv. Engg. Conf. Rec., pp. 1893 - 1895, August 1986.

4. P. K. Sood and T. A. Lipo, "Power conversion distribution system using a high frequency ac link system", IEEE Trans. Ind. Appl., vol. 24, pp. 288-300, Mar./Apr. 1988.

5. P. K. Sood and T. A. Lipo, "A versatile power converter for high frequency link system", IEEE Trans. Pow. Elec., vol. 3, pp. 383-390, Oct. 1988.

6. P. Jain and M. Tanju, "A 20 kHz hybrid resonant power source the space station", IEEE Trans. Aero. Elec. Syst., vol. 25, pp. 491-496, July 1989.

7. C. S. Leu et al., "A high frequency ac bus distributed power system", Proc. VPEC, pp. 98-107, Sept. 1990.

8. S. K. Sul and T. A. Lipo, "Design and performance of a high frequency link induction motor operating at unity power factor", IEEE Trans. Ind. Appl., vol. 26, pp. 434-440, May/June 1990.

9. S. K. Sul and T. A. Lipo, "Field oriented control of an induction machine in a high frequency link power system", IEEE Trans. Pow. Elec., vol. 5, pp. 436-445, Oct. 1990.

10. L. M. Burrows et al., "Field oriented control of induction motor", 25th Intersociety energy Conv. Engg. Conf. Rec., pp. 391-396, Aug. 1990.

11. O. Wasynczuk et al., "Steady state and dynamic characteristics of a 20kHz spacecraft power system: control of harmonics resonance", 25th Intersociety energy Conv. Engg. Conf. Rec., pp. 471 - 476, Aug. 1990.

12. B. K. Bose and P. M. Espalage, "High frequency link power conversion", IEEE Trans. Ind. Appl., pp. 387-393, Sept./Oct. 1977.

13. T. Lee, et al., "Performance of MCTs in a current regulated ac/ac PDM converter", IEEE PESC, pp. 935-941, 1993.

14. L. M. Burrows and I. G. Hansen, "Electromechanical systems with transient high power response operating from a resonant ac link", NASA Report, Aug. 1992.

15. M. C. Tanju and P. K. Jain, "High performance ac/dc converter for high frequency power distribution systems: analysis, design considerations and experimental results", IEEE Trans. PE, vol. 9, pp. 275-280, May 1994.

16. J. A. Sabate et al., "LLC resonant inverter with fixed frequency clamped mode operation", Proc. of VPEC Seminar, Blacksburg, pp. 131-141, Sept. 1991.

17. P. D. Ziogas and P. N. D. Photiodis, "An exact input current analysis of ideal static PWM Inverters", IEEE Trans. Ind. Appl., vol. 19, pp. 281-295, Mar./Apr. 1983.

18. D. Coates, "Advanced battery systems for electric vehicle applications", American Ch. Society magazine, pp. 2.273-2.278, 1993.

19. C. W. Seitz, "Industrial battery technologies and markets", IEEE AES Syst. Mag., pp. 11-15, May 1994.

20. B. Bates, "Battery systems for an advanced ac electric vehicle powertrain", Battery Symposium, Long Beach, 1987.

21. T. Moore, "Battery", EPRI Journal, pp. 7-13, April/May 1994.

22. W. A. O'Brien, "Electric vehicles (EVs): a look behind the scenes", IEEE AES Syst. Mag., pp. 38-41, May 1993

23. F. A. Wyczalek, "Heating and cooling battery electric vehicles - a final barrier", IEEE AES Syst. Mag., pp. 9-14, Nov. 1993.

24. R. Swaroop, "USABC jump-starts ev battery development", EPRI Journal, pp. 49-51, July/Aug. 1994.

25. D. H. Swan et al., "Demonstration of a zinc bromine battery in an electric vehicle", IEEE AES Syst. Mag., pp. 20-23, May 1994.

26. D. E. Reiner et al., "Bipolar nickel metal hydride battery for hybrid vehicle", IEEE AES Mag., pp. 24-28, May 1994.

27. T. Juergens et al., "A new high rate lead acid battery", IEEE AES Syst. Mag. pp. 7-9, May 1994.

28. H. Oman, "9th annual battery conference on advances and applications", IEEE AES Mag. pp. 25-31, April 1994.

29. H. Oman, "7th annual battery conf. '92 on applications and advances", IEEE AES Mag., pp. 2-5, April 1992.

30. O. Hman, "8th annual battery conf. on advances and applications", IEEE AES Mag., pp. 2-6, May 1993.

31. G. Tomazic, " Considerations regarding the comparison of traction batteries", IEEE AES Syst. Mag., pp. 37-41, April 1994.

32. U. Schaible, "A torque controlled high speed flywheel energy storage system for peak power transfer in electric vehicle", IEEE/IAS Annu. Meet. Conf. Rec., pp. 435-442, 1994.

33. S. C. Tripathy, "Electric drive for flywheel energy storage", Energy Conv. Mgmt., vol. 35, pp. 127-138, 1994.

34. T. A. Lipo and I. Alan, "Design and test of flywheel load levelling system utilizing a 20 khz parallel resonant high frequency ac voltage link", NASA Report, June 1992.

35. J. S. Lai et al., "High energy density double layer capacitors for energy storage applications", IEEE AES Mag. pp. 14-19, April 1992.

36. C. A. Amann, "How shall we power tomorrow's automobile", Automotive Eng., Alternatives, pp. 1-35, (Ed.) R. L. Evans.

37. G. Walker et al., :Automotive applications of Stirling engine", Automotive Engine Alternative, pp.105-124, (Ed.) R. L. Evans.

38. B. I. Robertsion, " The outlook for conventional automotive engine", Automotive Engine Alternatives, pp. 253-263, (Ed.) R. L. Evans.

39. V. K. Duggal et al., "The natural gas L10 urban bus engine - an alternative fuel option", Mech. Engineering, pp. 15-27, 1992.

40. D. J. Smith, "Advanced gas turbines provide high efficiency and low emissions", Power Engg., pp. 23-27, Mar. 1994.

41. J. R. Thomas and M. R. Fry, "Gas engines or fuel cells for future low emissions cogeneration", ASME Trans. Vol. 15, pp. 29-36, 1991.

42. H. Schreiber, "Gas turbine and combined cycle capacity enhancement", EPRI Journal, pp. 41-42, March 1994.

43. B. L. Koff, "Aircraft gas turbine emissions challenge", Trans. ASME, vol. 116, pp. 474-477, July 1994.

44. Y. S. H. Najjar, "Performance of simple cycle gas turbine engines in two modes of operation", Energy Conv. Mgmt., vol. 35, pp. 433-441, 1994.

45. H. Oman, "In this issue - technically", IEEE AES Syst. Mag., pp. 2-6, Nov. 1992.

46. M. Badger et al., "The PT6 engine: 30 years of gas turbine technology evolution", Trans. ASME, vol. 116, pp. 322-330, April 1994.

47. J. H. Hirschenhofer, "Latest progress in fuel call technology", IEEE AES Syst. Mag., pp. 18-27, Nov. 1992.

48. C. A. Forbes and J. F. Pierre, "The solid fuel cell future", IEEE Spectrum, pp. 40-44, Oct. 1993.

49. J. H. Hirschenhofer, "Fuel cell technology status", IEEE AES Syst. Mag., pp. 21-27, Nov. 1993.

50. J. Douglas, "Solid futures in fuel cells", EPRI Journals, pp. 6-13, March 1994.

51. J. R. Huff et al, "Fuel cell in transportation", Battery Symposium, Long Beach, 1987.

52. D. H. Swan et al., "Fuel cells and other long range tecgnology options for electric vehicles knowledge gaps and development priorities", OECD Documents (The Urban Electric Vehicle), pp. 457-468, May 1992.

53. R. A. Weinstock et al., "Optimum sizing and selection of hybrid electric vehicle components", IEEE/IAS Annu. Meet. Conf. Rec., pp. 251-256, 1993.

54. M. Valenti, "Hybrid car promises high performance and low emissions", Mechanical Engg. pp. 47-49, July 1994.

55. B. K. Bose et al., "A microcomputer based propulsion control system of a hybrid electric vehicle", IEEE Trans. Ind. Elec., vol. 31, pp. 61-68, Feb. 1984.

56. G. W. Davis et al., "The development of a series hybrid electric vehicle for near term applications", IEEE AES Syst. Mag., pp. 15-20, Nov. 1993

57. M. W. Cardullo, "Total life cycle cost analysis of conventional and alternate fueled vehicles", IEEE AES Syst. Mag., pp.39-43, Nov. 1993.

58. A. Kalberiah, "Electric hybrid drive systems for passenger cars and taxis", Int'l. Congress and Exposition, Detroit, pp. 69-77, Feb-March 1991.

59. J. Meisel, "A hybrid electric powertrain for meeting the super car mandate", Environmental Vehicle'95 Conf. , pp. 133-147, Jan.1995.

60. J. J. Brogan et al., "Diverse Choices for electric and hybrid motor vehicles", The urban Electric vehicle, pp. 77-88, 1992.

61. J. Delsey, "Environmental comparison of electric, Hybrid and advanced heat engine vehicles", pp. 103-113.

62. C. A. Amann, :Private vehicles for personal transportation", jour. of Gas Turbines and power, vol. 115, pp. 679-692, Oct. 1993.

63. C. C. Chan, "An overview of electric vehicle technology", Proceedings of IEEE, vol. 81, Sept. 1993.

64. C. C. Chan, "Power electronics challenges in electric vehicles", IEEE IECON Conf. Rec. pp. 701-706, 1993.

65. B. Bates, "Electric vehicle - a decade of transition", SAE, PT-40, 1992.

66. K. S. Rajashekara and R. Martin, "Present and future trends for electric vehicles: review of electrical propulsion system", IEEE Workshop on Pow. Elec. In Trans., pp. 7- 12, Oct. 1992.

67. K. S. Rajashekara, "History of electric vehicles in General Motors", IEEE Trans. Ind. Appl., Vol. 30, pp. 897-904, July/Aug. 1994.

68. K. S. Rajashekara, "Evaluation of power devices for electric vehicles", Workshop for Pow. Elec. In Transportation, pp. 43-47, Oct. 1992.

69. B. K. Bose, "A microcomputer based control system for a near term electric vehicle", IEEE Trans. Ind. Appl., vol. 17, Nov./Dec. 1981.

70. B. K. Bose, "A microcomputer based control and simulation of an advances IPM machine drive system for electric vehicle propulsion", IEEE Trans. Ind. Elec., vol. 24, pp. 547-559, Nov. 1988.

71. B.K.Bose et al., "Speed sensorless hybrid vector controlled induction motor drive",

IEEE IAS Annu. Meet. Conf. Rec., 1995. (To be presented).

72. B. K. Bose et al., "A microcomputer based propulsion control system of a hybrid electric vehicle", IEEE Trans. IE, vol. 31, pp. 61-68, Feb. 1984, .

73. B. K. Bose and G. Sousa, "Fuzzy logic based efficiency optimization control of electric vehicle drive", Project report to Delco Remy, Feb. 1994.

74. M. Riezenman, "Electric Vehicles", special report, IEEE Spectrum, pp. 18-101, Nov. 1992.

75. L. Chang, "Comparison of ac drives for electric vehicles - a report on experts' opinion survey", IEEE AES Syst. Mag. pp. 7-10. Aug. 1994.

76. I. Alan and T. A. Lipo, "Control of a polyphase induction Generator/induction motor power conversion system completely isolated from utility", IEEE/IAS, vol. 30, pp. 636-647, 1994.

77. Data points, "Harris to develop MCT based power electronic building blocks", p. 8, PCIM Magazine, Nov. 1994.

78. L. Chang, "Recent developments of electric vehicle and their propulsion systems", IEEE AES Syst. Mag., pp. 3-6, Dec. 1993.

79. X. Xu and V. A. Sankaran, "Power electronics in electric vehicles: challenges and opportunities", IEEE/IAS Annu. Meet. Conf. Rec., pp. 463-468, 1993.

80. W.A. O'Brien, "Electric vehicles: a look behind the scenes", IEEE AES Syst. Mag., pp. 38-41, May 1993.

81. H. Oman, " 28th Intersociety energy conversion engg. Conf." IEEE AES Syst. Mag., pp. 2-8, Nov. 1993.

82. D. Lynch, " The calstart consortium", IEEE Spectrum, pp. 54-57, 1994.

83. W. J. Gu and R. Liu, "A study of volume and weight vs. Frequency for high frequency transformers", IEEE PESC Rec. pp. 1123-1129, 1993.

84. D. M. Divan and G. Skibinski, "Zero switching loss inverters for high power applications", IEEE IAS Annu. Meet. Conf. Ref., pp. 627-634, 1987.

85. J. S. Lai and B. K. Bose, "An induction motor drive using an improved high frequency resonant dc link inverter", IEEE Trans. Power Electronics, vol. 6, pp. 504-513, July 1991.

86. Powerex, IGBT Module Technical Data Book, Publication No. 9A-000, 1989.

APPENDIX

SIMNON Simulation Program Listing

ADVANCED PROPULSION POWER DISTRIBUTION SYSTEM FOR NEXT GENERATION ELECTRIC/ HYBRID VEHICLE

Appendix A : Battery - Resonant Inverter - HFAC - RL_Load System

MACRO bnm   " Batary - HF Inverter - HFAC - RL_load

```
SYST hfc resl bainco
STORE Vdo[hfc] Vcr[hfc] V1[hfc]
STORE il[resl] Vs[resl] is[resl] -add
STORE Po[resl] Pavo[resl] -add
split 3 1
simu 0  0.002  1e-8
disp(lp)  -state
ashow Vdo Vcr
text 'Vdo, Vcr(=6.667, Delta=120deg) '
ashow V1
text 'V1 (Vab=300)'
ashow il
text 'il '
hcopy /nl 1
$sutil nl 1/jet
$copy /b nl 1.jet prn:
ashow Vs
text' vs (Vbus=440vrms, 622.2Vpp)'
ashow is
text 'is (Z=0.6+J0.8)'
ashow Po
text 'Po (=vs*is)'
hcopy /nl 1
$sutil nl 1/jet
$copy /b nl 1.jet prn:
ashow 4e-4 6e-4  vdo vcr
text 'Vdo, Vcr '
ashow 4e-4 6e-4 v1 il
text 'v1, il '
ashow 4e-4 6e-4 vs is
text 'vs, is'
hcopy /nl 1
$sutil nl 1/jet
$copy /b nl 1.jet prn:
ashow 4e-4 6e-4 v1 vs
text 'v1, vs'
ashow 4e-4 6e-4 il is
text 'il, is'
ashow 4e-4 6e-4 po pavo
text 'Po '
hcopy /nl 1
$sutil nl 1/jet
$copy /b nl 1.jet prn:

END-
```

DISCRETE SYSTEM hfc   " HF Voltage_Frequency control

"INPUT Vab
OUTPUT V1
TIME t
TSAMP Ts
pi = 3.1415926
"------- Voltage limiter ------
Vcr = 6.667   "180deg=10, 120deg=6.667, 75deg=4.155
Delt = (pi/10)* Vcr
"--------- Generate Vab Voltage ------
Vdo = (10/(Too/2)) * mod (t,(Too/2))
Vsq2 = 10*sqw(t/Too)
Vsq2p = if Vsq2>0 then 1 else 0
Vsq2n = if Vsq2<0 then 1 else 0
Vrp = if Vcr>Vdo then 1 else 0
Vrn = if Vcr<Vdo then 1 else 0
Sonp = Vsq2p   "G1
Sonn = Vsq2n   "G2
Soffp = (Vrp and Vsq2p) or (Vrn and Vsq2n)
Soffn = NOT soffp
S1 = Sonp and Soffp
S3 = Sonn and Soffn
S = S1 - S3
V1 = Vab * S
"-------- Parameters -------
fr = 20e+3   "20KHz, Base Frequency
wo = 2*pi*fr   "Angular Frequency = 125663.6 rad/sec when 20KHz
To = 1/fr   "50 usec when 20KHz
Too = To   "20Khz Fixed
Vab = 300   "Variable 380-245V, 180-75deg
Ts = t + h
h = 1e-7

END

CONTINUOUS SYSTEM resl   "Resonance Circuit and RL-Load

INPUT v1
OUTPUT i1 vs is
STATE iss vpp x y z
DER diss dvpp dx dy dz
TIME t
pi= 3.141592654
"---------- vs and is Calculaton ---------
dy = iss
dx = vpp
diss = (V1-vpp)/Lss - y/(Lss*Css) "- (Rss/Lss)*iss
dvpp = (iss-is)/Cpp - x/(Lpp*Cpp) "- vpp/(Rpp*Cpp)
i1 = iss *1.63

Vss = vpp
Vs = Vss*1.63   "Trans. Winding Ratio = 1 : 1.63
                  "Delta=180   - Vab = 244.95
                  "Delta=120   - Vab = 300
                  "Delta=74.79 - Vab = 380
P1 = V1*i1   " Input Power
"----------- L-load ------------------
dz = (vs - Rou*z)/Lou
is = z   " Z = 0.6 + J 0.8
Po = vs*is
pavo = 0
" --------- Parameters -----
"Rss : 0.01
"Rpp : 0.01
Lss : 28.95e-6   "10.5e-6   "31.5e-6
Css : 2.01e-6   "6.0e-6   "2.0e-6
Lpp : 19.3e-6   "7.0e-6   "21.e-6
Cpp : 3.29e-6   "9.0e-6   "3.0e-3
Rou = 0.6
Lou = 6.35e-6
iss : 50.2367   "481.047
vpp : 418.943   "459.11
x : -2.14199e-3 "2.71e-3
y : -6.4319e-3   "-3.24e-3
z : 58.7549   "-232.512

END

CONNECTING SYSTEM bainco   "Ba-Inv-Res-HFAC-RL_Load

TIME t
V1[resl] = V1[hfc]

END

Appendix B : HFAC - Converter - IM System

MACRO NM   "HFAC - CONVERTER - IM CONTROL SYSTEM

```
SYST nspco pdmc ma20 pmis nconn
STORE wr[ma20] wref[nspco] Vbus[nspco]
STORE Tl[ma20] Te[ma20] -add
STORE iar[nspco] ibr[nspco] icr[nspco] liz[nspco] -add
STORE idref[nspco] iqref[nspco] iq[ma20] id[ma20] -add
STORE Van[pdmc] Vbn[pdmc] Vcn[pdmc] -add
STORE ia[ma20] ib[ma20] ic[ma20] -add
STORE Pm[ma20] isn[pmis] -add
split 3 1
simu 0 0.012 1e-8
disp(lp) -state
ashow wref wr
text 'wr_ref, wr'
ashow vbus
text 'vs'
ashow isn liz
text 'is '
hcopy /nl1
$sutil nl1/jet
$copy /b nl1.jet prn:
ashow idref id iqref iq liz
text 'id_ref(=63A) id, iq_ref iq'
ashow iar ia ibr ib icr ic
text 'iam* and iam, ibm* and ibm, icm* and icm '
ashow te tl liz
text 'Te, Tl (KL=0.2, J=0.1)'
hcopy /nl1
$sutil nl1/jet
$copy /b nl1.jet prn:
ashow van
text ' vam'
ashow vbn
text ' Vbm'
ashow vcn
text ' vcm'
hcopy /nl1
$sutil nl1/jet
$copy /b nl1.jet prn:
ashow 0.0065 0.0075 van
text 'van'
ashow 0.0065 0.0075 vbn
text 'vbn'
ashow 0.0065 0.0075 vcn
text 'vcn'
hcopy /nl1
$sutil nl1/jet
$copy /b nl1.jet prn:
```

```
ashow 0.005 0.006 vbus
text 'vs'
ashow 0.005 0.006 isn
text 'is (Iqs_limit= 500A, KL=0.2, J=0.1)'
ashow 0.005 0.006 pm
text 'Pm (= vam*iam + vbm*ibm + vcm*icm)'
hcopy /nl l
$sutil nl l/jet
$copy /b nl l.jet prn:
ashow 0.0068 0.0072 vbus isn
text ' vs, is'
ashow 0.0068 0.0072 pm
text ' Pm'
ashow pm
text ' pm'
hcopy /nl l
$sutil nl l/jet
$copy /b nl l.jet prn:

END
```

CONTINUOUS SYSTEM nspco

```
INPUT wr
OUTPUT iar ibr icr  Vbus cosref sinref weref iqref
STATE  y1 x1
DER    dy1 dx1
TIME t
pi=3.14159265359
"-------------- Speed command and controller
Vbus = Vms * sin(wo*t)
wref = if t<6e-3 then 500 else 300      " Speed Control:450
spdref = wref/pole/pi*60
err = wref - wr
dx1 = Ki*err
Iqe = x1 + Kp*err
Iqre = IF Iqe<-Iqlim THEN -Iqlim ELSE IF Iqe>Iqlim THEN Iqlim ELSE Iqe
Idref = 63
Iqref = Iqre
"--------------- Wsl and We Calculation ------
wsl = Iqref/(Tr*Idref)
we = wr + wsl
dy1 = we
the = mod(y1, 2*pi)
cosrefo = cos(the)
sinrefo = sin(the)
cosref = cosrefo
sinref = sinrefo
weref = we
"-------- Vector rotation and phase 2/3 -----
iqs = Iqref * cosref + Idref * sinref
```

189

```
ids = -Iqref * sinref + Idref * cosref
ia = iqs
ib = -(ids * sqrt(3) + iqs) * 0.5
ic =  (ids * sqrt(3) - iqs) * 0.5    " -(ia+ib)
iar = ia
ibr = ib
icr = ic
"------------ Parameters ----------
Iqlim : 500
Ki : 1
Kp : 300
Rr =  12.43e-3
Llr=  43.8e-6 * 3
Lm =  2.13e-3
Lr = Llr + Lm
Tr = Lr/Rr
pole = 4
wo = 2*pi*fo
fo = 20e+3
Vms = 440*sqrt(2)
liz = 0
"------------- Initial Values
x1: 31.7593
y1: 20.7089     "Wr=672.115

END
```

```
DISCRETE SYSTEM pdmc

INPUT Vbus iarc ibrc icrc iam ibm icm
OUTPUT Van Vbn Vcn
STATE a b c
NEW  na nb nc
TIME t
TSAMP ts
"------- PDM PULSE GENERATOR -----
Vsb = Vbus/2
Vss = abs(vsb)
L= if (Vss<tod) then 1 else 0
Ka = if ira>0 then 1 else -1
Kb = if irb>0 then 1 else -1
Kc = if irc>0 then 1 else -1
na = if L>0.1 then Ka else a
nb = if L>0.1 then Kb else b
nc = if L>0.1 then Kc else c
Van = na*vss
Vbn = nb*vss
vcn = nc*vss
"Van = (2/3)*Vao - (1/3)*(Vbo+Vco)
"Vbn = (2/3)*Vbo - (1/3)*(Vao+Vco)
"Vcn = (2/3)*Vco - (1/3)*(Vbo+Vao)
```

```
ira = iarc - iam
irb = ibrc - ibm
irc = icrc - icm
"****** Initial Values
ts = t + dt
dt = 0.5e-6
tod = 5
a:-1
b:1
c:1

END
→
```

CONTINUOUS SYSTEM resvi   "Resonance Circuit

```
INPUT v1 is
OUTPUT vs il
STATE iss vpp  x y
DER   diss dvpp dx dy
TIME t
pi= 3.141592654
"---------- vss and iss, Calculaton ---------
dy = iss
dx = vpp
diss = (V1-vpp)/Lss - y/(Lss*Css)
dvpp = (iss-is)/Cpp - x/(Lpp*Cpp)
il = iss
Vss = vpp
Vs = Vss*1.63     " Vab=300V, Delta=120deg, Vbus=440rms
" --------- Parameters -----
Lss : 28.95e-6
Css : 2.19e-6
Lpp : 19.3e-6
Cpp : 3.28e-6
iss : -278.126      "-7.4431
vpp : -1.1          "-307.826
x   : -3.3863e-4    "3.50402e-6
y   : -2.6928e-3    "6.52761e-4

END
```

CONTINUOUS SYSTEM MA20   "IM 20kw

```
INPUT  Va Vb Vc  cosref sinref weref iqref
OUTPUT ia ib ic wr pm
STATE Iqs  Ids  Iqr  Idr  w
DER   DIqs DIds DIqr DIdr Dw
TIME t
pi = 3.141592654
```

```
sqr3 = sqrt(3)
we = weref
"------- State Equations
Diqs = (Lr*(Vqs-Rs*iqs)-fse*ids+Lm*Rr*iqr-Lrm*w*idr)/k1
Dids = (fse*iqs+Lr*(Vds-Rs*ids)+Lrm*w*iqr+Lm*Rr*idr)/k1
Diqr = (Lm*(Rs*Iqs-Vqs)+w*Lsm*ids-iqr*Rr*Ls+fre*idr)/k1
Didr = (-w*Lsm*Iqs+Lm*(ids*Rs-Vds)-fre*iqr-Ls*Rr*idr)/k1
"-------- Electromechanical Equations
dw = (Te-Tl)*Pole/(2*J) - (Bm/J)*w
Tl = IF wm>0 and 733>wm THEN Tl11 ELSE if wm>0 and 733<wm then Tl22 else 0
Tl11 = 0.2*wm  "2.72e-4*wm*wm    " Temax=141.6 Nm , Maximum Torque
Tl22 = 141.6 - (84.8/897)*(wm-733)   " wb=733 rad/sec, 7000rpm
                                     " wrmax=1465 rad/sec 14000rpm
Te = 0.75*pole*Lm*(Idr*Iqs-Iqr*Ids)
wr = w                "Electrical rotor speed
wm = wr*2/pole        "Mechanical rotor speed
Spdim = w/Pole/pi*60  "rpm
"-------- Voltage Transformations
Vqss = va
Vdss = (vc-vb)/sqr3
Vqs  = vqss*cosref-vdss*sinref
Vds  = vqss*sinref+vdss*cosref
"------- Relationships of Induction Machine
delw = we-w
fse = lsr*we-delw*lmm
fre = we*lmm-delw*lsr
lrm = Lr*Lm
lsm = Ls*Lm
lsr = Ls*Lr
lmm = Lm*Lm
k1 = lsr-lmm
"------- Current Transformations
Id = ids
Iq = iqs
Iqss = iqs*cosref+ids*sinref
Idss = ids*cosref-iqs*sinref
Iqrs = iqr*cosref+idr*sinref
Idrs = idr*cosref-iqr*sinref
Ias = Iqss
Ibs = -(0.5*Iqss)-(0.5*sqr3*Idss)
Ics = -(0.5*Iqss)+(0.5*sqr3*Idss)
Ia = Ias
Ib = Ibs
Ic = Ics
Vd = Vds
Vq = Vqs
"----------Power and is Current Cal. ------
Pa = va*ia
Pb = vb*ib
Pc = vc*ic
Pm1 = pa + pb + pc
pm2 = if pm1>0 then pm1 else if pm1<0 then -pm1 else 0
```

pm = if iqref>0 then pm2 else if iqref<0 then -pm2 else 0
"-------- Parameters
Rs = 11.21e-3   "0.0085
Rr = 12.43e-3   "0.00316
Ls = Lls + Lm   "1.934e-3
Lr = Llr + Lm   "1.927e-3
Lm = 2.13e-3   "1.89e-3
Lls = 43.8e-6 * 3
Llr = 43.8e-6 * 3
Tr = Lr/Rr
J : 0.1   "1.5764
Bm : 0.02   "[Kg m^2/sec]
pole = 4
"--------- Initial Values
Iqs: 500
Ids: 63
Iqr: -507.518
Idr: -22.0985
w : 400   "672.115

END

DISCRETE SYSTEM pmis

INPUT pm vs
OUTPUT isn
state x
new nx
TIME t
TSAMP Ts
ts = t + h
"------- Calculation of is ------
iso = pm/(vs+0.0000000001)
nx = iso
iss = if abs(vs) <30 then x else pm/vs
isn = iss
h = 5e-7
x : 100

END

CONNECTING SYSTEM nconn   " HFAC - CONVERTER - IM control

TIME t
wr[nspco] = wr[ma20]
Vbus[pdmc] = Vbus[nspco]
iarc[pdmc] = iar[nspco]
ibrc[pdmc] = ibr[nspco]

193

```
icrc[pdmc] = icr[nspco]
iam[pdmc] = ia[ma20]
ibm[pdmc] = ib[ma20]
icm[pdmc] = ic[ma20]
pm[pmis] = pm[ma20]
vs[pmis] = Vbus[nspco]
Va[ma20] = Van[pdmc]
Vb[ma20] = Vbn[pdmc]
Vc[ma20] = Vcn[pdmc]
cosref[ma20] = cosref[nspco]
sinref[ma20] = sinref[nspco]
weref[ma20] = weref[nspco]
iqref[ma20] = iqref[nspco]

END
```

Appendix C : Battery - Resonant Inverter - HFAC - Converter -IM System

MACRO bm   " Battery_Resonant Inverter_Converter_IM Control system

```
SYST hfvfc resvi nspco pdm ma20 isfilt pmis bmconn
STORE wr[ma20] wref[nspco]
STORE Vdo[hfvfc] Vcr[hfvfc] V1[hfvfc] -add
STORE Vrs[hfvfc] Vsm[hfvfc] -add
STORE isn[pmis] Vs[resvi] il[resvi] isi[isfilt] liz[nspco] -add
STORE van[pdm] vbn[pdm] vcn[pdm] -add
STORE ia[ma20] ib[ma20] ic[ma20] -add
Store iar[nspco] ibr[nspco] icr[nspco] -add
STORE iqref[nspco] idref[nspco] id[ma20] iq[ma20] -add
STORE pm[ma20] Te[ma20] Tl[ma20] -add
split 3 1
simu 0 0.01 1e-8
disp(lp) -state
ashow wr wref liz
text 'wr, wref(Iqs_limit=110A, J=0.1.Kl=0.2) '
ashow vcr liz
text 'Vcr (Max=10, Min=2.33)'
ashow Vsm Vrs
text 'Vsm (Ref=440Vrms and Vrs)'
hcopy /nl 1
$sutil nl 1/jet
$copy /b nl 1.jet prn:
ashow iqref iq liz
text 'Iqref and Iq '
ashow idref id liz
text 'Idref and Id'
ashow iar ia ibr ib icr ic
text 'iam* and iam, ibm* and ibm, icm* and icm'
hcopy /nl 1
$sutil nl 1/jet
$copy /b nl 1.jet prn:
ashow vs
text 'vs'
ashow isn
text 'is (= Pm/vs)'
ashow il
text 'il '
hcopy /nl 1
$sutil nl 1/jet
$copy /b nl 1.jet prn:
ashow van
text 'vam'
ashow vbn
text 'vbm'
ashow vcn
text 'vcm'
```

```
hcopy /nl l
$sutil nl l/jet
$copy /b nl l.jet prn:
ashow 0.0053 0.0057 vdo vcr
text ' Vdo and Vcr*'
ashow 0.0053 0.0057 V1
text ' V1 '
ashow 0.0053 0.0057 vs
text ' vs '
hcopy /nl l
$sutil nl l/jet
$copy /b nl l.jet prn:
ashow 0.005 0.0055 isn
text 'is (Bus Current)'
ashow 0.005 0.0055 isi
text 'isi (Filtered)'
ashow 0.005 0.0055 il
text 'il (Input current of Resonant current)'
hcopy /nl l
$sutil nl l/jet
$copy /b nl l.jet prn:
ashow 0.005 0.006 van
text 'vam'
ashow 0.005 0.006 vbn
text 'vbm'
ashow 0.005 0.006 vcn
text 'vcm'
hcopy /nl l
$sutil nl l/jet
$copy /b nl l.jet prn:
ashow 0.0062 0.007 vs
text 'vs'
ashow 0.0062 0.007 isn
text 'is'
ashow 0.0062 0.007 il
text 'il'
hcopy /nl l
$sutil nl l/jet
$copy /b nl l.jet prn:
ashow 0.0053 0.0057 vs isn
text 'vs and is'
ashow 0.0053 0.0057 il vl
text 'il and vl'
ashow 0.0053 0.0057 pm
text 'Pm'
hcopy /nl l
$sutil nl l/jet
$copy /b nl l.jet prn:
ashow te liz
text ' Te '
ashow Tl liz
text ' TL (= Kl*Wm, Kl=0.2) '
```

196

```
ashow pm
text ' pm (=vam*iam+vbm*ibm+vcm*icm)'
hcopy /nl1
$sutil nl1/jet
$copy /b nl1.jet pm:

END-
```

CONTINUOUS SYSTEM hfvfc   " HF Voltage_Frequency control

```
INPUT iqs Vs
OUTPUT Vl
STATE yl zl
DER dyl dzl
TIME t
pi = 3.1415926
"------- Frequency Controller ------
P = iqs   " M; P>0,  G; P<0
fdrr = if P>0 then fdr else if P<0 then -fdr else 0
frr = fo + fdrr
fro = if frr> frmax then frmax else if frr<frmin then frmin else frr
fdr = 400
frmax = 20500
frmin = 19500
"--------Vs Controller ------
Vrb = abs(Vs)
dzl = (1/filt)*Vrb - (1/filt)* zl
Vrs = zl
Vsm = 440
err = Vsm-Vrs
dyl = Ki*err
xl = yl + Kp*err
Vso = if xl<-Vsmin then -Vsmin else if xl>Vsmax then Vsmax else xl
Vcr = Vso + Vro
"---------- Generate Vab Voltage ------
Vdo = (10/(Too/2)) * mod (t,(Too/2))
Vsq2 = 10*sqw(t/Too)
Vsq2p = if Vsq2>0 then 1 else 0
Vsq2n = if Vsq2<0 then 1 else 0
Vrp = if Vcr>Vdo then 1 else 0
Vrn = if Vcr<Vdo then 1 else 0
Sonp = Vsq2p   "G1
Sonn = Vsq2n   "G2
Soffp = (Vrp and Vsq2p) or (Vrn and Vsq2n)
Soffn = NOT soffp
S1 = Sonp and Soffp
S3 = Sonn and Soffn
S = S1 - S3
Vab = Vb * S
Vl = Vab
"-------- Parameters -------
```

197

fo = 20e+3   "20KHz, Base Frequency
wo = 2*pi*fo   "Angular Frequency = 125663.6 rad/sec when 20KHz
To = 1/fo   "50 usec when 20KHz
Too = To * (fo/fr) "Frequency Control, 20KHz +- 400 Hz
fr = fro   "Variable Control Frequency
Vro = 6.666   "Delta = 120 deg
Vb = 300   "(=Vd)
h = 1e-7
Ki = 0.001
Kp = 0.2
Vsmax = 3.34
Vsmin = 4.33
y1 : -0.676
filt = 1/(2*pi*800)
z1 : 440

END

CONTINUOUS SYSTEM resvi   "Resonance Circuit

INPUT v1 is
OUTPUT vs i1
STATE iss vpp x y
DER   diss dvpp dx dy
TIME t
pi= 3.141592654
"---------- vss and iss, Calculaton ---------
dy = iss
dx = vpp
diss = (V1-vpp)/Lss - y/(Lss*Css)   "- (Rss/Lss)*iss
dvpp = (iss-isp)/Cpp - x/(Lpp*Cpp)   "- vpp/(Rpp*Cpp)
i1 = iss
isp = is
Vss = vpp
Vs = Vss*1.63   " Vab=300V, Delta=120deg, Vbus=440rms
" --------- Parameters -----
"Rss : 0.01
"Rpp : 0.01
Lss = 28.95e-6
Css = 2.01e-6
Lpp = (19.3e-6)/2
Cpp = (3.29e-6)*2
iss : -367.68
vpp : 27.195
x : -3.48391e-3
y : -2.82734e-4

END

CONTINUOUS SYSTEM nspco

```
INPUT wr
OUTPUT iar ibr icr cosref sinref weref Iqref
STATE y1 x1
DER   dy1 dx1
TIME t
pi=3.14159265359
"-------------- Speed command and controller
wref = 500
err = wref - wr
dx1 = Ki*err
Iqe = x1 + Kp*err
Iqre = IF Iqe<-Iqlim THEN -Iqlim ELSE IF Iqe>Iqlim THEN Iqlim ELSE Iqe
Idref = 63
Iqref = Iqre
"---------------- Wsl and We Calculation ------
wsl = Iqref/(Tr*Idref)
we = wr + wsl
dy1 = we
the = mod(y1, 2*pi)
cosrefo = cos(the)
sinrefo = sin(the)
cosref = cosrefo
sinref = sinrefo
weref = we
"-------- Vector rotation and phase 2/3 -----
iqs = Iqref * cosref + Idref * sinref
ids = -Iqref * sinref + Idref * cosref
ia = iqs
ib = -(ids * sqrt(3) + iqs) * 0.5
ic =  (ids * sqrt(3) - iqs) * 0.5    " -(ia+ib)
iar = ia
ibr = ib
icr = ic
liz = 0
"------------ Parameters ----------
Iqlim : 110
Ki : 1
Kp : 300
Rr = 12.43e-3
Llr= 43.8e-6 * 3
Lm = 2.13e-3
Lr = Llr + Lm
Tr = Lr/Rr
"------------- Initial Values
x1: 47.8
y1: 36.17

END
```

CONTINUOUS SYSTEM MA20 "INDUCTION MOTOR, Max 100kw

```
INPUT  Va Vb Vc cosref sinref weref iqref
OUTPUT ia ib ic wr pm pm1 spdim
STATE Iqs Ids Iqr Idr w
DER  DIqs DIds DIqr DIdr Dw
TIME t
pi = 3.141592654
sqr3 = sqrt(3)
we = weref
"------- State Equations
Diqs = (Lr*(Vqs-Rs*iqs)-fse*ids+Lm*Rr*iqr-Lrm*w*idr)/k1
Dids = (fse*iqs+Lr*(Vds-Rs*ids)+Lrm*w*iqr+Lm*Rr*idr)/k1
Diqr = (Lm*(Rs*Iqs-Vqs)+w*Lsm*ids-iqr*Rr*Ls+fre*idr)/k1
Didr = (-w*Lsm*Iqs+Lm*(ids*Rs-Vds)-fre*iqr-Ls*Rr*idr)/k1
"-------- Electromechanical Equations
"dw = Te*Pole/(2*J)
dw = (Te-Tl)*Pole/(2*J) - (Bm/J)*w
Tl = IF wm>0 and 733>wm THEN Tl11 ELSE if wm>0 and 733<wm then Tl22 else 0
Tl11 = 0.2*wm    "2.72e-4*wm*wm  " wm=733 rad/sec , Maximum Torque
Tl22 = 146.1 - (84.8/897)*(wm-733)  " wr=1465 rad/sec, 7000rpm
                                    " wr=2930, rad/sec 14000rpm
Te = 0.75*pole*Lm*(Idr*Iqs-Iqr*Ids)
wr = w          "Electrical rotor speed
wm = wr*2/pole    "Mechanical rotor speed
Spdim = w/Pole/pi*60 "rpm
"-------- Voltage Transformations
Vqss = va
Vdss = (vc-vb)/sqr3
Vqs  = vqss*cosref-vdss*sinref
Vds  = vqss*sinref+vdss*cosref
"------- Relationships of Induction Machine
delw = we-w
fse = lsr*we-delw*lmm
fre = we*lmm-delw*lsr
lrm = Lr*Lm
lsm = Ls*Lm
lsr = Ls*Lr
lmm = Lm*Lm
k1 = lsr-lmm
"------- Current Transformations
Id = ids
Iq = iqs
Iqss = iqs*cosref+ids*sinref
Idss = ids*cosref-iqs*sinref
Iqrs = iqr*cosref+idr*sinref
Idrs = idr*cosref-iqr*sinref
Ias = Iqss
Ibs = -(0.5*Iqss)-(0.5*sqr3*Idss)
Ics = -(0.5*Iqss)+(0.5*sqr3*Idss)
Ia = Ias
Ib = Ibs
```

```
Ic = Ics
Vd = Vds
Vq = Vqs
"----------Power and is Current Cal. ------
Pa = va*ia
Pb = vb*ib
Pc = vc*ic
Pm1 = Pa + Pb + Pc
pm2 = if pm1>0 then pm1 else if pm1<0 then -pm1 else 0
Pm = if iqref>0 then pm2 else if iqref<0 then -pm2 else 0
"pm3 = (3/2)*(Vq*iq + vd*id)
"-------- Parameters
Rs = 11.21e-3       "0.0085
Rr = 12.43e-3       "0.00316
Ls = Lls + Lm       "1.934e-3
Lr = Llr + Lm       "1.927e-3
Lm = 2.13e-3        "1.89e-3
Lls = 43.8e-6 * 3
Llr = 43.8e-6 * 3
Tr = Lr/Rr
J  = 0.1            "1.5764
Bm = 0.01           "[Kg m^2/sec]
pole = 4
"--------- Initial Values
Iqs: 110
Ids: 63
Iqr: -112.457
Idr: 19.5636
w  : 400    "433.61

END
⇁


CONTINUOUS SYSTEM isfilt

INPUT Vs is
OUTPUT isi
STATE  icr ilr ico
DER    dicr dilr dico
TIME t
pi=3.14159265359
"-------------- is filtering Circuit
iss = is * 1.63
qc = Cr*Vs
dilr = qc/(Lr*Cr)
dico = qc
dicr = ico
isi = icr + ilr + iss
"------------ Parameters ----------
Lr = (19.3e-6)/2
Cr = (3.23e-6)*2
"------------- Initial Values
```

icr : 6.166e-10
ilr : 621.777
ico : 5.217e-8

END

⌐

DISCRETE SYSTEM pdm   " CONVERTER FOR INDUCTION MOTOR

```
INPUT Vbus iar ibr icr iam ibm icm
OUTPUT Van Vbn Vcn
STATE a b c
NEW  na nb nc
TIME t
TSAMP ts
"------------- PDM PULSE GENERATOR -----
Vsb = Vbus /2
Vss = abs(Vsb)
L= if (Vss<tdd) then 1 else 0
Ka = if ira>0 then 1 else -1
Kb = if irb>0 then 1 else -1
Kc = if irc>0 then 1 else -1
na = if L>0.1 then Ka else a
nb = if L>0.1 then Kb else b
nc = if L>0.1 then Kc else c
Van = na*vss
Vbn = nb*vss
vcn = nc*vss
"Van = (2/3)*Vao - (1/3)*(Vbo+Vco)
"Vbn = (2/3)*Vbo - (1/3)*(Vao+Vco)
"Vcn = (2/3)*Vco - (1/3)*(Vbo+Vao)
ira = iar - iam
irb = ibr - ibm
irc = icr - icm
"-------------- Initial Values
ts = t + dt
dt = 1e-7    -
tdd = 5
a : 1
b : -1
c : 1
```

END

DISCRETE SYSTEM pmis

```
INPUT pm vs
OUTPUT isn
STATE x
NEW nx
```

```
TIME t
TSAMP Ts
Ts = t + h
pi = 3.141592654
"------- Calculation of is ------
iso = pm/(vs+0.000000001)
nx = iso
iss = if abs(vs) <30 then x else pm/vs
isn = iss
h = 1e-7
x : 500

END




CONNECTING SYSTEM bmconn  "Ba_Inv_Converter_IM Control


TIME t
wr[nspco] =wr[ma20]
iqs[hfvfc] = iqref[nspco]
Vs[hfvfc] = vs[resvi]
Vbus[pdm] = Vs[resvi]
V1[resvi] = V1[hfvfc]
pm[pmis] = pm[ma20]
vs[pmis] = vs[resvi]
is[resvi] = isi[isfilt]
Vs[isfilt] = Vs[resvi]
is[isfilt] = isn[pmis]
iar[pdm] = iar[nspco]
ibr[pdm] = ibr[nspco]
icr[pdm] = icr[nspco]
iam[pdm] = ia[ma20]
ibm[pdm] = ib[ma20]
icm[pdm] = ic[ma20]
Va[ma20] = Van[pdm]
Vb[ma20] = Vbn[pdm]
Vc[ma20] = Vcn[pdm]
iqref[ma20] = iqref[nspco]
cosref[ma20] = cosref[nspco]
sinref[ma20] = sinref[nspco]
weref[ma20] = weref[nspco]

END
```

Appendix D : Battery - Resonant Inverter - HFAC - Converter
-IM System
ICE - IG - Converter - HFAC-|

MACRO TBM   " Total Control system
                  " BA-INV-RES-|-HFAC-|- CONV.-IM
                  " ICE-IG-CONV-|-HFAC-|-RES-INV-BA

SYST thvfc resvi nspco pdm ma20 isfilt tpmis igtco ipdm ig30 tconn
STORE spdig[ig30] spdim[ma20] wref[nspco] wr[ma20] liz[nspco]
STORE Vcr[thvfc] V1[thvfc] Vdo[thvfc] -add
STORE Vrs[thvfc] Vsm[thvfc] Vs[resvi] i1[resvi] -add
STORE imm[tpmis] igg[tpmis] isn[tpmis] isi[isfilt] -add
STORE van[pdm] vbn[pdm] vcn[pdm] -add
STORE ia[ma20] ib[ma20] ic[ma20] -add
STORE iarc[nspco] ibrc[nspco] icrc[nspco] -add
STORE iqref[nspco] idref[nspco] iq[ma20] id[ma20] -add
STORE vag[ipdm] vbg[ipdm] vcg[ipdm] -add
STORE iar[igtco] ibr[igtco] icr[igtco] -add
STORE iag[ig30] ibg[ig30] icg[ig30] -add
STORE iqrefg[igtco] idrefg[igtco] idg[ig30] iqg[ig30] -add
STORE Pm[ma20] pg[ig30] pmg[tpmis] -add
STORE Tem[ma20] Tlm[ma20] Teg[ig30] -add
split 3 1
simu 0 0.01 1e-8
disp(lp) -state
ashow spdig spdim liz
text 'ICE(Constant 5000rpm) & IM Speed '
ashow vcr
text ' Vcr*'
ashow Vsm Vrs liz
text 'Vsm and Vrs'
hcopy /nl 1
$sutil nl 1/jet
$copy /b nl 1.jet prn:
ashow 6e-3 6.5e-3 vdo vcr
text ' Vdo and Vcr* '
ashow 6e-3 6.5e-3 V1
text ' V1'
ashow 6e-3 6.5e-3 vs
text ' vs'
hcopy /nl 1
$sutil nl 1/jet
$copy /b nl 1.jet prn:
ashow isn
text 'is (=Imm+igg, Bus Current)'
ashow imm
text 'imm (Motor Current, Iqsm=110A, Idsm=63A)'

204

```
ashow igg
text 'igg (Generator Currtnt, Iqsg=-50A, Idsg=63A)'
hcopy /nl l
$sutil nl l/jet
$copy /b nl l.jet prn:
ashow 6e-3 6.5e-3 isn
text ' is(=imm+igg)'
ashow 6e-3 6.5e-3 imm
text ' imm'
ashow 6e-3 6.5e-3 igg
text ' igg'
hcopy /nl l
$sutil nl l/jet
$copy /b nl l.jet prn:
ashow pm
text 'Pm'
ashow pg
text 'Pg'
ashow pmg
text 'Pb (=Pmg= Pm + Pg) '
hcopy /nl l
$sutil nl l/jet
$copy /b nl l.jet prn:
ashow 6e-3 6.5e-3 pm
text ' Pm'
ashow 6e-3 6.5e-3 Pg
text ' Pg'
ashow 6e-3 6.5e-3 Pmg
text ' Pb (=Pmg)'
hcopy /nl l
$sutil nl l/jet
$copy /b nl l.jet prn:
ashow 6e-3 6.5e-3 isn
text ' is'
ashow 6e-3 6.5e-3 isi
text ' isf
ashow 6e-3 6.5e-3 il
text ' il'
hcopy /nl l
$sutil nl l/jet
$copy /b nl l.jet prn:
ashow iq iqref liz
text 'iqrefm and iqm'
ashow id idref liz
text 'idrefm and idm'
ashow iarc ia ibrc ib icrc ic
text 'iam* and iam, ibm* and ibm, icm* and icm'
hcopy /nl l
$sutil nl l/jet
$copy /b nl l.jet prn:
ashow isn
text 'is (Bus Current)'
```

```
ashow vs
text 'vs (Bus Voltage)'
ashow il
text 'il (Resonant Inverter input current)'
hcopy /nl1
$sutil nl1/jet
$copy /b nl1.jet prn:
ashow van
text 'vam'
ashow vbn
text 'vbm'
ashow vcn
text 'vcm'
hcopy /nl1
$sutil nl1/jet
$copy /b nl1.jet prn:
ashow vag
text 'vag'
ashow vbg
text 'vbg'
ashow vcg
text 'vcg'
hcopy /nl1
$sutil nl1/jet
$copy /b nl1.jet prn:
ashow iqrefg iqg liz
text 'iqrefg, iqg'
ashow idrefg idg liz
text 'idrefg idg'
ashow iar ibr icr iag ibg icg
text 'iag* and iag, ibg* abd ibg, icg* and icg'
hcopy /nl1
$sutil nl1/jet
$copy /b nl1.jet prn:
ashow wref wr
text 'Wrm_ref and Wrm'
ashow Tem Tlm liz
text 'Tem amd Tlm '
ashow Teg liz
text 'Teg '
hcopy /nl1
$sutil nl1/jet
$copy /b nl1.jet prn:
ashow 0.006 0.007 van
text 'vam'
ashow 0.006 0.007 vbn
text 'vbm'
ashow 0.006 0.007 vcn
text 'vcm'
hcopy /nl1
$sutil nl1/jet
$copy /b nl1.jet prn:
```

```
ashow 0.006 0.007 vag
text 'vag'
ashow 0.006 0.007 vbg
text 'vbg'
ashow 0.006 0.007 vcg
text 'vcg'
hcopy /nl1
$sutil nl1/jet
$copy /b nl1.jet prn:

END


CONTINUOUS SYSTEM thvfc   " HF Voltage_Frequency control

INPUT iqs Vs
OUTPUT V1
STATE y1 z1
DER dy1 dz1
TIME t
pi = 3.1415926
"------- Frequency Controller ------
P = iqs        " M; P>0,  G; P<0
fdrr = if P>0 then fdr else if P<0 then -fdr else 0
frr = fo + fdrr
fro = if frr> frmax then frmax else if frr<frmin then frmin else frr
fdr = 400
frmax = 20500
frmin = 19500
"--------Vs Controller ------
Vrb = abs(Vs)
dz1 = (1/filt)*Vrb - (1/filt)* z1
Vrs = z1
Vsm = 440
err = Vsm-Vrs
dy1 = Ki*err
x1 = y1 + Kp*err
Vso = if x1<-Vsmin then -Vsmin else if x1>Vsmax then Vsmax else x1
Vcr = Vso + Vro
"---------- Generate Vab Voltage ------
Vdo = (10/(Too/2)) * mod (t,(Too/2))
Vsq2 = 10*sqw(t/Too)
Vsq2p = if Vsq2>0 then 1 else 0
Vsq2n = if Vsq2<0 then 1 else 0
Vrp = if Vcr>Vdo then 1 else 0
Vrn = if Vcr<Vdo then 1 else 0
Sonp = Vsq2p    "G1
Sonn = Vsq2n    "G2
Soffp = (Vrp and Vsq2p) or (Vrn and Vsq2n)
Soffn = NOT soffp
S1 = Sonp and Soffp
S3 = Sonn and Soffn
```

S = S1 - S3
Vab = Vb * S
V1 = Vab
"-------- Parameters -------
fo = 20e+3   "20KHz, Base Frequency
wo = 2*pi*fo   "Angular Frequency = 125663.6 rad/sec when 20KHz
To = 1/fo   "50 usec when 20KHz
Too = To * (fo/fr) "Frequency Control, 20KHz +- 400 Hz
fr = fro   "Variable Control Frequency
Vro = 6.666   "Delta = 120 deg
Vb = 300   "(=Vd)
h = 1e-7
Ki = 0.001
Kp = 0.2
Vsmax = 3.34
Vsmin = 4.33
filt = 1/(2*pi*800)
y1 : -0.676
z1 : 440

END

CONTINUOUS SYSTEM resvi   "Resonance Circuit

INPUT v1 is
OUTPUT Vs i1
STATE iss vpp x y
DER   diss dvpp dx dy
TIME t .
pi= 3.141592654
"---------- vss and iss, Calculaton ---------
dy = iss
dx = vpp
diss = (V1-vpp)/Lss - y/(Lss*Css)   "- (Rss/Lss)*iss
dvpp = (iss-isp)/Cpp - x/(Lpp*Cpp)   "- vpp/(Rpp*Cpp)
i1 = iss
isp = is
Vss = vpp
Vs = Vss*1.63   " Vab=300V, Delta=120deg, Vbus=440rms
" --------- Parameters -----
"Rss : 0.01
"Rpp : 0.01
Lss = 28.95e-6
Css = 2.01e-6
Lpp = (19.3e-6)/2
Cpp = (3.29e-6)*2
iss : -446.221   "481.047   "-367.68
vpp : -445.157   "459.11   "27.195
x   : -2.3291e-3 "2.71e-3   "-3.484e-3
y   : 2.5626e-3   "-3.24e-3   "-2.827e-4

END

SYSTEM nspco

```
INPUT wr
OUTPUT iarc ibrc icrc cosref sinref weref Iqref
STATE  y1 x1
DER   dy1 dx1
TIME t
pi=3.14159265359
"-------------- Speed command and controller
wref = 500
err = wref - wr
dx1 = Ki*err
Iqe = x1 + Kp*err
Iqre = IF Iqe<-Iqlim THEN -Iqlim ELSE IF Iqe>Iqlim THEN Iqlim ELSE Iqe
Idref = 63
Iqref = Iqre
"---------------- Wsl and We Calculation ------
wsl = Iqref/(Tr*Idref)
we = wr + wsl
dy1 = we
the = mod(y1, 2*pi)
cosrefo = cos(the)
sinrefo = sin(the)
cosref = cosrefo
sinref = sinrefo
weref = we
"-------- Vector rotation and phase 2/3 -----
iqs = Iqref * cosref + Idref * sinref
ids = -Iqref * sinref + Idref * cosref
ia = iqs
ib = -(ids * sqrt(3) + iqs) * 0.5
ic =  (ids * sqrt(3) - iqs) * 0.5    " -(ia+ib)
iarc = ia
ibrc = ib
icrc = ic
liz = 0
"------------ Parameters ----------
Iqlim : 110
Ki : 1
Kp : 300
Rr = 12.43e-3
Llr= 43.8e-6 * 3
Lm = 2.13e-3
Lr = Llr + Lm
Tr = Lr/Rr
"------------- Initial Values
x1: 48.8681 "47.8
y1: 37.0825 "36.17

END
```

DISCRETE SYSTEM pdm   " CONVERTER INDUCTION MOTOR

```
INPUT Vbus iarc ibrc icrc iam ibm icm
OUTPUT Van Vbn Vcn
STATE a b c
NEW  na nb nc
TIME t
TSAMP ts
"------- PDM PULSE GENERATOR -----
Vsb = Vbus /2
Vss = abs(Vsb)
L= if (Vss<tdd) then 1 else 0
Ka = if ira>0 then 1 else -1
Kb = if irb>0 then 1 else -1
Kc = if irc>0 then 1 else -1
na = if L>0.1 then Ka else a
nb = if L>0.1 then Kb else b
nc = if L>0.1 then Kc else c
Van = na*vss
Vbn = nb*vss
vcn = nc*vss
"Van = (2/3)*Vao - (1/3)*(Vbo+Vco)
"Vbn = (2/3)*Vbo - (1/3)*(Vao+Vco)
"Vcn = (2/3)*Vco - (1/3)*(Vbo+Vao)
ira = iarc - iam
irb = ibrc - ibm
irc = icrc - icm
"------------- Initial Values
ts = t + dt
dt = 1e-7
tdd = 5
a : -1
b : 1
c : -1

END
→
```

CONTINUOUS SYSTEM MA20   "INDUCTION MOTOR, Max 100kw

```
INPUT  Va Vb Vc cosref sinref weref iqrefm
OUTPUT ia ib ic wr pm pml spdim
STATE Iqs Ids Iqr Idr w
DER  DIqs DIds DIqr DIdr Dw
TIME t
pi = 3.141592654
sqr3 = sqrt(3)
we = weref
"------- State Equations
Diqs = (Lr*(Vqs-Rs*iqs)-fse*ids+Lm*Rr*iqr-Lrm*w*idr)/k1
```

Dids = (fse*iqs+Lr*(Vds-Rs*ids)+Lrm*w*iqr+Lm*Rr*idr)/k1
Diqr = (Lm*(Rs*Iqs-Vqs)+w*Lsm*ids-iqr*Rr*Ls+fre*idr)/k1
Didr = (-w*Lsm*Iqs+Lm*(ids*Rs-Vds)-fre*iqr-Ls*Rr*idr)/k1
"-------- Electromechanical Equations
"dw = Te*Pole/(2*J)
dw = (Te-Tl)*Pole/(2*J) - (Bm/J)*w
Tl = IF wm>0 and 733>wm THEN Tl11 ELSE if wm>0 and 733<wm then Tl22 else 0
Tl11 = 0.2*wm   "2.72e-4*wm*wm   " wm=733 rad/sec , Maximum Torque
Tl22 = 146.1 - (84.8/897)*(wm-733) " wr=1465 rad/sec, 7000rpm
                                   " wr=2930, rad/sec 14000rpm
Te = 0.75*pole*Lm*(Idr*Iqs-Iqr*Ids)
wr = w   "Electrical rotor speed
wm = wr*2/pole   "Mechanical rotor speed
Spdim = w/Pole/pi*60 "rpm
Tem = Te
Tlm = Tl
"-------- Voltage Transformations
Vqss = va
Vdss = (vc-vb)/sqr3
Vqs = vqss*cosref-vdss*sinref
Vds = vqss*sinref+vdss*cosref
"------- Relationships of Induction Machine
delw = we-w
fse = lsr*we-delw*lmm
fre = we*lmm-delw*lsr
lrm = Lr*Lm
lsm = Ls*Lm
lsr = Ls*Lr
lmm = Lm*Lm
k1 = lsr-lmm
"------- Current Transformations
Id = ids
Iq = iqs
Iqss = iqs*cosref+ids*sinref
Idss = ids*cosref-iqs*sinref
Iqrs = iqr*cosref+idr*sinref
Idrs = idr*cosref-iqr*sinref
Ias = Iqss
Ibs = -(0.5*Iqss)-(0.5*sqr3*Idss)
Ics = -(0.5*Iqss)+(0.5*sqr3*Idss)
Ia = Ias
Ib = Ibs
Ic = Ics
Vd = Vds
Vq = Vqs
"----------Power and is Current Cal. ------
Pa = va*ia
Pb = vb*ib
Pc = vc*ic
Pm1 = Pa + Pb + Pc
pm2 = if pm1>0 then pm1 else if pm1<0 then -pm1 else 0
pm = if iqrefm>0 then pm2 else if iqrefm<0 then -pm2 else 0

211

"pm1 = (3/2)*(Vq*iq + vd*id)
"-------- Parameters
Rs = 11.21e-3   "0.0085
Rr = 12.43e-3   "0.00316
Ls = Lls + Lm   "1.934e-3
Lr = Llr + Lm   "1.927e-3
Lm = 2.13e-3   "1.89e-3
Lls = 43.8e-6 * 3
Llr = 43.8e-6 * 3
Tr = Lr/Rr
J = 0.1   "1.5764
Bm = 0.01   "[Kg m^2/sec]
pole = 4
"--------- Initial Values
Iqs: 110
Ids: 63
Iqr: -112.457
Idr: 19.5636
w : 400   "433.61

END
→

CONTINUOUS SYSTEM isfilt

INPUT Vs is
OUTPUT isi
STATE icr ilr ico
DER   dicr dilr dico
TIME t
pi=3.14159265359
"-------------- is filtering Circuit
iss = is * 1.63
qc = Cr*Vs
dilr = qc/(Lr*Cr)
dico = qc
dicr = ico
isi = icr + ilr + iss
"------------ Parameters ----------
Lr = (19.3e-6)/2
Cr = (3.23e-6)*2
"------------- Initial Values
icr : 6.166e-10
ilr : 621.777
ico : 5.217e-8

END
→

DISCRETE SYSTEM tpmis   " is Bus Current Calculation

```
INPUT pm pml pg pgl vs
OUTPUT isn
STATE x y z
NEW nx ny nz
TIME t
TSAMP Ts
Ts = t + h
"------- Calculation of is ------
ism = pm/vs
nx = ism
imm = if abs(vs) <30 then x else ism
isg = pg/vs
ny = isg
igg = if abs(vs) <30 then y else isg
pmgl = pml + pgl
pmg = if pmgl>0 then pmgl else if pmgl<0 then -pmgl else 0
iss = pmg/vs
nz = iss
isn = if abs(vs) <30 then z else iss
img = imm + igg
ismg = ism + isg
"--------- Initial Values ---------
h = 1e-7
x : 100
y : 50
z : 100

END
```

CONTINUOUS SYSTEM igtco   " Torque Control of Generator

```
INPUT wr
OUTPUT iar ibr icr cosref sinref weref Iqref
STATE y1
DER   dy1
TIME t
pi=3.14159265359
"-------------- Torque command ---------
Idref = 63        " Flux Component Current
Iqref = - 50        " Torque Component Current
idrefg = idref
iqrefg = iqref
"-------------- Wsl and We Calculation ------
wsl = Iqref/(Tr*Idref)
we = wr + wsl
dy1 = we
the = mod(y1, 2*pi)
cosrefo = cos(the)
```

```
sinrefo = sin(the)
cosref = cosrefo
sinref = sinrefo
weref = we
"-------- Vector rotation and phase 2/3 -----
iqs = Iqref * cosref + Idref * sinref
ids = -Iqref * sinref + Idref * cosref
ia = iqs
ib = -(ids * sqrt(3) + iqs) * 0.5
ic =  (ids * sqrt(3) - iqs) * 0.5       " -(ia+ib)
iar = ia
ibr = ib
icr = ic
"------------ Parameters ----------
Rr = 12.43e-3
Llr= 43.8e-6 * 3
Lm = 2.13e-3
Lr = Llr + Lm
Tr = Lr/Rr
"------------- Initial Values
y1 : 30.645   "29.1   "13.6118  "11.5139

END
→


DISCRETE SYSTEM ipdm    "GENERATOR


INPUT Vbus iar ibr icr iag ibg icg
OUTPUT Vag Vbg Vcg
STATE a b c
NEW  na nb nc
TIME t
TSAMP ts
"------- PDM PULSE GENERATOR -----
Vsb = Vbus /2
Vss = abs(Vsb)
L= if (Vss<tdd) then 1 else 0
Ka = if ira>0 then 1 else -1
Kb = if irb>0 then 1 else -1
Kc = if irc>0 then 1 else -1
na = if L>0.1 then Ka else a
nb = if L>0.1 then Kb else b
nc = if L>0.1 then Kc else c
Vag = na*vss
Vbg = nb*vss
vcg = nc*vss
ira = iar - iag
irb = ibr - ibg
irc = icr - icg
"****** Initial Values
ts = t + dt
dt = 1e-7
```

tdd = 5
a : -1
b : -1
c : 1

END

CONTINUOUS SYSTEM ig30   "IG 30kw (Induction Generation)

INPUT Va Vb Vc cosref sinref weref iqrefg
OUTPUT iag ibg icg wr pg pgl
STATE Iqs Ids Iqr Idr
DER DIqs DIds DIqr DIdr
TIME t
pi = 3.141592654
sqr3 = sqrt(3)
"------- State Equations
Diqs = (Lr*(Vqs-Rs*iqs)-fse*ids+Lm*Rr*iqr-Lrm*w*idr)/k1
Dids = (fse*iqs+Lr*(Vds-Rs*ids)+Lrm*w*iqr+Lm*Rr*idr)/k1
Diqr = (Lm*(Rs*Iqs-Vqs)+w*Lsm*ids-iqr*Rr*Ls+fre*idr)/k1
Didr = (-w*Lsm*Iqs+Lm*(ids*Rs-Vds)-fre*iqr-Ls*Rr*idr)/k1
"-------- Electromechanical Equations
Teg = 0.75*pole*Lm*(Idr*Iqs-Iqr*Ids)
w = wr   " Electrical Generator speed(ICE)
wr = Wmig*(pole/2)   " Mechanical Generator speed(ICE)
Wmig = 0.1047* Spdig   " Rated Wm=523.6 rad/sec when Spdig=5000
Spdig = 5000
we = weref
"-------- Voltage Transformations
Vqss = va
Vdss = (vc-vb)/sqr3
Vqs = vqss*cosref-vdss*sinref
Vds = vqss*sinref+vdss*cosref
"------- Relationships of Induction Machine
delw = we-w
fse = lsr*we-delw*lmm
fre = we*lmm-delw*lsr
lrm = Lr*Lm
lsm = Ls*Lm
lsr = Ls*Lr
lmm = Lm*Lm
k1 = lsr-lmm
"------- Current Transformations
Idg = ids
Iqg = iqs
Iqss = iqs*cosref+ids*sinref
Idss = ids*cosref-iqs*sinref
Iqrs = iqr*cosref+idr*sinref
Idrs = idr*cosref-iqr*sinref
Ias = Iqss

215

Ibs = -(0.5*Iqss)-(0.5*sqr3*Idss)
Ics = -(0.5*Iqss)+(0.5*sqr3*Idss)
iag = Ias
ibg = Ibs
icg = Ics
Vd = Vds
Vq = Vqs
"----------Power and is Current Cal. ------
Pa = va*iag
Pb = vb*ibg
Pc = vc*icg
Pg1 = Pa + Pb + Pc
pg2 = if pg1<0 then pg1 else if pg1>0 then -pg1 else 0
pg = if iqrefg<0 then pg2 else if iqrefg>0 then -pg2 else 0
"pg1 = (3/2)*(Vqs*iqs + vds*ids)
"-------- Parameters
Rs = 11.21e-3   "0.0085
Rr = 12.43e-3   "0.00316
Ls = Lls + Lm   "1.934e-3
Lr = Llr + Lm   "1.927e-3
Lm = 2.13e-3   "1.89e-3
Lls = 43.8e-6 * 3
Llr = 43.8e-6 * 3
Tr = Lr/Rr
pole = 4
"--------- Initial Values
Iqs: -50   "50
Ids: 63   "63
Iqr: 66.8992   "-27
Idr: -2.77078   "-1.83

END
→

CONNECTING SYSTEM tconn   " TOTAL CONTROL SYSTEM
                               " BAT_INV_RES_HFAC_PDM_IM
                               " ICE_IG_PDM_HFAC

TIME t
iqs[thvfc] = iqref[nspco]
Vs[thvfc] = Vs[resvi]
V1[resvi] = V1[thvfc]
wr[nspco] = wr[ma20]
wr[igtco] = wr[ig30]
pm[tpmis] = pm[ma20]
pm1[tpmis] = pm1[ma20]
vs[tpmis] = vs[resvi]
"iqref[tpmis] = iqref[igtco]
pg[tpmis] = pg[ig30]
pg1[tpmis] = pg1[ig30]
is[resvi] = isi[isfilt]

```
Vs[isfilt] = Vs[resvi]
is[isfilt] = isn[tpmis]
Vbus[pdm] = Vs[resvi]
iarc[pdm] = iarc[nspco]
ibrc[pdm] = ibrc[nspco]
icrc[pdm] = icrc[nspco]
iam[pdm] = ia[ma20]
ibm[pdm] = ib[ma20]
icm[pdm] = ic[ma20]
Va[ma20] = Van[pdm]
Vb[ma20] = Vbn[pdm]
Vc[ma20] = Vcn[pdm]
cosref[ma20] = cosref[nspco]
sinref[ma20] = sinref[nspco]
weref[ma20] = weref[nspco]
iqrefm[ma20] = iqref[nspco]
Vbus[ipdm] = Vs[resvi]
iar[ipdm] = iar[igtco]
ibr[ipdm] = ibr[igtco]
icr[ipdm] = icr[igtco]
iag[ipdm] = iag[ig30]
ibg[ipdm] = ibg[ig30]
icg[ipdm] = icg[ig30]
va[ig30] = vag[ipdm]
vb[ig30] = vbg[ipdm]
vc[ig30] = vcg[ipdm]
cosref[ig30] = cosref[igtco]
sinref[ig30] = sinref[igtco]
weref[ig30] = weref[igtco]
iqrefg[ig30] = iqref[igtco]

END
```

Biography of Dr. Bimal K. Bose

Department of Electrical Engineering
419 Ferris Hall
The University of Tennessee
Knoxville, TN 37996-2100

Phone: (615) 974-8398
Fax: (615) 974-8289
E mail: BOSE@ECE.ENGR.UTK.EDU

Bimal K. Bose (S'59-M'60-SM'78-F'89) currently holds the Condra Chair of Excellence in Power Electronics at the University of Tennessee, Knoxville, where he is responsible for organizing the power electronics teaching and research program for the last seven years. He is also the Distinguished Scientist (formerly Chief Scientist) of EPRI-Power Electronics Applications Center, Knoxville, Honorary Professor of Sanghai University of Technology, China and Senior Adviser of Beijing Power Electronics Research and Development Center, China.

He received the B.E. degree from Calcutta University, India, the M.S. degree from the University of Wisconsin, Madison, and the Ph.D. degree from Calcutta University in 1956, 1960, and 1966, respectively. Early in his career, he served as a faculty member in Calcutta University (Bengal Engineering College) for 11 years. For his research contributions, he was awarded Premchand Roychand scholarship and Mouat gold medal by Calcutta University in 1968 and 1970, respectively. In 1971, he joined Rensselaer Polytechnic Institute, Troy, NY, as Associate Professor of Electrical Engineering. In 1976, he joined General Electric Corporate Research and Development, Schenectady, NY, as an Electrical Engineer, where he served for 11 years. During his time at GE, he also worked as Adjunct Professor in Rensselaer Polytechnic Institute. He has worked

as a consultant in various industries that include General Electric R & D Center, Bendix Corporation, Lutron Electronics, PCI Ozone Corporation, Electric Power Research Institute, Research Triangle Institute, Honeywell, Reliance Electric Company, and Motion Control Engineering Inc.

Dr. Bose's research interests are power converters, ac drives, microcomputer control, and application of expert system, fuzzy logic and neural network in power electronics. He has published more than 125 papers and holds 18 US patents. He is the author of Power Electronics and AC Drives (Prentice-Hall, 1986, translated into Japanese, Chinese and Korean) and Editor of the IEEE Press books Adjustable Speed AC Drive Systems (1981), Microcomputer Control of Power Electronics and Drives (1987) and Modern Power Electronics (1992). In addition, he contributed to Systems and Control Encyclopedia (Pergamon Press, 1987), Electrical Engineering Handbook (CRC Press, 1993), Power Electronics Technology and Applications (IEEE Press, 1993) and Encyclopedia of Applied Physics (VCH, to be published). He is the Guest Editor of the special issue of the Proceedings of the IEEE on Power Electronics and Motion Control (August 1994). He visited India, China, Brazil, Turkey, Japan, Korea, Europe, Australia, Chile, Hungary, Czech Republic and Puerto Rico with various sponsored missions that included addressing the conferences.

Dr. Bose has served the IEEE in various capacities that include Chairman of IAS Industrial Power Converter Committee, IAS member in Neural Network Council, Chairman of IE Society Power Electronics Council and Power Electronics Committee, Associate Editor of IE Transactions, Distinguished Lecturer of IE and IA Societies and various professional committees. He has been in the Editorial Board of IETE Journal (India), International Electrosoft Journal and Asia-Pacific Engineering Journal.

In addition, he has served on the National Power Electronics Committee, the International Council for Power Electronics Cooperation, the International Power Electronics Conference, Tokyo, European Power Electronics Conference, International Power Electronics Conference in Warshaw, etc. He is listed in Who's Who in America, Who's Who in Electro Magnetics Academy, Who's Who in Engineering, etc. He received Publication Award, Silver Patent Medal and Centennial Invention Disclosure recognition from GE, and a number of IEEE Prize Paper Awards. In 1993, he was awarded the IEEE Industry Applications Society's Outstanding Achievement Award "for contribution in the application of electricity to industry", and in 1994, he was awarded the IEEE Industrial Electronics Society's Dr. Ing. Eugene Mittlemann Achievement Award "in recognition of outstanding contributions to research and development in the field of Power Electronics and a lifetime achievement in the area of motor drive" and the IEEE Region 3 Outstanding Engineer Award "for contribution to power electronics and drives technology".

Biography of Dr. Min-Huei Kim

Min-Huei Kim (M'92) currently holds the Visiting Research Associate in Power Electronics Application Center at the University of Tennessee, Knoxville.

He received the B.S. and M.S. degree from Yeung-Nam University, Teagu, Korea, and Ph.D. degree in electrical engineering from the University of Chung-Ang, Seoul, Korea, in 1973, 1979, and 1988, respectively. He served the Military Service from 1974 to 1976, and he has worked the Research and Development for electric motor design of the Shinil Industry company from 1977 to 1978 in Seoul, Korea. In 1978, he joined an Instructor of the Yeung-Nam Junior College, Teagu, Korea. He became an Assistant Professor, Associate Professor and Professor in 1981, 1987, and 1992, respectively.

He has authored or coauthored over 15 research papers and two textbooks in electrical engineering. He received Advice Award for industrial company from Industrial Advancement Administration of Korean Government in 1991. He is teaching about a Power Electronics, Electronic Circuits and Electric Machinery in Yeung-Nam Junior College in Teagu, Korea.

Dr. Kim's research interests are a control system of drives, power converters, electromagnetic interference, neural networks and it's application of power electronics. He is a member of KIEE, JIEE and IEEE.